



PHARMACOLOGY 41st
CHIANG MAI UNIVERSITY



THE 41ST PHARMACOLOGICAL AND THERAPEUTIC SOCIETY OF THAILAND MEETING

PROCEEDINGS

HERBAL AND COMPLEMENTARY MEDICINE INNOVATION: EAST MEETS WEST

ประชุมวิชาการประจำปีสมาคมเภสัชวิทยาแห่งประเทศไทย

ครั้งที่ 41

14 – 15 กุมภาพันธ์ 2562

ณ โรงแรมเชียงใหม่ แกรนด์วิว แอนด์ คอนเวนชัน เซ็นเตอร์ จ.เชียงใหม่

Abstract E-Book



Abstract PDF file





**THE 41ST PHARMACOLOGICAL AND
THERAPEUTIC SOCIETY OF
THAILAND MEETING**

February 14 – 15, 2019

**Chiangmai Grandview Hotel & Convention Center,
Chiang Mai, Thailand**

**HERBAL AND
COMPLEMENTARY
MEDICINE INNOVATION:
EAST MEETS WEST**

Organized by Department of Pharmacology, Faculty of Medicine,
Chiang Mai University

Contents

List of the Conference Executive Organizing Committee	3
กรรมการฝ่ายวิชาการผู้ประเมินผลงาน (Assessor)	6
PH006: <i>in vitro</i> cytotoxicity of methanol extract from peels, flowers and twigs of <i>Mammea siamensis</i> against hepatocarcinoma cell lines	7
PH008: Detection of lipid radicals produced from cholesteryl esters oxidation using a fluorescence probe, NBD-Pen	13
PH016: Cytotoxic effects of bixanthones from lichen on human colorectal cancer cells	20
PH017: Cytotoxicity of mansonone G and ethoxy mansonone G from <i>Mansonia gagei</i> Drumm in non-small cell lung cancer	27
PH024: Pharmacokinetics of oral linezolid 300 mg/day in healthy volunteers	34
PH025: Preliminary study to investigate an <i>in vitro</i> chondroprotective effect of oxyresveratrol in inflammatory-activated C28/I2 human chondrocyte cell line	39
PH026: Evaluation of <i>in vitro</i> antioxidant activity of active compounds in the fingerroot	43
PH028: Pharmacoenhancing effect of piperine on disposition kinetics of oxyresveratrol in Rats	48
PH029: Interspecies differences in pharmacokinetic and metabolic profiles of triterpenoid glycosides in standardized extract of <i>Centella asiatica</i> , ECa 233	61

Contents

PH032: Tape stripping technique in rat skin model for the determination of substance penetration into the dermis	68
PH033: Plumbagin exerts anticancer activity by suppressing HIF-1 α expression under hypoxic condition in MCF-7 breast cancer cells	73
PH036: Luteolin induces apoptosis in non-small lung cancer cells	79
List of the Organizing Sponsors	86

คณะกรรมการจัดงานประชุมวิชาการประจำปีเภสัชวิทยาแห่งประเทศไทยครั้งที่ 41
(THE 41ST PHARMACOLOGICAL AND THERAPEUTIC SOCIETY OF THAILAND MEETING)



ประธานการจัดงานประชุมฯ (Chairman)

รศ. ดร. นพ.ศุภนิมิต ทีฆชอุณหเถียร

(Assoc. Prof. Dr. Supanimit Teekachunhatean, M.D., Ph.D.)



รองประธานฯ (Sub-chairman)

ผศ. ดร. ณัฐกานต์ จิรัณธนัฐ

(Asst. Prof. Natthakarn Chiranthanut, Ph.D.)



เลขานุการฯ (Secretary)

รศ. ดร. สิวบูรณ์ สิริรัฐวงศ์

(Assoc. Prof. Seewaboon Sireeratawong, Ph.D.)



ผู้ช่วยเลขานุการฯ (Secretary assistance)

ผศ. ดร. พญ.ศรัณยภิญ โปธิกานนท์

(Asst. Prof. Saranyapin Potikanond, M.D., Ph.D.)



กรรมการฯ (Committee)

ผศ. ดร. ภญ.ปริรัตน์ คนสูง

(Asst. Prof. Parirat Khonsung, Pharm.D.)



กรรมการฯ (Committee)

ผศ. ดร. พญ.ณัฐิยา หาญประเสริฐพงษ์
(Asst. Prof.Nutthiya Hanprasertpong, M.D., Ph.D.)



กรรมการฯ (Committee)

ผศ. ดร.พวงทิพย์ คุณานุสรณ์
(Asst. Prof.Puongtip Kuanusorn, Ph.D.)



กรรมการฯ (Committee)

ผศ. ดร. พญ.วารังคณา อารpornชยานนท์
(Asst. Prof.Warangkana Arpornchayanon, M.D., Ph.D.)



กรรมการฯ (Committee)

ผศ. ดร.วุฒิไกร นิมละมูล
(Asst. Prof.Wutigri Nimlamool, Ph.D.)



กรรมการฯ (Committee)

ผศ. ดร. นพ.สุกิจ รุ่งอภินันท์
(Asst. Prof.Sukit Roongapinun, M.D., Ph.D.)



กรรมการฯ (Committee)

อ. ดร .ภญ.มิ่งขวัญ ณ ตะกั่วทุ่ง
(Mingkwan Na Takuathung, Pharm.D.)



กรรมการฯ (Committee)

อ. ดร. นพ.ณัฐ คุณรังษีสมบูรณ์
(Nut Koonrungsomboon, M.D., Ph.D.)

กรรมการฝ่าย (Subcommittee)

กรรมการฝ่ายประชาสัมพันธ์ (Registration)

- นางปยุณนุช สุขสบาย
(Ms.Punyanuch Sukksabai)
- นายปทีป หาญกิตติชัย
(Mr.Phateep Hankittichai)
- นางสาวกัลยรัตน์ ชัยรักษา
(Ms.Kanyarat Chairaksa)
- นายนต์พันธ์ ชมภูศรี
(Mr.Nattapran Chompusri)

กรรมการฝ่ายวิชาการ (Academic scientific)

- นางสาวเบญจมาศ สุระเดช
(Ms.Benjamart Suradej)
- นางสาวมัทรีญาภาร์ เกาศรี
(Ms.Mattareeyapar Phaosri)
- นางสาวกัญจน์ณัฐ สันทราย
(Ms.Kanjanath Sansai)

กรรมการฝ่ายสถานที่และโสตทัศนูปกรณ์ (Exhibition)

- นางสาวนัทธ์หทัย เต็มยิ่งยง
(Ms.Nathathai Temyingyong)

- นายวิสิทธิ์ ฐิติณรงค์เวทย์
(Mr.Wisit Thitinarongwate)
- นายภัทรวัต ทะแก้วพันธ์
(Mr.Phatarawat Thaklaewphan)
- นางสาวอัจฉริยา เชื้อเย็น
(Ms.Achariya Churyen)

กรรมการฝ่ายการเงิน (Finance)

- นางยุพเรศ กองนาค
(Ms.Yupared Kongnak)
- นางสาวอังคณา ราชสีห์
(Ms.Aungkana Rachsee)
- นางสาวรุจิรา หลิมไพศาล
(Ms.Rujira Limpaisarn)
- นางสาวโสธรญา กลิ่นปรุง
(Ms.Soraya Klinprung)

กรรมการฝ่ายประสานงานทั่วไป (coordinate)

- นางสาวชिरวิภักดิ์ ัญญ์กัญจนธรณ์
(Ms.Sirawipak Thankanjanatorn)
- นางสาวพรรณพักตร์ หิรัญสฤติย์พร
(Ms.Pannaphak Hirunsatitpron)

กรรมการฝ่ายวิชาการผู้ประเมินผลงาน (Assessor)

1. ศ. ดร. ภก.วีรพล	คู้คงวิริยพันธุ์	มหาวิทยาลัยขอนแก่น
2. รศ. ดร. ภาณุ.รัตติมา	จึนาพงษา	มหาวิทยาลัยนเรศวร
3. รศ. ดร. ภาณุ.สุวรา	วัฒนพิทยกุล	มหาวิทยาลัยศรีนครินทรวิโรฒ
4. รศ. ดร. ภาณุ.ลินดา	จุฬาโรจน์มนตรี	มหาวิทยาลัยธรรมศาสตร์
5. ผศ. ดร. ภาณุ.วัชรี	ลิมนสิทธิกุล	มหาวิทยาลัยจุฬาลงกรณ์
6. ผศ. ดร.วันดี	อุดมศักดิ์	มหาวิทยาลัยสงขลานครินทร์
7. ผศ. ดร. นพ.สุกิจ	รุ่งอภินันท์	มหาวิทยาลัยเชียงใหม่
8. ผศ. ดร.วุฒิไกร	นิ่มละมุล	มหาวิทยาลัยเชียงใหม่
9. อ. ดร. นพ. ณ์ฐ	คุณรังสีสมบูรณ์	มหาวิทยาลัยเชียงใหม่

PH-006

Total phenolic content, antioxidant and cytotoxicity against HepG2 cell lines of methanol extract from flowers, twigs and peels of *Mammea siamensis*

Lamai Maikaeo^{1*}, Surasak Sajjabut¹ and Parichat Thepthong²

¹ Thailand Institute of Nuclear Technology (Public organization) Nakhon nayok 26120, Thailand.

² Department of Chemistry, Faculty of Science, Thaksin University, Phatthalung 93210, Thailand.

ABSTRACT

INTRODUCTION: *Mammea siamensis* is a Thai medicinal herb in the family Guttiferae, locally known as “Saraphi”. Its flowers are used as heart tonic. The chemical constituent of the genus *Mammea* has been known to be a rich source of coumarins and xanthenes which has been considered potential sources of anticancer agents. Liver cancer remains the first leading cause of cancer death in Thailand. The conventional drug resistances exist in current therapeutics. Natural products-derived from the plant are potential sources for the prevention from and the treatment of liver cancer.

OBJECTIVES: To evaluate the activities of methanol extracts from flowers, twigs, and peels of *M. siamensis* including total phenolic content, antioxidant activity and *in vitro* cytotoxicity against hepatocarcinoma cell lines (HepG2) for prevention and treatment of liver cancer.

METHODS: The flowers, twigs, and peels of *M. siamensis* were collected and extracted using methanol. The total phenolic content analysis was performed using Folin–Ciocalteu reagent; Antioxidant activity was evaluated as the scavenging activity of 1,1-diphenyl-2-picrylhydrazyl (DPPH) radical; the cytotoxicity was evaluated using HepG2 cell lines, and the cells were treated with 0-1000 µg/mL of the extract for 24 h and its cytotoxicity was identified by MTT assay.

RESULTS: The total phenolic content from flowers, twigs, and peels of *M. siamensis* were 43.34±0.51, 43.11±1.01, and 29.22±0.83 mg GAE/g, respectively and antioxidant capacity (DPPH) was 21.77±0.21, 19.2±0.21, and 10.65±0.31 mg AAE/g, respectively. The methanol extract from flowers and twigs showed potent cytotoxic activity against HepG2 cells greater than peels extract. The half maximal inhibitory concentration (IC₅₀) from flowers, twigs, and peels against HepG2 were 26.97±3.62, 27.99±1.04, and 187.19±4.71 µg/mL, respectively.

CONCLUSIONS: The study presents the first report on the methanol extract from flowers and twigs of *M. siamensis* against HepG2 cell cultures. There is a correlation between total phenolic content, antioxidant activity and anticancer activity. The bioactive compound from the flowers and twigs of *M. siamensis* prove to be the abundant- source for anti-liver cancer agents. Further studies of the molecular mechanism of the extracts against the HepG2 cell and normal cell lines are under investigation.

Keywords: Total phenolic content, antioxidant activity, cytotoxicity, hepatocarcinoma cell lines, *Mammea siamensis*

INTRODUCTION

The phytochemical from plant especially phenolic compound have been gradually discovered to be potential sources of antitumor drugs. The antioxidant activity of phenolic compounds is mainly due to their redox properties, which can be of high importance in

adsorbing and neutralizing free radicals or decomposing peroxides.¹ Currently, many plants with high contents of phenolics and high antioxidant activity are recommended for several human diseases preventive and treatment.^{2,3}

Mammea siamensis is a Thai medicinal herb in the family Guttiferae, locally known as “Saraphi”. The flower is used as a heart tonic, fever-lowering and enhancement of appetite in Thailand.⁴ The fruit is generally considered edible and used as a vasodilator. The chemical constituent of the genus *mammea* are known to be a rich source of coumarins and xanthenes.⁵⁻⁷ These phenolic compounds possess multiple biological properties such as antimicrobial, anti-inflammatory, antioxidant and anticancer. A part of these plant have cytotoxic activity on many cancer cell lines including colon cancer (DLD-1), breast cancer (MCF-7), cervical cancer (HeLa), lung cancer (NCI-H460),⁸ liver cancer (HepG2),⁹ and leukaemic cells (K562).¹⁰

In 2017, Data from death certificate found that liver cancer is the first leading cause of cancer death in Thailand by the mortality rate of liver cancer per 100,000 population are 25, followed by lung cancer (21), breast cancer (12.6), cervix cancer (6.8) and leukaemia (3.9).¹¹ The primary cancer of liver, comprises with 2 types including hepatocellular carcinoma (HCC) is 95% and cholangiocarcinoma (CCA) is 5% in patients of Thailand.¹² The major risk factors for HCC are viral (chronic hepatitis B and hepatitis C) and toxic (alcohol and aflatoxins),¹³ and CCA are parasitic infection in dietary.¹⁴ A variety of therapies have been used for the treatment of liver cancer, such as chemotherapy,¹⁵ radiotherapy,¹⁶ cryo-ablation,¹⁷ and transarterial chemoembolization (TACE).¹⁸ However, these treatments cause serious side effects, including bone marrow depression, hair loss, postembolization syndrome, and liver and renal failure. Therefore, an urgent need is arising for new active and well-tolerated treatments to improve survival among HCC patients.

The abundant herb resource has also provided an essential material foundation to look for new anticancer drugs. Bioactive plant compounds could affect the normal biological process of cancer cells, including initiation, promotion and progression.¹⁹ *M. siamensis* are one of the potential sources for cancer prevention and treatment; however, there is no information about the total phenolic content and antioxidant activity of *M. siamensis*. Indeed, only a small number of reports about the cytotoxicity against liver cancer (HepG2) therefore it remains unclear.^{9,4} This study was undertaken to assess the different parts of *M. siamensis* for their total phenolic content and antioxidant activity, as well as their potential *in vitro* toxicity against HepG2 cell lines.

This study presents the first report on the methanol extract from flowers and twigs of *M. siamensis* against HepG2 cell cultures. A significant correlation exists between total phenolic content, antioxidant activity, and anticancer activity. The active development of innovative therapeutic approaches and molecularly targeted agents using herbal medicine could put insights into the cancer agents and raise new opportunities for the future.

METHODS

1. Plant extract preparation

The flowers, twigs and peels of *M. siamensis* were collected from Prince of Songkla University, Songkhla province. Each part was dried in 40°C in oven, then grained. Each dried powdered material was extracted in methanol for 7 days. The extracts were filtered using Whatman no.1 filter paper. The methanol extract was concentrated to dryness using rotary evaporator under vacuum. Extracts were stored at 25°C until the use.

2. Total phenolic content assay

The total phenolic content was estimated using the Folin-Ciocalteu assay. Briefly, the extract was weighed and dissolved with 100 µL of distilled water in a test tube. The 0.75 mL of 10-fold diluted Folin-Ciocalteu reagent was added and allowed to stand at room temperature for 5 min. Then, 0.75 mL of 6% (w/v) sodium carbonate solution was added. The mixture was homogenized and allowed to stand at room temperature for 90 min. The total phenolic content

was determined via the absorbance measurements at 725 nm using a spectrophotometer. The standard calibration curve was plotted using gallic acid at the concentrations of 0.02 - 0.1 mg/mL. The total phenolic content was expressed in mg gallic acid equivalent (GAE)/g sample.

3. Antioxidant assay (DPPH assay)

The radical scavenging activity was determined by 1,1-diphenyl-2-picrylhydrazyl (DPPH) assay. Shortly, the 100 μ L of each extract was added to 900 μ L of DPPH in methanol solution (150 μ M) and the solution was shaken vigorously. After incubation at room temperature for 15 min in darkness, the absorbance of each solution was determined at 517 nm. The free radical scavenging power was expressed as ascorbic acid equivalent (AAE)/g sample.

4. Cytotoxic test against HepG2

4.1 Cell culture

HepG2 (ATCC-HB-8065) were cultured in DMEM-low glucose (Gibco, USA) supplement with 3.7 g/L of sodium bicarbonate buffer system, 10% fetal bovine serum (Hyclone, USA), penicillin (100U/mL) and streptomycin (100 μ g/mL) (Gibco, USA) and then incubated at 37 °C at 95% humidity and 5 % CO₂.

4.2 MTT assay

HepG2 cells (1x10⁴ cells/well) were seeded in 96 well plates. After 24 h, the old media were replaced with 100 μ L of filtrated media mixed with plant extract which was diluted in DMSO (<0.4% v/v in culture media) at 10-fold concentration range 0-1000 μ g/mL. The vehicles treatment, cells were treated with 0.4 v/v of DMSO, following 24 h incubation. The cytotoxicity was observed by 3–4,5-dimethylthiazol-2,5-diphenyl-tetrazolium bromide (MTT) (Sigma, USA) assay. Shortly, the old medium was discarded carefully, then 20 μ L of 1 mg/mL of MTT was added into each well and left the plate in incubator for 3 h. Subsequently, the MTT solution was removed and 100 μ L of isopropanol was added into each well. The presence of viable cells was indicated by purple coloring due to the formation of formazan crystals. The color reading was taken at 570 nm using an automated microplate reader (Molecular Devices, USA). All tests were conducted in triplicate. The percentage of cell survival was calculated using the following formula: $(A_{\text{Sample}}/A_{\text{Control}}) \times 100$. The concentration corresponding to a survival rate of a 50% is defined as inhibition concentration 50% (IC₅₀)

RESULTS AND DISCUSSION

Herbal medicinal is one of the major traditional medicine which has been gained a remarkable effect on the treatment of various diseases as well as cancer. Many Thai traditional medicines have been tested for their cytotoxicity activity against cancer cell line. In the present study, the total phenolic content, antioxidant capacity, and cytotoxicity against HepG2 cell lines from flowers, twigs, and peels of *M. siamensis* were investigated. Results from the initial screening showed that the total phenolic content from flowers, twigs, and peels were 43.34±0.51, 43.11±1.01, and 29.22±0.83 mg GAE/g, respectively, antioxidant capacity (DPPH) were 21.77±0.21, 19.2±0.21, and 10.65±0.31 mg AAE/g, respectively, and the cytotoxic activity against HepG2 with IC₅₀ were 26.97±3.62, 27.99±1.04, and 187.19±4.71 μ g/mL, respectively (Table 1.).

A positive correlation between total phenolic content, antioxidant activity, and anticancer activity was found in the methanol extract from *M. siamensis*. Table. 1 indicates the total phenolic content, antioxidant activity, and potent cytotoxic activity against HepG2 of the flowers and twigs were higher than peels extract. Evidence suggests the antioxidant capacity of phenolics will increase with the number of free hydroxyls and conjugation of side chains to the aromatic rings.²⁰ In addition, phenolic compounds are known to induce the cytotoxicity on various cancer cell line, the increasing of anticancer activity correlates with the higher amount of polyphenols and antioxidant capacity.²¹

The cytotoxic activity against cancer cell lines from apart of *M. siamensis* extracts have been reported. The coumarins (thetraphin C) from bark strongly inhibited DLD-1 (colon

cancer), MCF-7 (breast adenocarcinoma), HeLa (human cervical cancer), and NCI-H460 (human lung cancer) with IC_{50} in the range of 1.6-5.7 μ M.⁸ Hexane fraction from flowers demonstrated the strongest effect on leukemic cell (EoL-1) with IC_{50} of 3.8 \pm 0.8 μ g/mL. Moreover, the methanol extract from flowers showed antiproliferative activity against human leukemia (HL-60) and stomach cancer (KATO-III) IC_{50} in the range of 9-30 μ M and 10-24 μ M, respectively, but it had no cytotoxic against HepG2.⁴ Our results contradicts previous reports, and we found that the methanol extract from flowers strongly suppressed HepG2 cell proliferation (IC_{50} =27 μ g/mL).

The cytotoxicity on HepG2 might be due to the compounds or DMSO as vehicles solvent. The DMSO in culture medium above 0.1-0.5% often decrease the proliferation of cultured cells. Our results found that the 0.4% DMSO which was the highest concentration contained in culture media had some cytotoxicity for HepG2 by decreased cell viability about 15% compared to untreated control. However, the comparison effect between 0.4% DMSO and the highest concentration of each methanol extracts on HepG2 cell viability showed that a significant difference in cell viability (Figure. 1). These data indicated that the compounds in the highest concentration of each methanol extracts have strongly affected on inhibit HepG2 cell viability than vehicles solvent. Therefore, the cytotoxic effect on HepG2 cell viability are resulted from the compounds in methanol extracts.

Table 1. Total phenolic content, antioxidant activity, and cytotoxicity against HepG2 (IC_{50}) of methanol extract from *M. siamensis*

Part of plant	Total phenolic content (mg GAE/g)	Antioxidant activity (DPPH) (mg AAE/g)	Cytotoxicity IC_{50} (μ g/mL)
Flowers	43.34 \pm 0.51	21.77 \pm 0.21	26.97 \pm 3.62
Twigs	43.11 \pm 1.01	19.2 \pm 0.21	27.99 \pm 1.04
Peels	29.22 \pm 0.83	10.65 \pm 0.31	187.19 \pm 4.71

Total phenolic content and antioxidant activity are reported as gallic acid equivalents (GAE) and ascorbic acid equivalents (AAE) respectively. IC_{50} was the inhibitory concentration corresponding to a survival rate of a 50% (Values expressed as mean \pm SD, n=3)

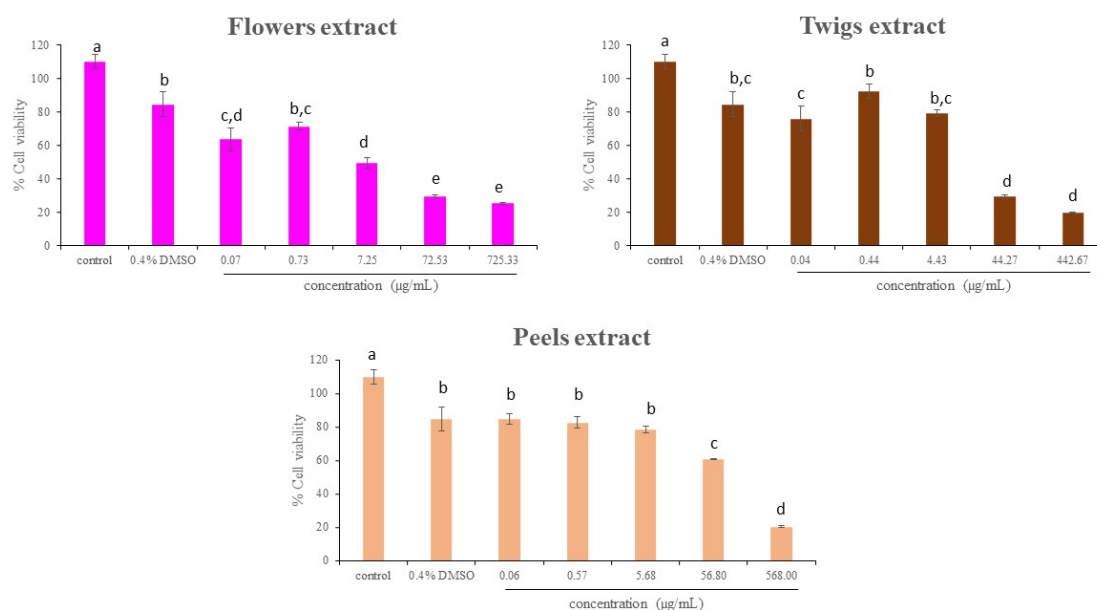


Figure 1. Effect of DMSO and methanol extract from *M. siamensis* on HepG2 cell viability (Results are shown as mean \pm SD, n=3). The different alphabet letters indicated statistically different means of each group ($p < 0.05$, one-way ANOVA, Scheffe)

CONCLUSIONS

There is a correlation between and total phenolic content, antioxidant activity, and anticancer activity. The total phenolic content, antioxidant activity, and potent cytotoxic activity against HepG2 of the flowers and twigs were higher than peels extract. The bioactive compound from the flowers and twigs of *M. siamensis* are the good sources for anti-liver cancer agent. The molecular mechanism of the extract against the HepG2 cell and normal cell lines are under future investigation.

ACKNOWLEDGEMENT

The authors are grateful to the project “Cell cytotoxicity laboratory” of Thailand institute of nuclear technology (Public organization) for finance support. And also thanks to Mrs. Kaylene Ballard (University of the Sunshine Coast) for her thoughtful proofreading of our manuscript.

CONFLICT OF INTEREST

The authors declare that they have no conflicts of interest.

REFERENCES

1. Forman S, Kas J, Fini F, Steinberg M, Ruml T. The effect of different solvents on the ATP/ADP content and growth properties of HeLa cells. *J Biochem Mol Toxicol*. 1999;13(1):11–5.
2. Boutennoun H, Boussouf L, Rawashdeh A, Al-Qaoud K, Abdelhafez S, Kebieche M, et al. In vitro cytotoxic and antioxidant activities of phenolic components of Algerian *Achillea odorata* leaves. *Arab J Chem* [Internet]. 2017;10(3):403–9.
3. Qader SW, Abdulla MA, Chua LS, Najim N, Zain MM, Hamdan S. Antioxidant, Total Phenolic Content and Cytotoxicity Evaluation of Selected Malaysian Plants. Vol. 16, *Molecules*. 2011.
4. Tung NH, Uto T, Sakamoto A, Hayashida Y, Hidaka Y, Morinaga O, et al. Antiproliferative and apoptotic effects of compounds from the flower of *Mammea siamensis* (Miq.) T. Anders. on human cancer cell lines. *Bioorg Med Chem Lett* [Internet]. 2013;23(1):158–62.
5. Mahidol C, Kawetripob W, Prawat H, Ruchirawat S. *Mammea* coumarins from the flowers of *Mammea siamensis*. *J Nat Prod*. 2002 May;65(5):757–60.
6. Laphookhieo S, Promnart P, Karalai JKSAK-OCPC. Coumarins and xanthenes from the seeds of *Mammea siamensis*. *J Braz Chem Soc*. 2007;1077–1080.
7. Poobrasert O, Constant HL, Beecher CWW, Farnsworth NR, Kinghorn AD, Pezzuto JM, et al. Xanthenes from the twigs of *Mammea siamensis*. *Phytochemistry* [Internet]. 1998;47(8):1661–3.
8. Ngo NTN, Nguyen VT, Vo H Van, Vang O, Duus F, Ho T-DH, et al. Cytotoxic Coumarins from the Bark of *Mammea siamensis*. *Chem Pharm Bull (Tokyo)*. 2010 Nov;58(11):1487–91.
9. Mahavorasirikul W, Viyanant V, Chaijaroenkul W, Itharat A, Na-Bangchang K. Cytotoxic activity of Thai medicinal plants against human cholangiocarcinoma, laryngeal and hepatocarcinoma cells in vitro. *BMC Complement Altern Med*. 2010 Sep;10:55.
10. Rungrojsakul M, Saiai A, Ampasavate C, Anuchapreeda S, Okonogi S. Inhibitory effect of *mammea E/BB* from *Mammea siamensis* seed extract on Wilms’ tumour 1 protein expression in a K562 leukaemic cell line. *Nat Prod Res*. 2016;30(4):443–7.
11. Strategy and Planning Division M of PH. *Public Health Statistics A.D.2017*. 2017. 146 p.

12. Srivatanakul P. Epidemiology of Liver Cancer in Thailand. *Asian Pac J Cancer Prev*. 2001;2(2):117–21.
13. Gomaa AI, Khan SA, Toledano MB, Waked I, Taylor-Robinson SD. Hepatocellular carcinoma: epidemiology, risk factors and pathogenesis. *World J Gastroenterol*. 2008 Jul 21;14(27):4300–8.
14. Kirstein MM, Vogel A. Epidemiology and Risk Factors of Cholangiocarcinoma. *Visc Med*. 2016 Dec;32(6):395–400.
15. Le Grazie M, Biagini MR, Tarocchi M, Polvani S, Galli A. Chemotherapy for hepatocellular carcinoma: The present and the future. *World J Hepatol*. 2017 Jul 28;9(21):907–20.
16. Jae Lee I, Seong J. Radiotherapeutic Strategies in the Management of Hepatocellular Carcinoma. Vol. 81 Suppl 1, *Oncology*. 2011. 123-133 p.
17. Song KD. Percutaneous cryoablation for hepatocellular carcinoma. *Clin Mol Hepatol*. 2016 Dec;22(4):509–15.
18. Van Ha TG. Transarterial chemoembolization for hepatocellular carcinoma. *Semin Intervent Radiol*. 2009 Sep;26(3):270–5.
19. Treasure J. Herbal medicine and cancer: an introductory overview. *Semin Oncol Nurs*. 2005 Aug;21(3):177–83.
20. Mathew S, Abraham TE, Zakaria ZA. Reactivity of phenolic compounds towards free radicals under in vitro conditions. *J Food Sci Technol*. 2015 Sep;52(9):5790–8.
21. Danciu C, Vlaia L, Fetea F, Hancianu M, Coricovac DE, Ciurlea SA, et al. Evaluation of phenolic profile, antioxidant and anticancer potential of two main representants of Zingiberaceae family against B164A5 murine melanoma cells. *Biol Res*. 2015 Jan 12;48(1):1.

PH-008

Detection of lipid radicals produced from cholesteryl esters oxidation using a fluorescence probe, NBD-Pen

Pakawit Lerksaipheng¹, Rataya Luechapudiporn², Kittiphong Paiboonsukwong³,
Pimtip Sanvarinda¹ and Noppawan Phumala Morales^{1*}

¹ Department of Pharmacology, Faculty of Science, Mahidol University, Bangkok 10400, Thailand.

² Department of Pharmacology and Physiology, Faculty of Pharmaceutical Sciences, Chulalongkorn University, Bangkok 10330, Thailand.

³ Thalassemia Research Center, Institute of Molecular Biosciences, Mahidol University, Nakhon Pathom 73170, Thailand.

ABSTRACT

INTRODUCTION: Oxidative modification of low-density lipoprotein (LDL) and high-density lipoprotein (HDL) are regarded as causative events of cardiovascular diseases. Lipid peroxidation is primarily initiated by reactive oxygen species and produces lipid radicals (L[•]) as mediators. Cholesteryl esters (CE), especially cholesteryl linoleate (CL) and cholesteryl arachidonate (CA) are the major core components of LDL and HDL. Therefore, the formation of L[•] and lipid hydroperoxide (LOOH) during CL and CA oxidation has been considered as a key step in the cardiovascular pathogenesis. A fluorescence probe, NBD-Pen, has been developed for specific detection of L[•]. The kinetics of L[•] formation and lipid identification, thus, are simply investigated by following fluorescence of adducts of NBD-Pen and L[•].

OBJECTIVES: This study aims to investigate the kinetics of L[•] generation using NBD-pen, and LOOH formation during CL and CA oxidation in 2,2'-azobis(2-amidinopropane) dihydrochloride (AAPH)- and hemin-induced lipid peroxidation model.

METHODS: CA, CL as well as linoleic acid (LA) and free cholesterol (FC) were oxidized by 2 mM AAPH or 2 μM hemin. During the oxidation, the generated L[•] was trapped by NBD-Pen and continuously measured fluorescence intensity ($\lambda_{ex}=470$ nm, $\lambda_{em}=530$ nm) for 2 h. After the reaction stop, lipids were extracted and analyzed by reversed-phase HPLC tandem UV-Visible and fluorescence detector to determine LOOH and NBD-Pen adducts.

RESULTS: The different kinetic profiles of AAPH- and hemin-induced L[•] formation was demonstrated. Hemin manifested a stronger oxidizing property than AAPH. The initial rate of L[•] formation from AAPH oxidation was ranked as CA > LA > CL, and from hemin oxidation was CA > CL > LA. Chromatographic results also revealed the different species of L[•] and LOOH formation after oxidation with AAPH and hemin.

CONCLUSIONS: This study showed that L[•] rapidly produced from CE oxidation and detected by a specific fluorescent probe. Moreover, the results suggested that AAPH and hemin interacted with lipids at different rate and target. CA showed a higher susceptibility to oxidation than CL based on an initial rate of L[•] formation.

Keywords: cholesteryl ester, lipid radical, lipid peroxidation, AAPH, hemin

INTRODUCTION

Oxidative modification of LDL and HDL are regarded as causative agents of cardiovascular diseases. LDL and HDL are oxidized by enzymatic and non-enzymatic reaction producing several bioactive lipid products. However, the primary reaction *in vivo* has not been

elucidated. Generally, lipid peroxidation is primarily initiated by reactive oxygen species and produces L[•] as mediators. Cholesteryl esters (CE), especially cholesteryl linoleate (CL) and cholesteryl arachidonate (CA) are the major core components of LDL and HDL. Therefore, the formation of L[•] and lipid hydroperoxide (LOOH) during CL and CA oxidation has been considered as a key step in the cardiovascular pathogenesis.

NBD-Pen is a specific fluorescence probe for L[•] developed by Yamada et al. since 2016 (1). NBD-Pen consists of a nitroxide and a fluorophore group moiety. Without the environment of L[•], nitrosyl radical on the nitroxide group will act as a quencher for the fluorophore group. On the other hand, the presence of L[•] makes a single electron on the nitroxide group interacts with a single electron on L[•] instead of the fluorophore group. This allows electrons of fluorophore group to delocalize and able to emit a fluorescence signal after its light absorption in a specific wavelength. The emitted signal is proportionate to the quantity of L[•] in the system providing a high selectivity and sensitivity of L[•] measurement though L[•] is very reactive.

In this study, Oxidation of CL and CA were investigated using two initiators including AAPH, an azo compound generating free radicals; and hemin, a protoporphyrin IX-containing ferric ion (Fe³⁺). Kinetics profiles of L[•] generation during CL and CA oxidation was examined by using NBD-Pen, and the formation of LOOH was also determined.

Our results may predict the main target lipids during of LDL and HDL oxidation, whether CL or CA. An initial rate of L[•] production as well as several unidentified L[•] obtained from chromatograms of CL and CA oxidation would be beneficial for understanding more about cardiovascular diseases developed via LDL and HDL oxidation. Moreover, this may lead to the finding of novel biomarkers in LDL and HDL-related diseases in further study.

METHODS

FC, CA, CL and LA were dissolved in acetonitrile:isopropanol (1:1) to make various concentrations (500, 250, 125, 62.5, 31.2, 15.6, 7.81, 3.91 μM) and then oxidized by AAPH or hemin. The oxidation reaction was performed by mixing 50 μL of each lipid sample with 100 μL phosphate buffer (pH 7.4) and 10 μL of 100 μM NBD-Pen in 96-well plate. The mixture was incubated at 40 °C before starting the reaction with 40 μL of 10 mM AAPH or 10 μM hemin. The fluorescence intensity of NBD-Pen-L[•] adduct was continuously measured at 470 nm of excitation wavelength (λ_{ex}) and 530 nm of emission wavelength (λ_{em}) for 2 h by Varioskan Flash Microplate Reader (Thermo Fisher Scientific, USA).

After oxidation, a 200 μL of the reaction mixture was extracted by 500 μL ice-cold methanol and followed by 2.5 mL hexane in sequence. The mixture was vortexed vigorously and centrifuged at 1700 rpm at 4 °C for 5 min. The upper hexane layer was collected, evaporated using N₂ gas, and finally re-dissolved in 600 μL acetonitrile:isopropanol (1:1) for HPLC analysis.

A reversed-phase HPLC tandem UV-Visible and fluorescence detector were used to measure CE (at 210 nm), LOOH (at 234 nm), and NBD-Pen-L[•] adduct (at 470 nm of λ_{ex} and 530 nm of λ_{em}). The HPLC systems consisted of Waters Alliance 2695 separations module with Waters 2487 dual wavelength and Waters 474 scanning fluorescence detectors. All samples were separated on a Hypersil BDS C-18 stainless-steel column (5 μm; 4.6 x 250 mm), with 1.0 mL/min flow rate of acetonitrile:isopropanol:water (46:51:3) as a mobile phase and column temperature 50 °C.

RESULTS

Kinetic curves of NBD-Pen-L[•] adduct derived by oxidation FC, CA, CL and LA with 2 mM AAPH and 2 μM hemin are illustrated in Figure 1. The initial rate of L[•] formation is calculated from the slope of the kinetics curves and demonstrated in Table 1. The maximum end point of fluorescent intensity (at 2 h) is demonstrated in Table 2.

The results showed that cholesteryl esters, CA and CL were rapidly oxidized by hemin with the initial rate of 6.24 and 2.49 min^{-1} , respectively. The reaction reached the terminal phase of lipid peroxidation within 30 min. In AAPH oxidation, the initial rate of CA and CL was 1.72 and 0.14 min^{-1} , respectively.

Maximum fluorescent intensity was used to estimate the amount of L^\bullet formation. Table 2 demonstrated that both CA and CL produced a comparative amount of L^\bullet in hemin oxidation, fluorescent intensity was 182.58 and 143.65, respectively. However, the different L^\bullet formation was observed in AAPH oxidation, fluorescent intensity was 134.36 and 43.84, respectively.

FC and LA were used as a representative of cholesterol and fatty acid chain moiety in CE, respectively. The results of rate and maximum intensity of FC and LA strongly revealed that polyunsaturated fatty acids were a target of oxidation rather than cholesterol moiety.

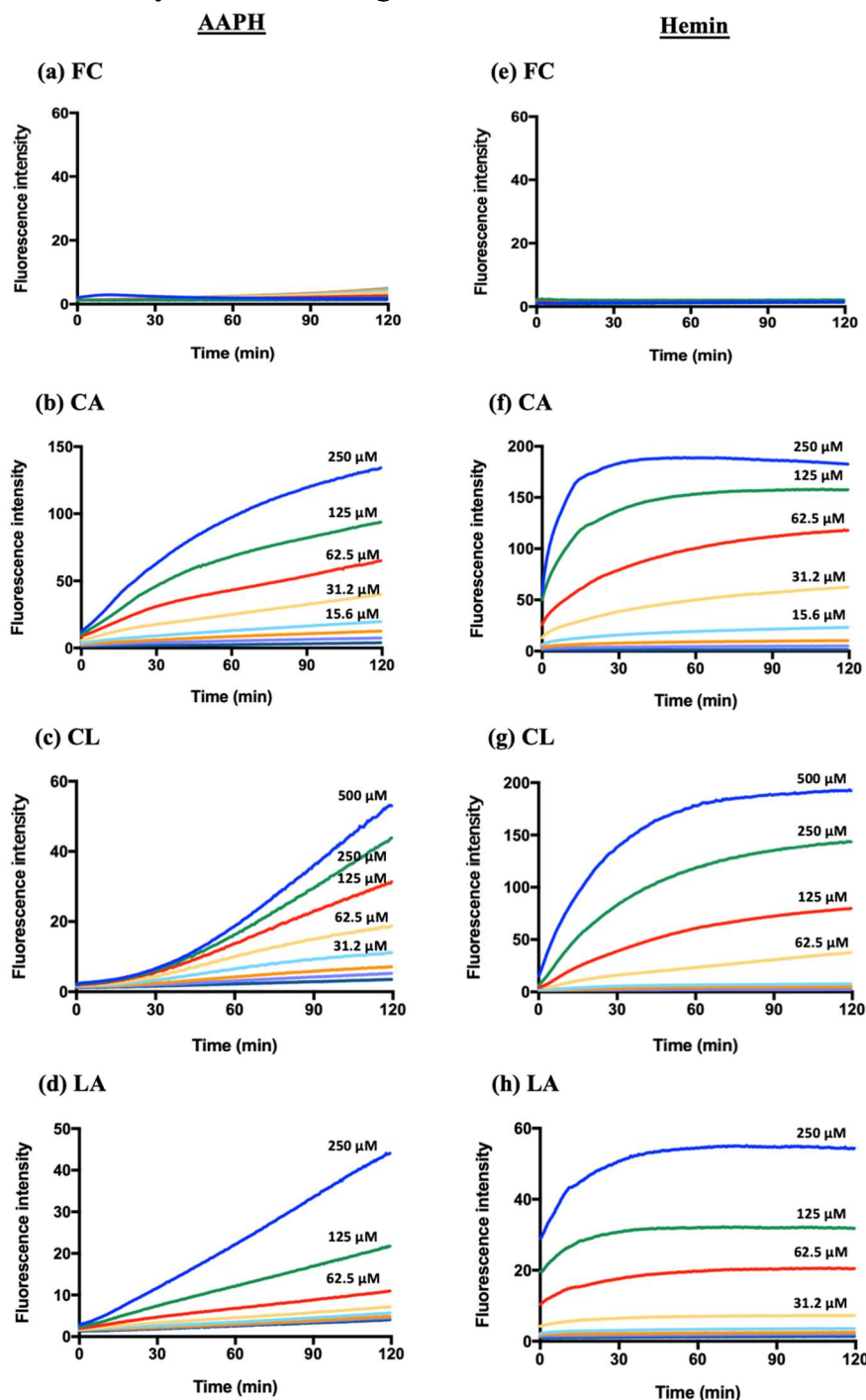


Figure 1. Kinetics curve of L^\bullet formation derived by AAPH induced FC (a), CA (b), CL (c) and LA (d) oxidation; and by hemin-induced FC (e), CA (f), CL (g) and LA (h).

Table 1. Initial rate of L[•] formation derived from FC, CA, CL and LA oxidation by AAPH and hemin

Lipid	Initial rate of oxidation (min ⁻¹)	
	2 mM AAPH	2 μM Hemin
FC	0.01 ± 0.00	ND
CA	1.72 ± 0.04	6.24 ± 0.34
CL	0.14 ± 0.01	2.49 ± 0.14
LA	0.27 ± 0.01	1.04 ± 0.06

The concentration of lipids was 250 μM. Data were mean ± S.D. from 3 independent experiments.

Table 2. Maximum fluorescent intensity of FC, CA, CL and LA oxidation by AAPH and hemin

Lipid	Maximum intensity (A.U)	
	2 mM AAPH	2 μM Hemin
FC	2.01 ± 0.07	2.11 ± 0.05
CA	134.36 ± 1.14	182.58 ± 16.88
CL	43.84 ± 5.15	143.65 ± 8.07
LA	44.05 ± 5.46	54.40 ± 2.10

The concentration of lipids was 250 μM. Maximum fluorescent intensity was detected at 2 h after starting the reaction with AAPH or hemin. Data were mean ± S.D. from 3 independent experiments.

The products of lipid peroxidation were separated and characterized by HPLC. Chromatograms of NBD-Pen-L[•] adduct of CA and CL oxidation by AAPH and hemin are demonstrated in Figure 2. Oxidation of CA and CL gave the different L[•] products as indicated by different fluorescent chromatogram patterns. Although AAPH and hemin showed the different rate of reaction, they produced a similar chromatogram pattern in CA oxidation. However, AAPH and hemin produced different products in CL oxidation. The major differences found in the chromatogram pattern of CL oxidation were a group of peaks at retention time 10.8 min and at 7.7 to 8.356 min. For AAPH, the peak at retention time 10.8 was observed with high intensity. While the peaks at retention time 7.7 to 8.3 min are the major products for hemin-induced CL oxidation.

Oxidation of CL resulted in the production of lipid peroxides (LOOH) as showed in Figure 3. Chromatograms detected at 210 nm and 234 nm were used to monitored CE and LOOH, respectively. The levels of FC, CA, CL and LA were decreased more than 80% after 2 h oxidation by AAPH and hemin. Corresponding with decreasing of lipids, their peroxide products LOOH were increased. An example of CL oxidation by hemin is shown. Here, the peak of CL (retention time 13.2 min) was decreasing approximately 97% and LOOH was clearly detected at retention time 7.1 min.

DISCUSSION

CA and CL are the most abundant lipids in the core of lipoproteins. Their chemical structures are cholesterol links with polyunsaturated fatty acid by an ester bond. There are 4 and 2 unsaturated bonds in arachidonic acid (20:4) and linoleic acids (18:2), respectively. CA was suggested to have a higher susceptibility to oxidation than CL. In regard to our results, fatty acid moiety was a primary target for L[•] production, not cholesterol moiety. Moreover, the initial rate of L[•] production verified that the different number of unsaturated bonds might be the major factor determining the initial rate of oxidation. In addition, the oxidizing agents could

attack at several unsaturated bonds, thus accelerated the reaction and produced a higher amount of L^{\bullet} . Therefore, CA oxidation showed a higher initial rate and reached the terminal phase of lipid peroxidation faster than CL.

AAPH is an azo compound that liberates LOOH at a constant rate, while hemin initiates lipid peroxidation via Fenton-like reaction. Our results clearly showed that hemin was more potent than AAPH in lipid peroxidation induction. We observed that the initial rate of L^{\bullet} formation was ranked as $CA > LA > CL$ for AAPH, and $CA > CL > LA$ for hemin. This suggested that AAPH may selectively attack CE in the fatty acid moiety, making LA produced more L^{\bullet} than CL due to the hindrance effect from cholesterol moiety. On the other hand, hemin may attack CE molecule with less selectivity, therefore, L^{\bullet} could produce from both cholesterol and fatty acid moiety.

Since hemin is an integral part of hemoglobin and also plays a role in hemoglobin regulation and erythropoiesis *in vivo*, therefore, patients with diseases of hemolytic anemia usually have elevated blood levels of hemin and often exceed $10 \mu\text{M}$ (2). As hemin contains Fe^{3+} ion, it leads to the highly oxidative stress status and induces oxidation making harmful effects to the numerous biological molecules. Because hemin has a high lipid solubility, it may be a key oxidizing agent to induce core lipoprotein oxidation *in vivo*.

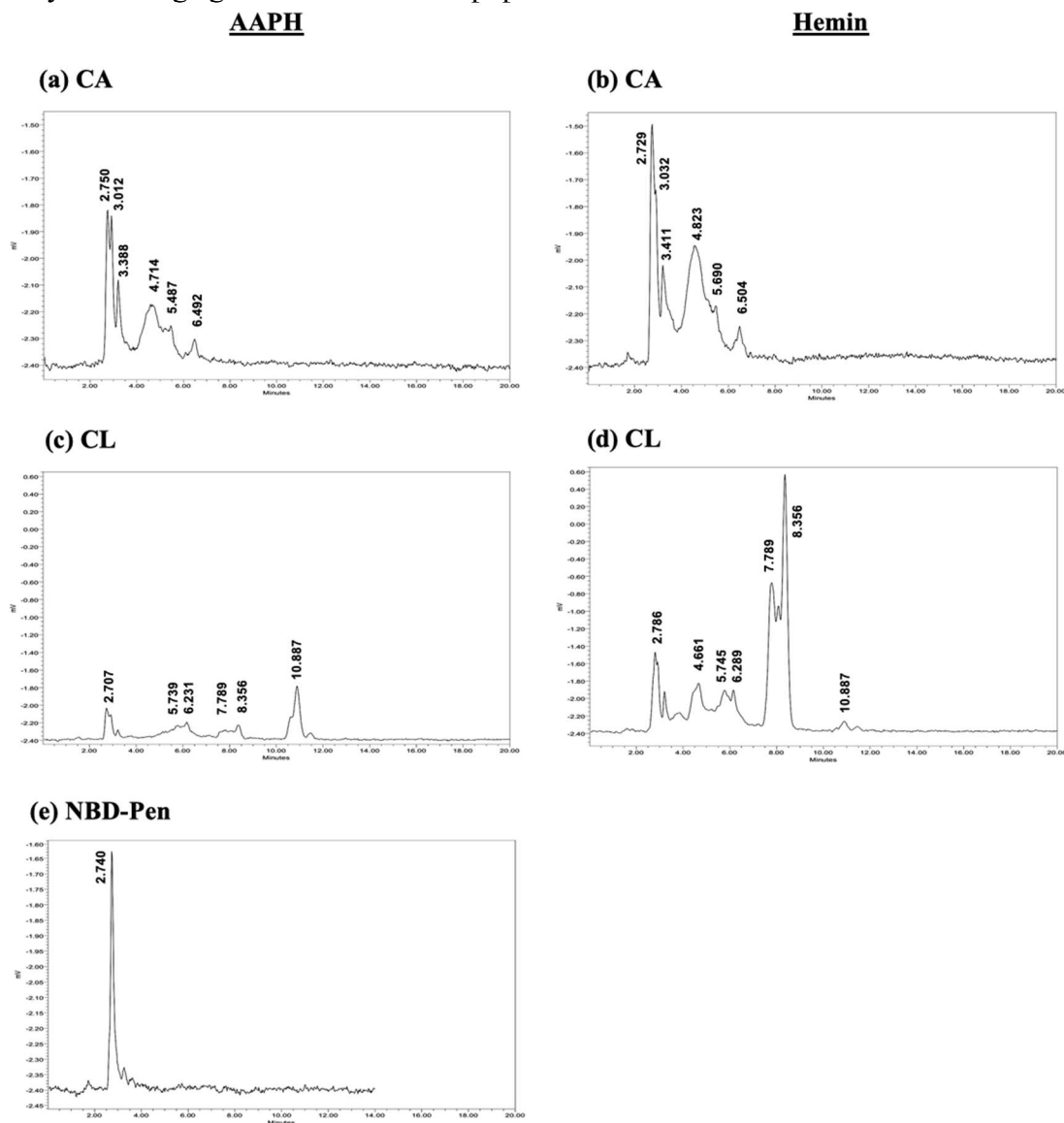


Figure 2. Chromatograms of NBD-Pen- L^{\bullet} adduct monitoring at 470 nm of λ_{ex} and 530 nm of λ_{em} of CA oxidation induced by AAPH (a) and hemin (b); CL oxidation induced by AAPH (c) and hemin (d). Baseline NBD-Pen is shown in (e).

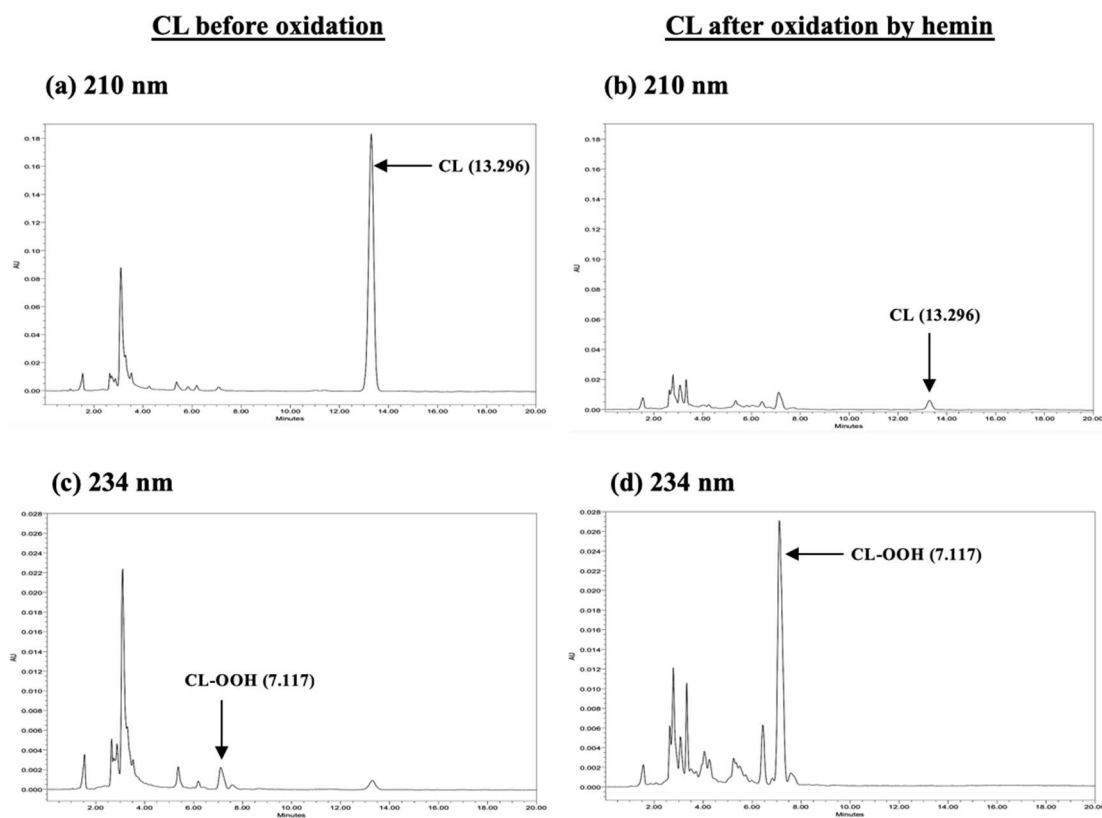


Figure 3. Chromatograms monitoring at 210 and 234 nm of CL before (a, c) and 2 h after oxidation (b, d) by hemin.

Chromatograms of NBD-Pen-L^{*} adduct demonstrated the different L^{*} products from CA and CL oxidation. The L^{*} products were also depended on oxidizing agents. Therefore, identification of L^{*} as well as LOOH produced from various oxidizing agents in pathologic lesion will lead to the understanding of lipid peroxidation mechanism *in vivo*.

Oxidized lipid products have several biological activities; however, there is no direct evidence indicates which oxidized CE involves in the pathogenesis of diseases in human, such as atherosclerosis. Several studies suggested that CE is the major substrate for 12/15-lipoxygenase. The products, especially from CA, can be further oxidized by ROS and become polyoxygenated products with bicyclic endoperoxide and hydroperoxide group (BEP-CE) that plays many roles in inflammation in cardiovascular diseases via toll-like receptor-4 (TLR4)/myeloid differentiation-2 (MD-2) (3).

CA might be susceptible and producing more L^{*} when compared at the same concentration, however, the most abundant CE in plasma and lipoproteins is CL. Thus, CL that might be more affected by oxidizing agents and producing more L^{*} as well as biological effects than CA. One interesting study about LDL and HDL oxidation in β -thalassemia/Hb E demonstrated that the primary target of oxidative modification due to a highly oxidative stress condition for LDL and HDL is CL (4). To support that, another study also indicated 23% of oxidized CL were found in atherosclerotic lesions, followed by 16% of CA (5).

Taken together, CA and CL are suggested to be the 2 important targets of oxidation producing L^{*}. CL might be the main target of oxidation due to its highest percentage of CE composition. While CA might be the main target of oxidation as well, due to its highest susceptibility to the oxidation.

CONCLUSIONS

This study showed that L[•] rapidly produced from CE oxidation and detected by a specific fluorescent probe. Moreover, the results suggested that AAPH and hemin interacted with lipids in different rate and target. CA showed a higher susceptibility to oxidation than CL based on an initial rate of L[•] formation.

CONFLICT OF INTEREST

The authors declare that there is no conflict of interest.

ACKNOWLEDGEMENTS

The authors would like to thank Professor Yamada Ken-Ichi, Department of Chemo-Pharmaceutical Sciences, Faculty of Pharmaceutical Sciences, Kyushu University, Japan for kindly providing NBD-Pen and Science Achievement Scholarship of Thailand (SAST) for in part financial support. The authors also appreciate Miss Jindaporn Janprasit for her technical assistance and Central Instrument Facilities, Faculty of Science, Mahidol University, Thailand for research facilities.

REFERENCES

1. Yamada KI, Mito F, Matsuoka Y, Ide S, Shikimachi K, Fujiki A, Kusakabe D, Ishida Y, Enoki M, Tada A, Ariyoshi M. Fluorescence probes to detect lipid-derived radicals. *Nature chemical biology*. 2016;12(8):608.
2. Kaye FJ, Weinberg RS, Schofield JM, Alter BP. The effect of hemin in vitro and in vivo on human erythroid progenitor cells. *The International Journal of Cell Cloning*. 1986;4(6):432-46.
3. Choi SH, Yin H, Ravandi A, Armando A, Dumlao D, Kim J, Almazan F, Taylor AM, McNamara CA, Tsimikas S, Dennis EA. Polyoxygenated cholesterol ester hydroperoxide activates TLR4 and SYK dependent signaling in macrophages. *PLoS One*. 2013;8(12):e83145.
4. Luechapudiporn R, Morales NP, Fucharoen S, Chantharaksri U. The reduction of cholesteryl linoleate in lipoproteins: an index of clinical severity in β -thalassemia/Hb E. *Clinical Chemistry and Laboratory Medicine (CCLM)*. 2006;44(5):574-81.
5. Hutchins PM, Moore EE, Murphy RC. Electrospray tandem mass spectrometry reveals extensive and non-specific oxidation of cholesterol esters in human peripheral vascular lesions. *Journal of lipid research*. 2011;jlr-M019174.

PH-016

Cytotoxic effects of bixanthenes from lichen on human colorectal cancer cells

Nuttida Maksuksai¹, Warinthorn Chavasiri², Tuong Lam Truong², Piyanuch Wonganan³,
and Wacharee Limpanasithikul³

¹Interdisciplinary Program in Pharmacology, Graduate School, Chulalongkorn University, Bangkok 10330, Thailand.

²Department of Chemistry, Faculty of Science, Chulalongkorn University, Bangkok 10330, Thailand.

³Department of Pharmacology, Faculty of Medicine, Chulalongkorn University, Bangkok 10330, Thailand.

ABSTRACT

INTRODUCTION: Bixanthenes are natural compounds found in plants, fungi and lichens. Many bixanthenes from plants and fungi have been reported to have several pharmacological activities as well as anticancer activities. Novel bixanthenes were isolated from lichen *Usnea aciculifera* with unknown activities.

OBJECTIVES: To evaluate the cytotoxic activities of novel bixanthenes, TT01-TT08, from *U. aciculifera* against human colorectal cancer HT-29 cells.

METHODS: Human colorectal cancer HT-29 cells were treated with various concentrations of bixanthenes TT01-TT08. Viability of the treated cells were determined by MTT assay. Normal human cells were also used to determining cytotoxic activities of some bixanthenes with potential antitumor agents for evaluating their selectivity against cancer cells.

RESULTS: All bixanthenes decreased viability of HT-29 cells with different degree. The three potent bixanthenes were TT-03, TT-05, and TT-08 with their IC₅₀ values at 2.41± 0.19 μM, 16.17± 2.14 μM and 3.49± 0.12 μM respectively. These bixanthenes were also determined their cytotoxic activities against human normal cells. TT-08 demonstrated the highest selectivity against HT-29 cells. TT-08 was chosen for further study. TT-08 at 1.25-20 μM had cytotoxic effect on HT-29 cells in a concentration and time dependent manner. Its IC₅₀ value were 3.87± 0.13 μM, 2.05 ± 0.06 μM, 1.51± 0.11 μM at 24, 48 and 72h, respectively.

CONCLUSIONS: The results from this study revealed cytotoxic activities of novel bixanthenes from *U. aciculifera* against human colorectal cancer cells. Bixanthone TT-08 demonstrated a good candidate anticancer agent with low IC₅₀ value and toxic to cancer cell higher than to normal cells. Further study are needed to evaluate its anticancer potential at cellular and molecular levels.

Keywords: Bixanthenes, colorectal cancer cells, lichen

INTRODUCTION

Bixanthenes are natural compounds found in plants, fungi and lichens. Their core structures are xanthone dimers composed of two xanthenes with a variety of linkages.¹ Previous studies demonstrated several pharmacological activities of bixanthenes including antimicrobial²⁻⁷, antioxidant⁸⁻¹⁰ and anticancer activities.^{11, 12} Bixanthenes from several plants and fungi demonstrated anticancer activities against many cancer cells such as breast cancer, colon cancer, lung cancer, liver cancer, prostatic cancer and esophageal cancer.^{13,14} However, anticancer activities of bixanthenes from lichen have not been reported. Eight novel

bixanthonones were isolated from lichen *Usnea aciculifera* with unknown pharmacological activities.

Colorectal cancer (CRC) is the third most common cancer worldwide.¹⁵ Treatment of CRC is basically based on the stage of the cancer. Treatment options for CRC include surgery, radiation, chemotherapy and targeted therapy.¹⁶ 5-fluorouracil (5-FU) based chemotherapy has been widely used for CRC. Major problems of CRC chemotherapy are common side effects on normal dividing cells of the drugs in combined therapy as well as drug resistance of the cancer cells which leads to the treatment failure.^{15, 16} Development of novel anticancer agents to improve CRC treatments are needed. Development of novel anticancer agents from high technology as well as from nature are still needed. This study aimed to evaluate potential anticancer activities of novel bixanthonones from *U. aciculifera* against human colorectal cancer HT-29 cells.

METHODS

Cells: Human colorectal cancer cells (HT-29) and human normal cells (PCS201-010) were obtained from ATCC (Rockville, MD, USA). HT-29 cells were maintained in complete Dulbecco's Modified Eagle's Medium (DMEM) containing 10% v/v fetal bovine serum (Gibco, USA), 100 units/ml penicillin and 0.1 mg/mL streptomycin (Gibco, USA) at 37 °C in a humidified atmosphere in 5% CO₂. PCS201-010 cells were maintained in complete DMEM with high glucose.

Bixanthonones from *U. aciculifera*: Eight bixanthonones TT01-TT08 were isolated from *U. aciculifera*. These bixanthonones were dissolved in dimethyl sulfoxide (DMSO) as the stock solutions. The stock solutions were diluted with complete DMEM to required final concentrations in constant 0.2% DMSO. The maximum final concentration of these bixanthonones used in this study was 30 µM.

Study cytotoxic effects of bixanthonones by MTT assay

Human colorectal cancer HT-29 cells at the density of 5×10^4 cells/ml in 96-well plate were treated with various concentrations of bixanthonones TT01-TT08 for optimal time. Viability of the treated cells was determined by adding thiazolylblue tetrazoliumbromide (MTT) solution (Sigma, USA) to each well, incubating for 4 h, removing the supernatants, dissolving the formazan product in DMSO, and measuring the dissolved product at 570 nm using a microplate reader. The percentage of cytotoxicity of these bixanthonones and their IC₅₀ values were determined.

Effects of some bixanthonones with potential anticancer activities on viability of normal PCS201-010 cells were also determined by MTT assay. The degree of selective toxicity towards cancer cells was also evaluated as selective index (SI) values (SI= IC₅₀ normal cells/ IC₅₀ cancer cells).

Study apoptotic induction effect of TT-08

HT-29 cells at 5×10^4 cells/ml in 6-well plate were treated with TT-08 at 1.25, 2.5 and 5 µM for 24 h. The treated cells were stained with annexin V-FITC and propidium iodide (PI) (Santa Cruz Biotechnology, USA) and detected with flow cytometer. 5-FU at 100 µM was used as the positive control. The patterns of the treated cells were evaluated as follow; viable cells were annexin V-FITC-/PI- cells, early apoptotic cells were annexin V-FITC+/PI- cells, necrotic cells were annexin V-FITC/PI+ cells, and late apoptotic cells were annexin V-FITC+/PI+ cells.

All experiments were performed in triplication with n=3. Data were presented as mean ± standard error of mean (S.E.). Statistical comparisons were made by one-way ANOVA followed by Tukey's post hoc test. All statistical analysis was performed according to the statistic program, SPSS version 22.0. Any *p*-value < 0.05 was considered statistically significant.

RESULTS

Cytotoxic effects of bixanthones on cancer and normal cells

All eight bixanthones decreased viability of HT-29 colorectal cancer cells with different IC_{50} values. Two bixanthones demonstrated potent cytotoxic effect. They are TT-03 and TT-08 with their IC_{50} values at $2.41 \pm 0.19 \mu\text{M}$ and $3.49 \pm 0.12 \mu\text{M}$ respectively (Table1). Cytotoxic effects of these two bixanthones against normal cells were also determined for their selectivity towards cancer cells. The results showed that TT-03 and TT-08 had cytotoxic effects on PCS201-010 normal cells with IC_{50} values at $3.78 \pm 0.25 \mu\text{M}$ and $7.29 \pm 0.78 \mu\text{M}$, respectively (Table2). TT-08 demonstrated the higher selectivity against HT-29 cells than TT-03. The SI values were TT-03 and TT-08 were 1.56 and 2.08, respectively. TT-08 was chosen for further study.

Table 1. IC_{50} values of bixanthones TT01-TT08 from *U. aciculifera* on HT-29 cells

Bixanthones	IC_{50} (μM)
TT-01	> 30
TT-02	> 30
TT-03	2.41 ± 0.19
TT-04	> 30
TT-05	16.17 ± 2.14
TT-06	> 30
TT-07	> 10
TT-08	3.49 ± 0.12

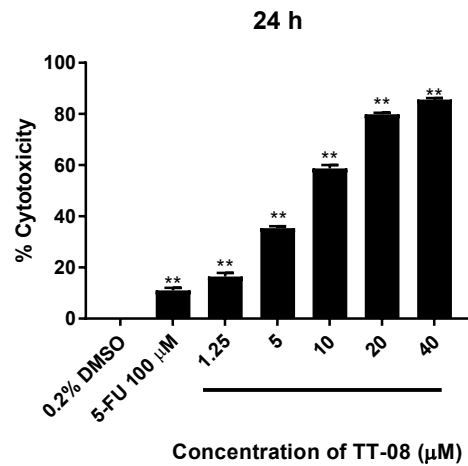
Table 2. Cytotoxic activities of TT-03 and TT-08 on colorectal HT-29 cancer cells and PCS201-010 normal cells and their SI values.

Bixanthones	HT-29 cells IC_{50} (μM)	PCS201-010 cells IC_{50} (μM)	SI value
TT-03	2.41 ± 0.19	3.78 ± 0.25	1.56
TT-08	3.49 ± 0.12	7.29 ± 0.78	2.08

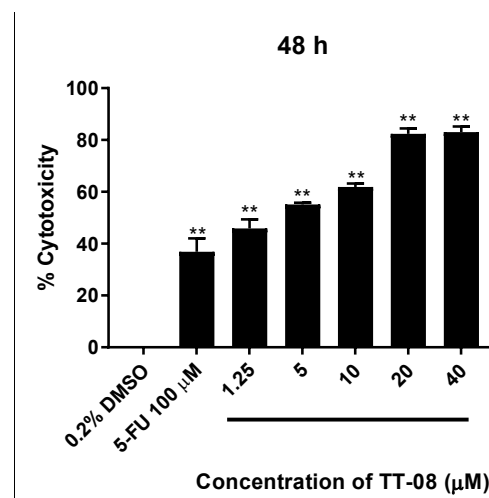
Cytotoxic activity of bixanthones TT-08 in human colorectal cancer cell at 24, 48 and 72 h

Cytotoxic effect of TT-08 at 1.25-20 μM against HT-29 cells was determined after 24, 48 and 72 h of exposure. 5-fluorouracil (5-FU) was used as the positive controls. The resulted showed that TT-08 at 1.25-20 μM had cytotoxic effect on HT-29 cells in a concentration and time dependent manner. Its IC_{50} values were $3.87 \pm 0.13 \mu\text{M}$, $2.05 \pm 0.06 \mu\text{M}$, $1.51 \pm 0.11 \mu\text{M}$ at 24, 48 and 72h, respectively (Figure 1: A-C).

A



B



C

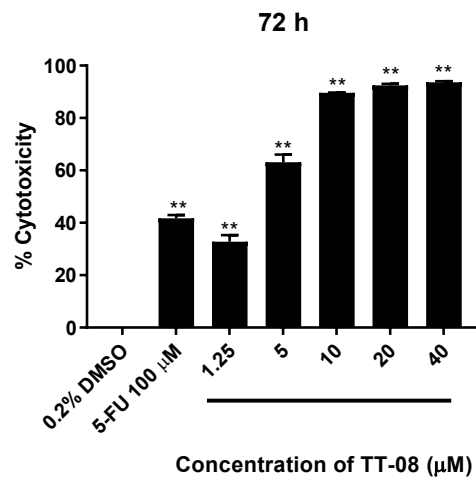


Figure 1. Cytotoxic effects of bixanthone TT-08 against HT-29 cells. The cells were treated with TT-08 at 1.25-20 μM for 24 (A), 48 (B), and 72 (C) h. The cytotoxic effects were determined by MTT assay. The data represent the mean \pm SEM of three independent experiments. ** $p < 0.001$ when compared to the solvent control (0.2% DMSO).

The apoptotic induction effect of TT-08 on human colorectal cancer cells

The apoptotic effect of TT-08 at 1.25-5 μM in HT-29 cells was determined after 24 h of exposure. TT-08 induced apoptotic cell death, both early and late apoptosis, in a concentration manner (Figure 2: A-B). The compound at 2.5 and 5 μM significantly increased apoptotic cell death when compared to the solvent control. The percentage of apoptotic cell death of TT-08 at these concentrations were $20.56 \pm 2.70\%$ and $54.23 \pm 0.91\%$, respectively.

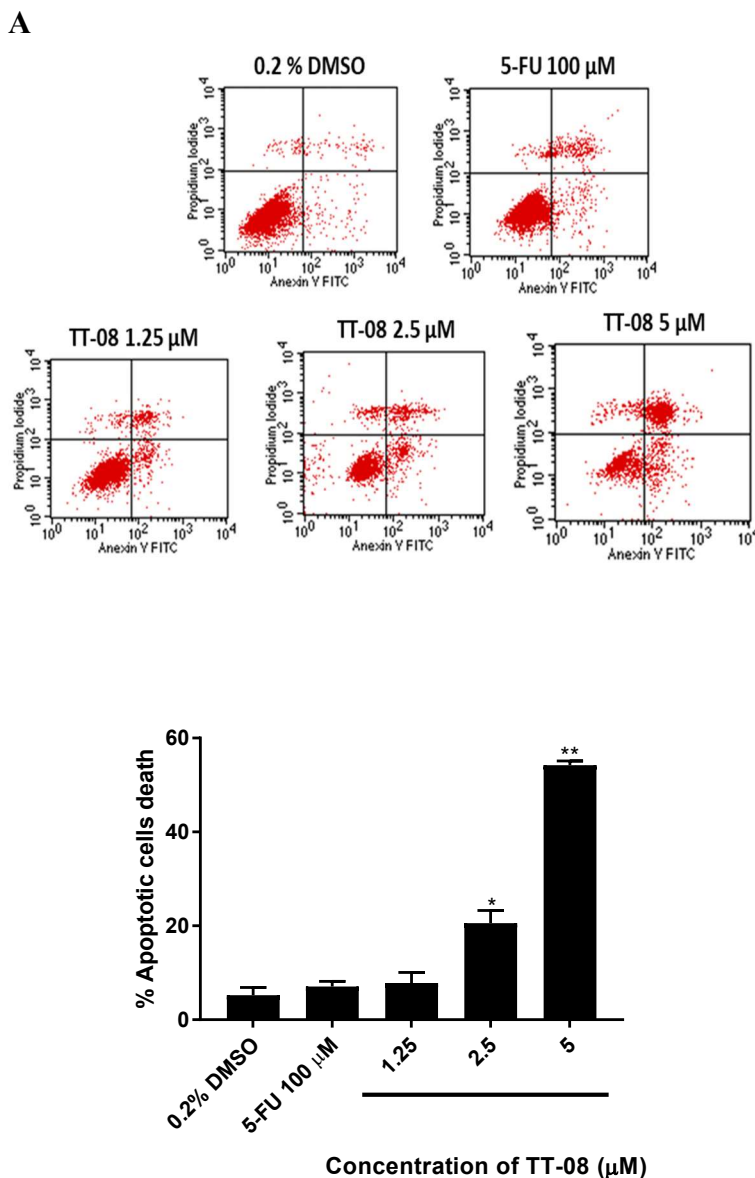


Figure 2. The apoptotic effect of TT-08 on HT-29 cells. The cells were treated with 1.25-5 μM of TT-08 for 24 h. The death patterns of the treated cells were determined by annexin V-FITC/PI staining using flow cytometer, (A) Representative cytograms of cell death patterns of one experiment. (B) The percentage of early and late apoptotic cells of the treated cells. The data represent the mean \pm SEM of three independent experiments. * $p < 0.01$, ** $p < 0.001$ when compare to the solvent control (0.2% DMSO).

DISCUSSION

Bixanthenes is a group of natural compounds that have many pharmacological activities as well as anticancer activities of several bixanthenes from plants and fungi.²⁻¹² Plant bixanthenes, griffipavixanthone and cratoxyxanthone, had anticancer activities against

leukemic, lung cancer, breast cancer, prostatic cancer and esophageal cancer with no cytotoxicity to normal kidney epidermal cells.^{11,12} Griffipavixanthone induced apoptosis in non-small-cell lung cancer (NSCLC) cells in a dose-dependent manner via mitochondrial-dependent pathway.¹⁴ Fungal bixanthenes, dicerandrols (dicerandrols A, B, C) and preanaxanthone A, demonstrated anticancer effects against human breast cancer, colon cancer, lung cancer, liver cancer. Phomoxanthone A caused DNA fragmentation and induced apoptosis in murine lymphoma cells.^{17,18} None of bixanthenes from lichen was reported to have anticancer effects. Since novel of bixanthenes were isolated from lichen *Usnea aciculifera* with unknown activities, their anticancer effect was the most interest in this study. We first revealed that some bixanthenes from *U. aciculifera* demonstrated potential anticancer effects against colorectal cancer HT-29 cells. TT-03 and TT-08 had potent cytotoxic effect on the cancer cells with low IC₅₀ values. TT-08 demonstrated higher cytotoxic selectivity towards cancer cells with SI \geq 2. It decreased HT-29 cell viability in a concentration-dependent and time dependent manners. It also induced HT-29 cell death mainly via apoptosis in a concentration dependent manner.

CONCLUSIONS

The results from this study first revealed that bixanthenes from lichen have anticancer activities against colorectal cancer cells. TT-08 from *U. aciculifera* had potent anticancer effect with high selective index. It caused cell death mainly by apoptosis. It may be a candidate anticancer agent for treatment CRC. In depth investigation are needed to reveal this potential both in vitro and in vivo.

CONFLICT OF INTEREST

The authors declare no conflicts of interest.

REFERENCES

1. Wezeman T, Brase S, Masters KS. Xanthone dimers: a compound family which is both common and privileged. *Natural Product Reports* 2015; 32(1):6-28.
2. Lim C, Kim J, Choi JN, Ponnusamy K, Jeon Y, Kim SU, et al. Identification, fermentation, and bioactivity against *Xanthomonas oryzae* of antimicrobial metabolites isolated from *Phomopsis longicolla* S1B4. *Journal of Microbiology and Biotechnology* 2010; 20(3):494-500.
3. Mbwambo ZH, Kapingu MC, Moshi MJ, Machumi F, Apers S, Cos P, et al. Antiparasitic activity of some xanthenes and biflavonoids from the root bark of *Garcinia livingstonei*. *Journal of Natural Products* 2006; 69(3):369-72.
4. Stewart M, Capon RJ, White JM, Lacey E, Tennant S, Gill JH, et al. Rugulotrosins A and B: Two new antibacterial metabolites from an Australian isolate of a *Penicillium* sp. *Journal of Natural Products* 2004; 67(4):728-30.
5. Ondeyka JG, Dombrowski AW, Polishook JP, Felcetto T, Shoop WL, Guan Z, et al. Isolation and insecticidal/anthelmintic activity of xanthanol, a novel bis-xanthone, from a non-sporulating fungal species. *The Journal of Antibiotics* 2006; 59 (5): 288-92.
6. Schuffler A, Liermann JC, Kolshorn H, Opatz T, Anke H. Isolation, structure elucidation, and biological evaluation of the unusual heterodimer chrysoxanthone from the ascomycete IBWF1195A. *Tetrahedron Letters* 2009; 50(34):4813-5.
7. Shim SH, Baltrusaitis J, Gloer JB, Wicklow DT. Phomalevones A-C: dimeric and pseudodimeric polyketides from a fungicolous Hawaiian isolate of *Phoma* sp. (Cucurbitariaceae). *Journal of Natural Products* 2011; 74(3):395-401.

8. Chen Y, Fan H, Yang GZ, Jiang Y, Zhong FF, He HW. Prenylated xanthenes from the bark of *Garcinia xanthochymus* and their 1, 1-diphenyl-2-picrylhydrazyl (DPPH) radical scavenging activities. *Molecules* 2010; 15(10):7438-49.
9. Chen Y, Fan H, Yang GZ, Jiang Y, Zhong FF, He HW. Two unusual xanthenes from the bark of *Garcinia xanthochymus*. *Helvetica Chimica Acta* 2011; 94(4):662-668.
10. Xu YJ, Cao SG, Wu XH, Lai YH, Tan BHK, Pereira JT, et al. Griffipavixanthone, a novel cytotoxic bixanthone from *Garcinia griffithii* and *G. pavifolia*. *Tetrahedron Letters* 1998; 39(49):9103-6.
11. Ding Z, Lao Y, Zhang H, Fu W, Zhu L, Tan H, et al. Griffipavixanthone, a dimeric xanthone extracted from edible plants, inhibits tumor metastasis and proliferation via downregulation of the RAF pathway in esophageal cancer. *Oncotarget* 2016; 7(2):1826-37.
12. Han AR, Kim JA, Lantvit DD, Kardono LB, Riswan S, Chai H, et al. Cytotoxic xanthone constituents of the stem bark of *Garcinia mangostana* (mangosteen). *Journal of Natural Products* 2009; 72(11):2028-31.
13. Cao S, McMillin DW, Tamayo G, Delmore J, Mitsiades CS, Clardy J. Inhibition of tumor cells interacting with stromal cells by xanthenes isolated from a Costa Rican *Penicillium* sp. *Journal of Natural Products* 2012; 75(4):793-7.
14. Shi JM, Huang HJ, Qiu SX, Feng SX, Li XE. Griffipavixanthone from *Garcinia oblongifolia* champ induces cell apoptosis in human non-small-cell lung cancer H520 cells in vitro. *Molecules* 2014; 19(2):1422-31.
15. American Cancer Society. *Colorectal Cancer Facts & Figures 2017-2019*. Atlanta: American Cancer Society, 2017.
16. Shead DA, Hanisch LJ, Clarke R, Corrigan A. Colon cancer, version 1.2017, NCCN Guidelines for Patients. Washington: National Comprehensive Cancer Network, 2017.
17. Ding B, Yuan J, Huang X, Wen W, Zhu X, Liu Y, et al. New dimeric members of the phomoxanthone family: phomolactonexanthenes A, B and deacetylphomoxanthone C isolated from the fungus *Phomopsis* sp. *Marine drugs* 2013; 11(12):4961-72.
18. Ronsberg D, Debbab A, Mandi A, Vasylyeva V, Bohler P, Stork B, et al. Pro-apoptotic and immunostimulatory tetrahydroxanthone dimers from the endophytic fungus *Phomopsis longicolla*. *The Journal of Organic Chemistry* 2013; 78(24):12409-25.

PH-017

Cytotoxicity of mansonone G and ethoxy mansonone G from *Mansonia gagei* Drumm in non-small cell lung cancer

Arachawipa Wannachote¹, Wacharee Limpanasithikul², Warinthorn Chavasiri³
and Piyanuch Wonganan^{2*}

¹ *Interdisciplinary Program in Pharmacology, Graduate School, Chulalongkorn University, Bangkok 10330, Thailand.*

² *Department of Pharmacology, Faculty of Medicine, Chulalongkorn University, Bangkok 10330, Thailand.*

³ *Department of Chemistry, Faculty of Science, Chulalongkorn University, Bangkok 10330, Thailand.*

* *E-mail: Piyanuch.W@chula.ac.th*

ABSTRACT

INTRODUCTION: Mansonones are naphthoquinone-containing compounds extracted from the heartwood of *Mansonia gagei*. Several studies reported that mansonones have various pharmacological activities such as antibacterial, antifungal, antioxidant, antiestrogenic, antiadipogenic and antitumor. Previous study reported that ether analogues of mansonone G (MG), a major compound isolated from *Mansonia gagei* Drumm, displayed higher antibacterial activity than parent MG.

OBJECTIVES: This study aimed to investigate the cytotoxicity of MG and ethoxy MG (EMG) and the underlying mechanism(s) in non-small cell lung cancer (NSCLC).

METHODS: The cytotoxicity of MG and EMG was evaluated by MTT assay. The apoptotic and ROS generating effects of EMG were determined by flow cytometry analysis and DCFH-DA assay, respectively.

RESULTS: Our results demonstrated that MG and EMG significantly inhibited the growth of A549 NSCLC cell line with IC₅₀ values of 20.88 ± 0.44 and 9.49 ± 0.58 μM, respectively. Notably, EMG was more toxic to A549 cancer cells than PCS201-010 normal cells. EMG at 10 and 20 μM significantly induced early apoptosis cell death by 12.24 ± 5.4% and 58.2 ± 6.9%, respectively. EMG also significantly increased reactive oxygen species (ROS) level in A549 cells. Remarkably, N-acetylcysteine could significantly prevent EMG-induced cell death following treatment with EMG at 5, 10 and 20 μM by 1.2, 1.2 and 2.2 folds, respectively.

CONCLUSIONS: The results of this study demonstrated that the cytotoxicity of EMG involves induction of apoptosis and generation of ROS in A549 cell. These results suggest that EMG is a promising anticancer agent for lung cancer.

Keywords: *Mansonia gagei* Drumm, ethoxy mansonone G, lung cancer, cytotoxicity

INTRODUCTION

Lung cancer is the leading cause of cancer deaths worldwide (1). Non-small cell lung cancer (NSCLC) is the most common form of lung cancer, accounting for approximately 85% of all cases (2). The National Cancer Institute of Thailand reported that lung cancer is the fourth most commonly diagnosed cancer in Thais after breast cancer, liver cancer, and colorectal

cancer, respectively (3). Treatment options for lung cancer include surgery, radiotherapy, chemotherapy, and targeted therapy (4). Although chemotherapeutic agents such as cisplatin, gemcitabine and paclitaxel have been commonly used to treat lung cancer patients, serious side effects often limit their clinical application. Therefore, new compounds with high anticancer activity and low toxicity are critically needed.

Mansonones are naphthoquinone-containing compounds extracted from the heartwood of *Mansonia gagei* (5). Several studies reported that mansonones have various pharmacological activities such as antibacterial, antifungal, antioxidant, antiestrogenic, antiadipogenic and antitumor (6-9). Previous study reported that ether analogues of mansonone G (MG), a major compound isolated from *Mansonia gagei* Drumm, displayed antibacterial activity higher than parent MG (5). In the present study, we therefore determined cytotoxic activity of MG and ethoxy MG (EMG) and the underlying mechanism(s) in NSCLCs.

METHODS

Preparation of test compound stock solutions

MG was isolated from the heartwood of *M.gagei* by repeatedly soaking in CH₂Cl₂. Then, the crude CH₂Cl₂ extract was fractionated with EtOAc in hexane. Fractions were further separated using silica gel column and MG was structurally identified by spectroscopy. EMG was synthesized by incubating MG with K₂CO₃ and subsequently with aliphatic alkyl halides for 5-8 h. The reaction mixture was then extracted with EtOAc three times, dried over anhydrous Na₂SO₄. After filtration and evaporation, the residue was purified by a silica gel column using hexane:EtOAc and hexane:CH₂Cl₂:EtOAc. EMG was structurally validated by ¹H nuclear magnetic resonance (NMR), ¹³C NMR, and high-resolution mass spectroscopy (HRMS) analyses (6).

Stock solutions of MG, EMG and cisplatin were prepared in dimethyl sulfoxide (DMSO) at 50 mM and stored at 4°C until use. In the experiments, the stock solution was diluted in culture medium to give appropriate final concentrations. The 0.2% DMSO was used as a vehicle control.

Cell culture

A human lung adenocarcinoma (A549) cell line was from American Type Culture Collection (ATCC, USA) and normal human primary dermal fibroblasts (PCS201-010) was kindly provided by Ms. Nalinee Pradubyat from College of Pharmacy, Rangsit University. A549 cells were maintained in Dulbecco's modified Eagle's medium (DMEM) supplemented with 10% fetal bovine serum (FBS) and 100 units/mL penicillin and 100 µg/mL streptomycin. PCS201-010 cells were maintained in DMEM with high glucose supplemented with 10% FBS and 100 units/mL penicillin and 100 µg/mL streptomycin. The cells were maintained in 5% CO₂ humidified at 37°C.

Cytotoxicity assay

The cytotoxic effects of MG and EMG were determined by methyl thiazolyl tetrazolium (MTT) assay. Briefly, A549 cells and PCS201-101 cells were seeded in a 96-well plate at a density 2.5x10⁴ cells/mL and incubated overnight at 37°C and 5% CO₂. Cells were then treated with 2.5, 5, 10, 20 or 40 µM of MG, EMG or cisplatin (positive control) or 0.2% DMSO (vehicle control) for 48 h. After treatment, 15 µL of MTT (5 mg/mL) was added in each well and incubated at 37°C for 4 h. The formazan crystals created after incubation were dissolved in DMSO. Absorbances of obtained colored solutions were measured at 570 nm using a microplate reader (Thermo, Finland). The selective index (SI) which indicates the cytotoxic selectivity of a test compound against cancer cells was calculated from the IC₅₀ of the test compound in normal cells versus cancer cells.

Apoptosis assay

A549 cells were seeded in a 6-well plate at a density 2.5×10^4 cells/mL and incubated overnight at 37°C and 5% CO_2 . Then, the cells were treated with different concentrations of EMG for 24 h. Subsequently, cells were washed twice with cold PBS, harvested by trypsinization and centrifuged for 5 min. The cell pellets were re-suspended with 500 μL of assay buffer and stained with 1 μL of propidium iodide (BD Pharmingen™, USA) and 1 μL Annexin-V fluorescein dye (Invitrogen, USA) at room temperature in the dark for 15 min. The percentage of apoptotic cells were quantitatively measured using flow cytometer (BD LSR II, Biosciences).

ROS generation detection assay

Effect of EMG on ROS generation were determined by DCFH-DA assay. Briefly, A549 cells were seeded in a 96-well plate at a density 2.5×10^4 cells/mL and incubated overnight at 37°C and 5% CO_2 . Then, the cells were incubated with 100 μL of 10 μM DCFH-DA (Sigma, USA) in Hank's buffered salt solution (Sigma, USA) at 37°C for 30 min in dark. After incubation, the cells were removed and washed with PBS. Subsequently, cells were treated with different concentrations of EMG or 200 μM of H_2O_2 (positive control) for 1 h. After treatment, the cells were washed twice with cold PBS and 200 μL of 1% triton-X in 0.3 M NaOH was added. The levels of ROS were analysed by measuring the DCF fluorescence intensity at an excitation wavelength of 502 nm and an emission wavelength of 523 nm (Thermo, Finland).

Statistical analysis

Data are presented as mean \pm standard error of mean (SEM) from three independent experiments performed in triplicate. Statistical analysis was performed by one-way analysis of variance (ANOVA) followed by LSD using SPSS software program. Difference is considered significant if P value < 0.05 .

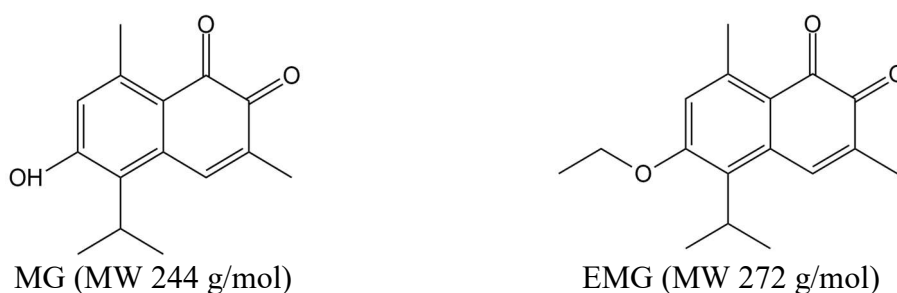


Figure 1. Structures of MG and EMG

RESULTS

Cytotoxicity of MG and EMG on A549 cells

As shown in Figure 2. MG, EMG and cisplatin significantly inhibited the growth of A549 cells with IC_{50} values of 20.88 ± 0.44 , 9.49 ± 0.58 and 12.70 ± 0.61 μM , respectively. MG, EMG and cisplatin also significantly inhibited the growth of PCS201-010 cells with IC_{50} values of 27.59 ± 1.99 , 26.19 ± 1.31 and 28.66 ± 2.15 μM , respectively. It however should be noted that EMG displayed the most potent cytotoxicity toward A549 cells, compared to MG and cisplatin. Moreover, we found that normal cells were more sensitive to MG and cisplatin than EMG. (Table 1)

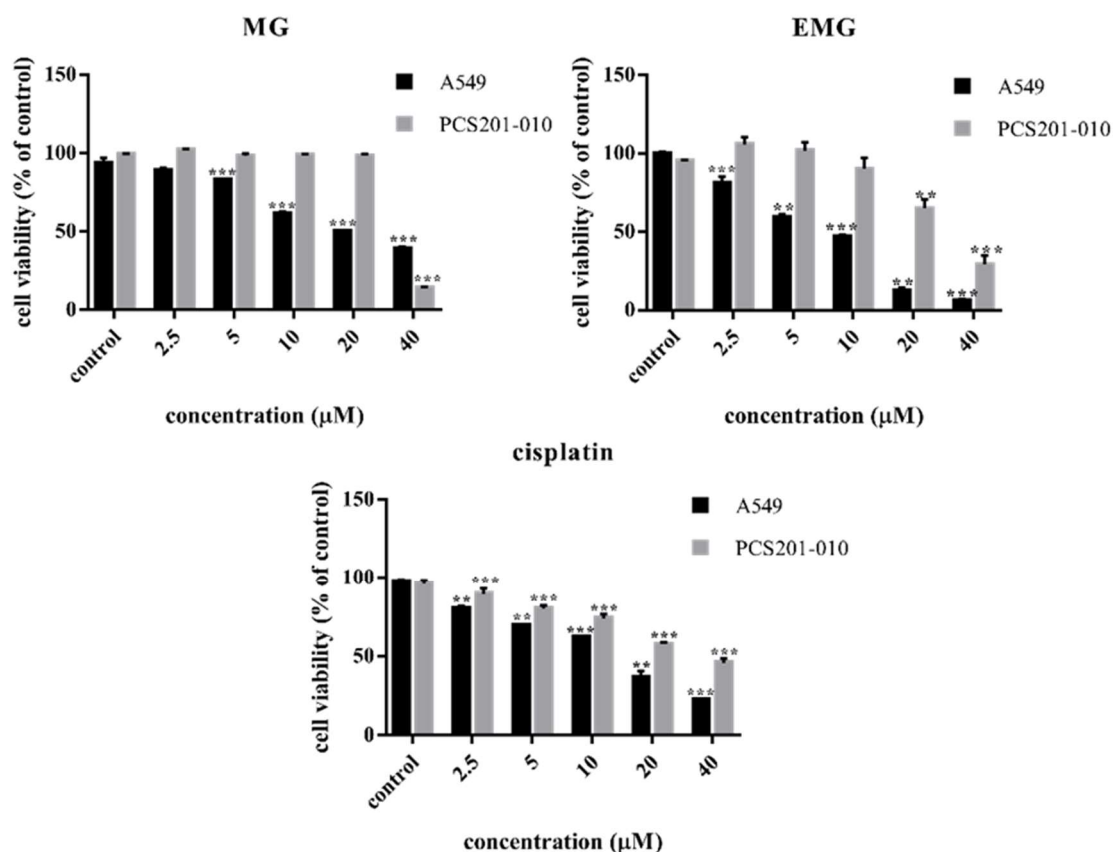


Figure 2. Effect of MG, EMG and cisplatin on viability of A549 and PCS201-010 cells. The cells were treated with MG, EMG or cisplatin at 2.5, 5, 10, 20 or 40 μM for 48 h. Cell viability was evaluated using MTT assay. Data are presented as mean ± SEM. (n=3). **P < 0.01, ***P < 0.001 compared with vehicle control (0.2% DMSO).

Table 1. IC₅₀ and selectivity index values of MG, EMG and cisplatin on A549 and PCS201-010 cells

Compound	IC ₅₀ (μM)		SI Index
	A549	PCS201-010	
MG	20.88 ± 0.44	27.59 ± 1.99	1.32
EMG	9.49 ± 0.58	26.19 ± 1.31	2.76
Cisplatin	12.70 ± 0.61	28.66 ± 2.15	2.26

Apoptosis induction and ROS generation in A549 cells by EMG

Apoptosis-inducing effects of EMG was evaluated by flow cytometry after annexin-V/PI staining. As shown in Figure 3, EMG induced A549 cells to undergo apoptosis. Treatment of A549 cells with EMG at 10 and 20 μM significantly increased early apoptosis cell death by 12.24 ± 5.4% and 58.2 ± 6.9%, respectively. Moreover, EMG at 20 μM and H₂O₂ at 200 μM also significantly increased the level of ROS from 100% to approximately 165% and 175%, respectively. We then determined whether EMG-induced A549 cell death is mediated through increased ROS production. As shown in Figure 4, EMG-induced cell death was significantly attenuated by pretreatment with 5 mM N-acetylcysteine (NAC), a free radical scavenger. NAC could significantly prevent EMG-induced cell death following treatment with EMG at 5, 10 and 20 μM by 1.2, 1.2 and 2.2 folds, respectively. These results suggest that EMG-induced cell death in A549 cells is partly mediated through increased ROS production.

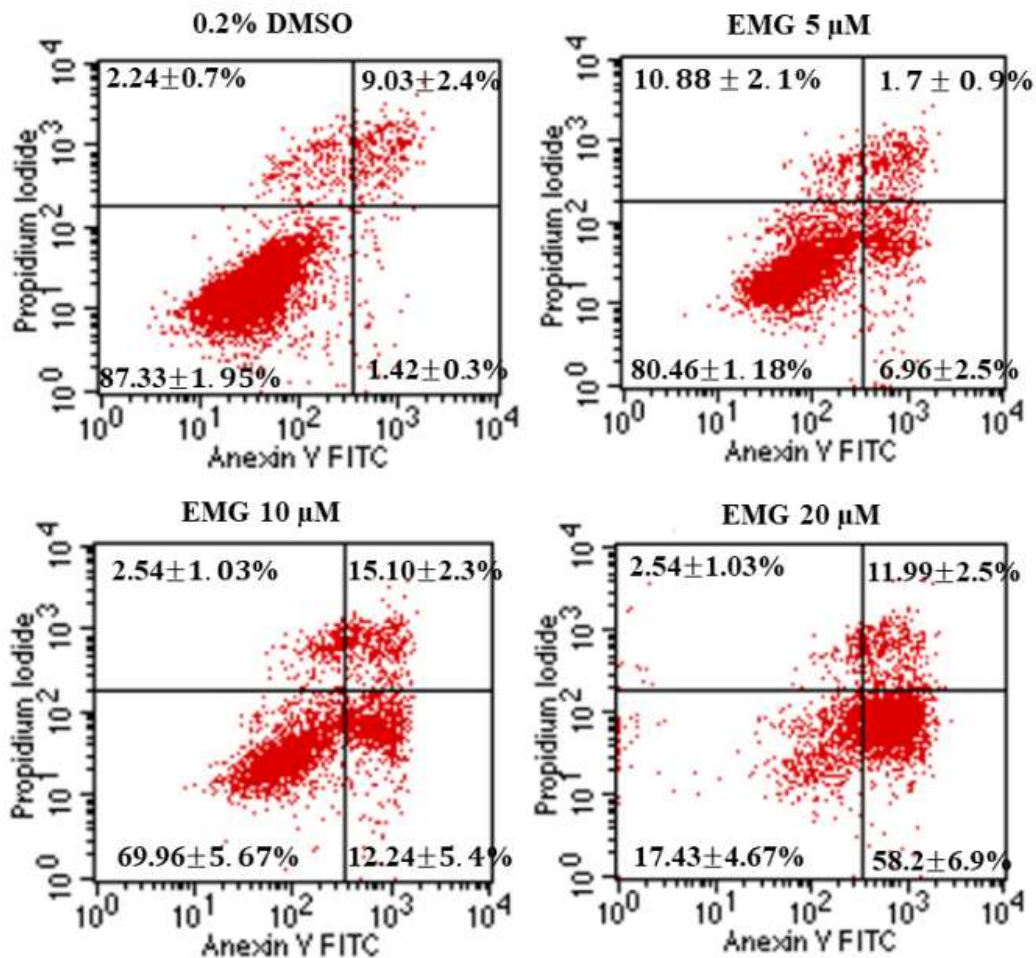


Figure 3. Apoptosis-inducing effects of EMG on A549 cells. Representative cytograms of apoptosis in A549 cells after treatment with EMG 5, 10, 20 μM for 24 h. Data are presented as mean \pm SEM (n=3).

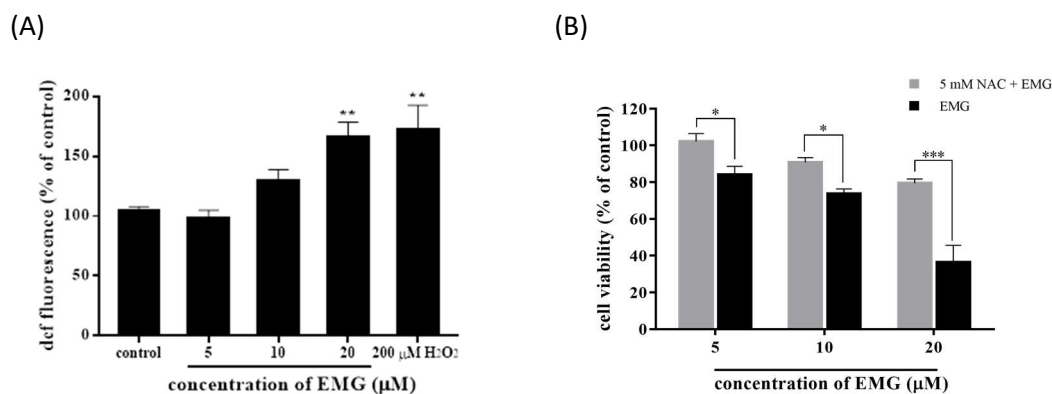


Figure 4. Effect of EMG on ROS generation in A549 cells. (A) The cells were treated with EMG at 5, 10, 20 μM or H₂O₂ at 200 μM for 1 h. The levels of ROS were determined by measuring the DCF fluorescence intensity using a fluorescence microplate reader. Data are presented as mean \pm SEM. (n=3). **P<0.01 compared with vehicle control (0.2% DMSO). (B) The cells were treated with EMG at various concentrations for 24 h, in the presence or absence of 5 mM NAC. The percentages of cell viability were evaluated using MTT assay. Data are presented as mean \pm SEM (n=3). *P<0.05 and ***P<0.001 compare with EMG-treated cells.

DISCUSSION

Previous studies reported that mansonones, naphthoquinone-containing compounds, isolated from the dichloromethane extract of *Mansonia gagei* Drumm, have shown several pharmacological activities such as anti-bacterial, anti-fungal, anti-estrogenic, anti-adipogenic and anti-cancer (5-9). The present study found that both MG and EMG exhibited cytotoxicity against A549 NSCLC cells. Remarkably, A549 cells were more sensitive to cytotoxicity of EMG than MG. Previously, it was reported that increasing alkyl chain length on ether analogues of MG, made the compounds more hydrophobic which could facilitate the access of compounds to bacterial cells (5). Thus, it is likely that higher hydrophobicity of EMG than MG resulted in higher cytotoxicity of EMG than MG on A549 cells. Though ROS are considered to be essential for regulation of normal physiological functions such as cell proliferation, migration and cell death, excess cellular levels of ROS can cause damage to proteins, nucleic acids, lipids, membranes and organelles, leading to apoptotic cell death (10). In the present study, we found that EMG significantly increased ROS level in A549 cells and the cytotoxicity of EMG was significantly abolished by NAC, indicating that cytotoxicity of EMG is mediated through ROS generation. Previous studies demonstrated that juglone (5-hydroxy-1,4-naphthoquinone) induces apoptosis through ROS generation in human leukemia HL-60 cell (11). Thus, it is likely that ROS are involved in EMG-induced apoptosis in A549 cells. However, this speculation needs to be further investigated.

CONCLUSION

The results of this study demonstrated that the cytotoxicity of EMG is mediated through induction of apoptosis and generation of ROS in A549 cell. These results suggest that EMG is a promising anticancer agent for lung cancer.

ACKNOWLEDGEMENTS

We thank Asst. Prof. Dr. Warinthorn Chavasiri from Department of Chemistry, Faculty of Science, Chulalongkorn University for kindly providing mansonone G and ethoxy mansonone G.

We thank Ms. Nalinee Pradubyat from College of Pharmacy, Rangsit University for kindly providing normal human primary dermal fibroblasts (PCS201-010).

CONFLICT OF INTEREST

The authors declare no conflicts of interest.

REFERENCES

1. Bray F, *et al.* Global cancer statistics 2018: GLOBOCAN estimates of incidence and mortality worldwide for 36 cancers in 185 countries. *CA Cancer J Clin.* 2018;68(6):394-424.
2. Ohnuma T, *et al.* Enhanced sensitivity of A549 cells to the cytotoxic action of anticancer drugs via suppression of Nrf2 by procyanidins from Cinnamomi Cortex extract. *Biochem Biophys Res Commun.* 2011;413(4):623-9.
3. Imsamran W, *et al.* Hospital-based cancer registry annual report 2017. *J Natl Cancer Inst.* 2018;32:1-94.
4. Lemjabbar-Alaoui H, *et al.* Lung cancer: Biology and treatment options. *Biochim Biophys Acta.* 2015;1856(2):189-210.
5. Hairani R, *et al.* Allyl and prenyl ethers of mansonone G, new potential semisynthetic antibacterial agents. *Bioorg Med Chem Lett.* 2016;26(21):5300-3.

6. Kim HK, *et al.* CBMG, a novel derivative of mansonone G suppresses adipocyte differentiation via suppression of PPAR γ activity. *Chem Biol Interact.* 2017;273(Supplement C):160-70.
7. Tiew P, *et al.* Antifungal, antioxidant and larvicidal activities of compounds isolated from the heartwood of *Mansonia gagei*. *Phytother Res.* 2003;17(2):190-3.
8. El-Halawany AM, *et al.* Anti-estrogenic activity of mansonone G and mansorin A derivatives. *Pharm Biol.* 2013;51(8):948-54.
9. Wang D, *et al.* Cytotoxic effects of mansonone E and F isolated from *Ulmus pumila*. *Biol Pharm Bull.* 2004;27(7):1025-30.
10. Redza-Dutordoir M and Averill-Bates DA. Activation of apoptosis signalling pathways by reactive oxygen species. *Biochim Biophys Acta.* 2016;1863(12):2977-92.
11. Xu HL, *et al.* Juglone, from *Juglans mandshruica* Maxim, inhibits growth and induces apoptosis in human leukemia cell HL-60 through a reactive oxygen species-dependent mechanism. *Food Chem Toxicol.* 2012;50(3):590-6.

PH-024

**Pharmacokinetics of oral linezolid 300 mg/day
in healthy volunteers**

Jetsada Piwluang¹, Somchai Sriwiriyajan¹ and Sutep Jaruratanasirikul²

¹ Department of Pharmacology, Faculty of Science, Prince of Songkla University, Songkhla 90110, Thailand.

² Department of internal medicine, Faculty of Medicine, Prince of Songkla University, Songkhla 90110, Thailand.

ABSTRACT

INTRODUCTION: Linezolid is the first synthetic antibiotic of oxazolidinone group that can inhibit bacterial protein synthesis. Previous studies have found that linezolid was an effective treatment for multidrug-resistant (MDR) and extensively drug-resistant (XDR) tuberculosis (TB). In addition, the current dosage recommendation (1,200 mg/day) occasionally results in serious adverse events including bone marrow suppression and peripheral neuropathy.

OBJECTIVES: To determine the pharmacokinetics of oral linezolid 300 mg /day in healthy volunteers.

METHODS: This study conducted in six healthy volunteers. All subjects received an oral linezolid 300 mg/day by directly observed treatment (DOT) at the same time each day for 5 days. Blood samples were collected on day 5 before and at 0.5, 1, 1.5, 2, 2.5, 3, 4, 6, 8, 12 and 24 h after dosing. The separated plasma samples were evaluated by ultra-performance liquid chromatography (UPLC). All pharmacokinetic parameters were calculated by Winnonlin version 1.1.

RESULTS: The mean parameter were: $T_{max} 0.75 \pm 0.42$ h, $C_{max} 11.29 \pm 0.71$ $\mu\text{g/mL}$, $AUC_{0-\infty} 132.36 \pm 89.53$ $\mu\text{g.h/mL}$, $AUC_{last} 89.21 \pm 23.45$ $\mu\text{g.h/mL}$, $t_{1/2} 12.09 \pm 12.92$ h, $V_d 8.87 \pm 5.58$ L/kg, $Cl 50.35 \pm 27.73$ mL/min. All participants completed the study without reporting any adverse effects.

CONCLUSIONS: The results of this study showed that an oral administration of linezolid 300 mg/day has demonstrated good bioavailability in healthy volunteers. Further studies may be required for pharmacodynamics and clinical treatment outcome.

Keywords: Pharmacokinetics, Pharmacodynamics, Linezolid

INTRODUCTION

Linezolid is the first synthetic antibiotic in the oxazolidinone group that able to inhibit bacterial protein synthesis by time-dependent activity. Linezolid has been approved for treatment of gram – positive and difficult-to-treat aerobic bacterial infections, especially multi-drug resistant or extensively drug resistant (MDR/XDR) *Mycobacterium tuberculosis* infection. Linezolid is well absorbed, with a bioavailability of approximately 100%, allowing this agent to be used early intravenously, then switching to oral¹. The characteristics of linezolid are non-linear, that is, mean pharmacokinetic parameters may not be specified by dosage administration. The efficacy of linezolid depends on concentration above the MIC or $AUC_{0-\infty}/MIC$ value in range of 80-120².

Recommendation dosage of linezolid for adults is 400 or 600 mg every 12 hours which has been proven to treat difficult-to-treat bacteria such as MDR/XDR-TB effectively³.

In addition, the current recommend dosage occasionally resulted in serious adverse events (SAE) including bone marrow suppression and peripheral neuropathy. A previous study showed that daily dose lowering (600 mg/day) of oral linezolid could reduce bone marrow suppression, but not peripheral neuropathy when compared with 1,200 mg/day then 300 mg/day could reduce both SAEs⁴. However, the pharmacokinetics and bioavailability of oral linezolid 300 mg/day is still unclear.

This study aimed to determine the pharmacokinetics and oral bioavailability of linezolid 300 mg /day in healthy volunteers.

METHODS

Study population

We prospectively recruited six healthy volunteers using inclusion criteria: age of 20-40 years, BMI 19-24 kg/m², no underlying disease or current medications, CrCl \geq 90 mL/min by Cockcroft and Gault equation, normal liver function test, non-smoking, non-alcohol, non-pregnant or lactation in women subjects and able to take medication. Subjects obtained physical examination and blood testing: CBC, BUN, Cr, liver function test, total bilirubin, direct bilirubin, serum albumin alkaline phosphatase and pregnancy testing. Blood testing was collected on screening, day 5 and day 17 of study.

Ethics

The study protocol was approved by Ethic committee of Faculty of medicine, Prince of Songkla University (REC 61-087-14-1) and informed consent was obtained from all subjects prior to their participation in this study.

Pharmacokinetics evaluation

All subjects received an oral linezolid 300 mg/day at the same time under directly observed treatment (DOT) for 5 days. Blood samples were collected on day 5 before and at 0.5, 1, 1.5, 2, 2.5, 3, 4, 6, 8, 12 and 24 h after dosing.

After blood sample collection, plasma was separated from blood samples by centrifugation at 15,000 rpm for 15 minutes at 10 C° and then collected at -80 C° until assayed. The assay was reference from Cios A et al.³, plasma 300 μ L was added to 70 μ L of 2-ethoxybenzamide (IS) with concentration 1 mg/mL and vortex 10 s then the tube was added with 500 μ L methanol for deprotonized. The mixture was vortex-mixed for 30 s and centrifuged 15 min at 10 C°. The sample were analyzed by Agilent UPLC 1290 infinity II.

The mobile phase was a mixture of 50 mM Potassium dihydrogen phosphate buffer pH 3.5 and acetonitrile by ratio 74 : 26 v/v with flow rate 0.6 mL/min. The linezolid was monitored at 258 nm with run time 7 min⁵. The lower limit of quantification (LLOQ) of linezolid under the UPLC condition is 0.2 μ g/mL. The pharmacokinetic parameters were calculated by Winnonlin version 1.1.

RESULTS

The study was conducted in three men and three women with mean age 22.83 ± 1.17 years, body weight 59.5 ± 5.68 kg and BMI 21.88 kg/m². All subjects did not take any other medications or supplements.

Pharmacokinetic parameters were summarized in table 1. The study was completed without loss to follow up.

There were no reported of adverse effects, including bone marrow suppression. CBC results were summarized in table 2.

Table1. Descriptive summary of pharmacokinetic parameters

Parameter	Oral Linezolid 300 mg/day N = 6
AUC _{0-∞} (µg.h/mL), mean ± S.D.	132.36 ± 89.53
AUC _{last} (µg.h/mL), mean ± S.D.	89.21 ± 23.45
C _{max} (µg/mL), mean ± S.D.	11.29 ± 0.71
T _{max} (h), mean ± S.D.	0.75 ± 0.42
t _{1/2} (h), mean ± S.D.	12.09 ± 12.92
Vd (L/kg), mean ± S.D.)	8.87 ± 5.58
Cl (mL/min), mean ± S.D.)	50.35 ± 27.73

AUC_{0-∞} area under plasma concentration-time curve from time zero to infinite time; AUC_{last-∞} area under plasma concentration-time curve from time zero to the time of the last quantifiable; C_{max} maximum concentration; T time to maximum concentration; t_{1/2} half-life; Vd volume of distribution; Cl clearance

Table2. Descriptive summary of CBC testing

Parameter	Screening	Day 5	Day 17
WBC (×10 ³ /uL), mean ± S.D.	7.41 ± 1.81	5.89 ± 0.78	7.06 ± 1.56
RBC (×10 ⁶ /uL), mean ± S.D.	4.72 ± 0.58	4.79 ± 0.76	4.77 ± 0.61
Hct (%), mean ± S.D.	40.9 ± 5.05	41.35 ± 5.91	41.38 ± 4.94
Plt (×10 ³ /uL), mean ± S.D.	262.00 ± 45.29	277.50 ± 43.52	281.00 ± 51.27
Hb (g/dL), mean ± S.D.	13.67 ± 1.62	13.65 ± 2.01	13.75 ± 1.79
MCV (fL), mean ± S.D.	86.75 ± 4.78	86.63 ± 5.25	86.98 ± 4.88
MCH (pg), mean ± S.D.	28.97 ± 1.26	28.58 ± 1.12	28.85 ± 4.88
MCHC (g/dL), mean ± S.D.	33.47 ± 1.10	33.00 ± 0.74	33.22 ± 1.12

WBC white blood cell; RBC red blood cell; Hct hematocrit; Plt platelet; Hb hemoglobin; MCV mean corpuscular volume; MCH mean corpuscular hemoglobin; MCHC mean corpuscular hemoglobin concentration

DISCUSSION

This is the first report of full pharmacokinetics in daily 300 mg of oral linezolid. The absorption of oral linezolid 300 mg/day is rapid and achieved C_{max} in 0.75 (± 0.42) h after taking medication. The property of linezolid is good penetration in epithelial lining fluid which also is consistent with V_d of this study. Previous study has shown linezolid 300 mg/day may be enough to keep the concentration above MIC for *M. tuberculosis*². A previous study reported that pharmacokinetics of 600 mg linezolid compared with oral tablet and oral suspension in healthy Chinese subjects, the mean parameters; AUC_{0-∞} 112.6 ± 24.5 and 109.2 ± 21.7 µg.h/mL, C_{max} 13.7 ± 3.5 and 15.5 ± 3.5 µg/mL, T_{max} 1.50 ± 0.5 and 0.63 ± 0.5 h and t_{1/2} 5.13 ± 0.92 and 5.08 ± 0.7 h, respectively³. It seems like AUC_{0-∞} and C_{max} between 600 mg/day and 300 mg/day are equivalent, even their dosage is as much as doubling. The non-linear characteristic of linezolid is not relevant over the dosage. Consequently, higher dosage was not associated with higher AUC_{0-∞}. In addition, the study in Korean patients who were diagnosed with intractable MDR/XDR-TB infection. They prescribe linezolid 300 mg/day for 7 days that reported only steady-state serum C_{max} and C_{min}: C_{min} 0.4 mg/L and C_{max} 11.6 ± 4.4 mg/L⁴, which C_{max} similar to our study. That result can hypothesized the linezolid concentration after daily 300 mg would exceed MIC (0.2 mg/L) for *M. tuberculosis*⁶.

Linezolid 300 mg/day was safe and well tolerated in our healthy volunteers because CBC testing on screening, day 5 and day 17 remain normal testing and were not different between 3 times of testing. Serious adverse effects can occur related to high dose and longtime use. Although, 300 mg/day of linezolid has low adverse effects, the treatment for long time

should have been monitored closely. Finally, the non-linear pharmacokinetic character of linezolid shows that 300 mg daily is sufficient and safe compares to high-dose linezolid.

The limitations of our study include a small group of healthy volunteers and short duration of treatment. Therefore, it is hard to explain a long –term pharmacokinetic. Further studies with more subjects and duration of treatment is recommended to confirm its pharmacokinetic properties.

CONCLUSIONS

The orally 300mg per day linezolid provides good bioavailability and safety in healthy volunteers. However, further studies is required to demonstrate effective pharmacodynamics and clinical treatment outcome to develop an oral 300 mg/day linezolid as one of drug of choice in treatment for MDR/XDR-TB.

ACKNOWLEDGEMENT

None

CONFLICT OF INTEREST

None

REFERENCES

1. S. D Matthew. 2011. Linezolid pharmacokinetic and pharmacodynamics in clinical treatment. *Journal of Antimicrobial Chemotherapy*. 66: iv7 – 15.
2. C Roger, L. Muller, S.C. Wallis, et al. 2016. Population pharmacokinetics of linezolid in critically ill patients on renal replacement therapy: comparison of equal doses in continuous vevovenous haemofiltration and continuous venovenous haemofiltration. *Journal of Antimicrobial Chemotherapy*. 71: 464-470.
3. J Zhang, Y Zhang, R Wang, et al. 2014. Pharmacokinetics and bioequivalence comparison of 600 mg single-dose linezolid oral suspension and tablet formulation in healthy Chinese subjects. 6(5): 153-157
4. Koh WJ, Kwon OJ, Gwak H, Chung JW, Cho SN, Kim WS. et al. 2009. Daily 300 mg dose of linezolid for the treatment of intractable multidrug-resistant and extensively drug-resistant tuberculosis. *J Antimicrob Chemother*. 64:388-91.
5. Cios A, Kus K, Szymura-Oleksiak J. 2013. Determination of linezolid in human serum by reversed-phase high-performance liquid chromatography with ultraviolet and diode array detection. *Acta Pol Pharm*. 70:631-41.
6. Stevens DL, Dotter B, Madaras-Kelly K. 2004. A review of linezolid: the first oxazolidinone antibiotic. *Expert Rev Anti Infect Ther*. 2: 51-9.
7. World Health Organization. 2016. WHO treatment guidelines for drug – resistant tuberculosis 2016 update. Geneva: World Health Organization.
8. Pfizer. [Internet]. Zyvox® [LAB-0139-20.1, Revised November 2011]. Available from: https://www.accessdata.fda.gov/drugsatfda_docs/label/2012/021130s028lbl.pdf.
9. Burkhardt O, Borner K, Von der Hoh N, Koppe P, Pletz MW, Nord CE. et al. 2005. Single- and multiple-dose pharmacokinetics of linezolid and co-amoxiclav in healthy human volunteers. *J Antimicrob Chemother*. 50:707-12.
10. Zou JJ, Ji HJ, Wu DW, Yao J, Hu Q, Xiao DW. et al. 2008. Bioequivalence and pharmacokinetic comparison of a single 200-mg dose of meclofenoxate hydrochloride

- capsule and tablet formulations in healthy Chinese adult male volunteers: a randomized sequence, open-label, two-period crossover study. *Clin Ther.* 30:1651-7.
11. Koh WJ, Kang YR, Jeon K, Kwon OJ, Lyu J, Kim WS. et al. 2012. Daily 300 mg dose of linezolid for multidrug-resistant and extensively drug-resistant tuberculosis: updated analysis of 51 patients. *J Antimicrob Chemother.* 67:1503-7.
 12. Lee M, Lee J, Carroll MW, Choi H, Min S, Song T. et al. 2012. Linezolid for treatment of chronic extensively drug-resistant tuberculosis. *N Engl J Med.* 367:1508-18.
 13. Farshidpour M, Ebrahimi G, Mirsaeidi M. 2013. Multidrug-resistant tuberculosis treatment with linezolid-containing regimen. *Int Mycobacteriol.* 2:233-6.
 14. Srivastava S, Magomedze G, Koeuth T, Sherman C, Pasipanodya JG, Raj P. 2016. Linezolid dose that maximizes sterilizing effect while minimizing toxicity and resistance emergence for tuberculosis. *Antimicrob Agents Chemother.* 61:e00751-17.

PH-025

Preliminary study to investigate an *in vitro* chondroprotective effect of oxyresveratrol in inflammatory-activated C28/I2 human chondrocyte cell line

Chayanee Laowittawat¹, Pongsak Utaisincharoen², Tulyapruet Tawonsawatruk³,
Pimtip Sanvarinda¹ and Ruedee Hemstapat^{1*}

¹ Department of Pharmacology, Faculty of Science, Mahidol University, Bangkok 10400, Thailand.

² Department of Microbiology, Faculty of Science, Mahidol University, Bangkok 10400, Thailand.

³ Department of Orthopedics, Faculty of Medicine, Mahidol University, Bangkok 10400, Thailand.

ABSTRACT

INTRODUCTION: *Morus alba* L., a plant from the family of Moraceae, contains several of bioactive compounds, which shows many pharmacological effects, including wound healing, anti-inflammatory and antioxidant activities. Based on our previous *in vitro* and *in vivo* studies, *M. alba* stem extract containing oxyresveratrol, a bioactive compound found abundantly in this plant, exhibited anti-inflammatory activity in LPS-Stimulated RAW 264.7 Cells and cartilage protective effect in the ACLT-induced rat model of osteoarthritis (OA), respectively. The mechanisms underlying chondroprotective effect of this plant is currently unknown; however, oxyresveratrol may partly be responsible for the chondroprotective effect on chondrocytes.

OBJECTIVES: To investigate cytotoxicity and the chondroprotective activity of oxyresveratrol through stimulation of gene expression in inflammatory-activated C28/I2 human chondrocyte cell line.

METHODS: Cytotoxicity and optimal concentrations were assessed using MTT assay. C-28/I2 cells were treated with different concentrations of oxyresveratrol including 0, 6.25, 12.5, 25 and 50 μ M. The optimal concentrations were selected for gene expression analysis. The gene expression level of ACAN (aggrecan) and COL2A1 (collagen type II) were investigated by a reverse transcription polymerase chain reaction (RT-PCR).

RESULTS: The results showed that, oxyresveratrol at 25 and 50 μ M significantly increased the expression of aggrecan synthesis in IL-1 β -activated cells compared to the non-activated cells ($p < 0.05$). An increasing trend of collagen type II expression in inflammatory-activated C28/I2 cell line was also observed; however, no significant difference was noted compared to the non-activated cells.

CONCLUSIONS: These preliminary results showed that oxyresveratrol may exhibit its chondroprotective effect by increasing gene expression of proteoglycan synthesis in inflammatory-activated C28/I2 cell line.

Keywords: *Morus alba*, Osteoarthritis, Oxyresveratrol

INTRODUCTION

Morus alba. (Mulberry), a herbal from the family of Moraceae, contain several bioactive compounds, including oxyresveratrol, kuwanons, morusin, moracin M, mulberrofuran G, sanggenons D, and mulberroside A. This plant has been reported to exhibit excellent pharmacological effects such as anti-inflammatory, antioxidant and antimicrobial

activities¹. Based on our previous findings, oxyresveratrol, the bioactive compound abundantly found in the stem part of *M. alba* exhibited anti-inflammatory activity in LPS-Stimulated RAW 264.7 cells through the inhibition of iNOS, NO, and COX-2 production². In addition, *M. alba* also showed the anti-nociceptive effect and cartilage protective effect in the ACLT-induced rat model of osteoarthritis (OA) in a dose-dependent manner³.

Since type II collagen and aggrecan are the main extracellular matrix, which are found in the articular cartilage. It could be postulated that any substance that can stimulate extracellular matrix synthesis would help delay or prevent the progression of OA. Despite several previous studies of *M. alba* activities, a lot of attention has been paid to anti-inflammatory and antioxidant activities. However, the mechanisms underlying the chondroprotective effect of *M. alba* is still unknown. Therefore, the present study aimed to investigate chondroprotective effect of oxyresveratrol through stimulation of gene expression of COL2A1 (collagen type II) and ACAN (aggrecan) in inflammatory-activated C28/I2 human chondrocyte cell line.

MATERIALS AND METHODS

Materials: C28/I2 human chondrocyte cell line was purchased from Merck (Darmstadt, Germany). Dulbecco's Modified Eagle Medium (DMEM), penicillin/streptomycin, L-glutamine and fetal bovine serum were purchased from GIBCO (NY, USA). Oxyresveratrol was purchased from Sigma Aldrich (St.Louis, USA). Agarose and tris-borate-EDTA (TBE) was purchased from Vivantis (Selangor Darul Ehsan, Malaysia).

Cell culture and cell viability: C28/I2 were cultured in 96-well plates (0.5×10^4 cells/well) and maintained in a humidified incubator at 37°C in 5% CO₂ for 24 hours. Cells were then treated with oxyresveratrol 0, 6.25, 12.5, 25 and 50 µM, and incubated at 37°C for 24 hours. Cell viability was determined by MTT assay as described previously⁴.

Reverse Transcription-Polymerase Chain Reaction (RT-PCR) assay: C28/I2 were seeded in 6-well plates at a density of 3×10^5 cells/well. After 24 hours, cells were treated with various concentrations of oxyresveratrol (12.5, 25 and 50 µM) for 2 hours. After that cells were treated with or without IL-1β (10 ng/mL) for 24 hours. Total RNA from the cultured cells was then extracted using illustra RNAspin Mini Kit (GE Healthcare, USA). Complementary DNA (cDNA) was synthesized using HyperScriptTM RT master mix (with oligo dT; Seoul, Korea). The AccuStartTM PCR SuperMix (QuantaBio, USA) was used to determine mRNA gene expression of COL2A1 (collagen type II) and ACAN (aggrecan). GAPDH was used as internal control. PCR products were loaded to 2% agarose gel. The gels were electrophoresed in 1X TBE buffer at a constant voltage of 90 for 40 minutes.

Statistical analysis: All data were expressed as the mean ± standard deviation (SD). Statistical analyses were performed using GraphPad Prism (version 6.0) software and conducted using ANOVA (one-way analysis of variance) followed by the Tukey's test for multiple comparisons. A P-value less than 0.05 was considered statistically significant.

RESULTS AND DISCUSSION

The MTT results showed that the cell viability decreased with increasing concentration of oxyresveratrol from 6.25 to 50 µM. However, all the concentrations of oxyresveratrol yielded cells viability greater than 80% (Figure 1).

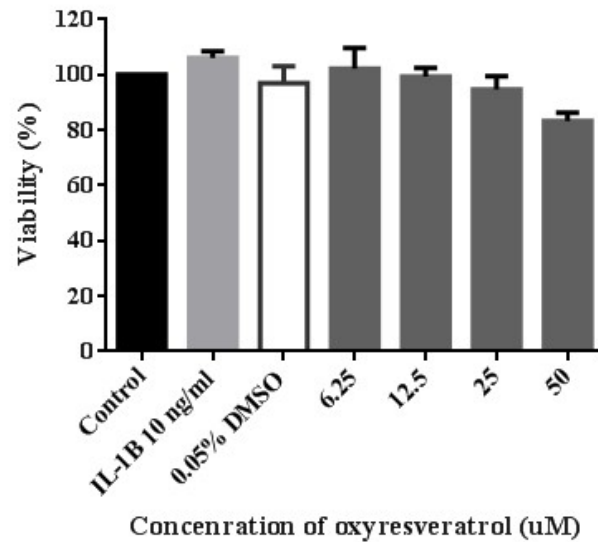


Figure 1. The percentage viability of C28/I2 chondrocyte cells which was untreated (control), treated with 0.05% DMSO (control vehicle) and various concentrations of oxyresveratrol for 24 h. The viability of cells was assessed using MTT assay. Data are expressed as the mean \pm SD (n=3).

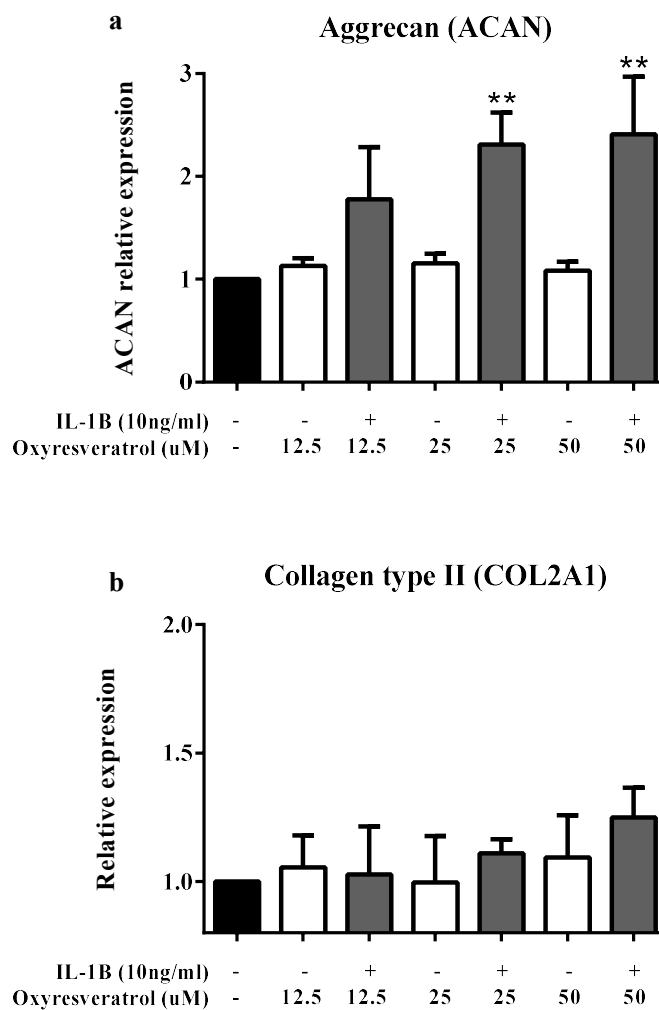


Figure 2. The effect of oxyresveratrol on gene expression of aggrecan (ACAN) and type II collagen (COL2A1) in non-activated and IL-1 β activated C28/I2 cells. Data are expressed as the mean \pm SD (n=3). ** $p < 0.01$ vs non-activated chondrocytes.

To investigate the chondroprotective effect of oxyresveratrol, mRNA expression levels of both aggrecan (ACAN), a major component of proteoglycan molecules and type II collagen (COL2A1), a major component of collagen molecules in extracellular matrix of articular cartilage were assessed in non-activated and IL-1 β -activated chondrocytes treated with oxyresveratrol (12.5, 25 and 50 μ M). The result showed that oxyresveratrol significantly increased the expression of ACAN mRNA of IL-1 β -activated chondrocytes compared with non-activated chondrocytes in a dose-dependent manner ($p < 0.05$) (Figure 2a). However, the effect of oxyresveratrol on the expression of COL2A1 mRNA was not statistically significant (Figure 2b). In addition, oxyresveratrol had no effect on the expression of both ACAN and COL2A1 mRNA in non-activated chondrocytes.

Although the precise mechanisms responsible for the chondroprotective effect of oxyresveratrol cannot be explained in the present study, it is possible that oxyresveratrol may exert its chondroprotective effect by stimulating the mRNA expression of aggrecan and thereby promoting the proteoglycan synthesis.

CONCLUSIONS

This study demonstrated that oxyresveratrol, a bioactive compound found abundantly in *M.alba* may exhibit its chondroprotective effect by stimulating the mRNA expression of aggrecan and thereby promoting the proteoglycan synthesis. However, further study is required to confirm the relative protein expression levels of both proteoglycan and type II collagen by using western blotting. This finding may provide a potential candidate for further development as an alternative treatment for OA.

ACKNOWLEDGEMENTS

Ms. Chayanee Laowittawat was supported by Science Achievement Scholarship of Thailand (SAST). This work is also supported in part by the Faculty of Science, Mahidol University.

REFERENCES

1. Chan EW-C, Lye P-Y, Wong S-K. Phytochemistry, pharmacology, and clinical trials of *Morus alba*. Chinese Journal of Natural Medicines. 2016;14(1):17-30.
2. Soonthornsit N, Pitaksutheepong C, Hemstapat W, Utaisincharoen P, Pitaksuteepong T. *In Vitro* Anti-Inflammatory Activity of *Morus alba* L. Stem Extract in LPS-Stimulated RAW 264.7 Cells. Evidence-based complementary and alternative medicine : eCAM. 2017;2017:3928956.
3. Khunakornvichaya A, Lekmeechai S, Pham PP, Himakoun W, Pitaksuteepong T, Morales NP, et al. *Morus alba* L. Stem Extract Attenuates Pain and Articular Cartilage Damage in the Anterior Cruciate Ligament Transection-Induced Rat Model of Osteoarthritis. Pharmacology. 2016;98(5-6):209-16.
4. Jeong JW, Lee HH, Lee KW, Kim KY, Kim SG, Hong SH, et al. Mori folium inhibits interleukin-1 β -induced expression of matrix metalloproteinases and inflammatory mediators by suppressing the activation of NF- κ B and p38 MAPK in SW1353 human chondrocytes. International journal of molecular medicine. 2016;37(2):452-60.

PH-026

Evaluation of *in vitro* antioxidant activity of active compounds in the fingerroot

Chanathip Duangtha¹, Noppawan Phumala Morales¹, Pongsak Uthaisincharoen², Sunhapas Soodvilai³ and Ruedee Hemstapat^{1*}

¹Department of Pharmacology, Faculty of Science, Mahidol University, Bangkok 10400, Thailand.

²Department of Microbiology, Faculty of Science, Mahidol University, Bangkok 10400, Thailand.

³Department of Physiology, Faculty of Science, Mahidol University, Bangkok 10400, Thailand.

ABSTRACT

INTRODUCTION: Fingerroot (*Boesenbergia rotunda*), a plant in Zingiberaceae or ginger family, is a traditional medicinal plant which is usually found in Southeast Asia and Indo-China. This plant is an excellent source of several vitamins, minerals, dietary fibers, flavonoids, etc., which provide a variety of pharmacological benefits, such as anti-cancer, anti-inflammatory, and anti-oxidant activity. Panduratin A (PA), pinostrobin (PS), and pinocembrin (PC) are bioactive compounds present in this plant. Since oxidative stress has been implicated in the progression of OA, any compound exhibit antioxidant activity might have a potential attenuation of disease progression. Thus, the present study was designed to examine the antioxidant mechanisms of these bioactive compounds.

OBJECTIVES: To evaluate and compare the potential antioxidant activity of panduratin A, pinostrobin, and pinocembrin.

METHODS: The antioxidant activities were determined using various radical scavenging assays, including DPPH radical scavenging, ferric reducing antioxidant power (FRAP), nitric oxide radical scavenging, as well as superoxide radical scavenging assay.

RESULTS: Among the active compounds, Panduratin A (PA) showed the highest ability to scavenge DPPH radical, while the other compounds showed weak DPPH scavenging activity. Although none of these compounds exhibited ferric reducing capacity and nitric oxide scavenging activity, all of them exhibited superoxide radical scavenging capacity.

CONCLUSIONS: This *in vitro* antioxidant study suggested that PA exhibited positive results for DPPH radical and superoxide radical scavenging capabilities, while PS and PC showed only the capability to scavenge superoxide radical. However, further studies are required to investigate the antioxidant activity of these compounds in the oxidative-stress stimulated chondrocytes assays.

Keywords: fingerroot, antioxidant, human chondrocytes

INTRODUCTION

Boesenbergia rotunda (Family: Zingiberaceae), fingerroot, is a traditional medicinal plant that usually found in Southeast Asia and Indo-China. It contains several bioactive molecules, such as flavonoids, polyphenols, vitamins, and minerals. Local people use fingerroot as a daily ingredient in food and as the active ingredient in traditional medicines. Fingerroot extract has been known to possess several pharmacological activities, including

anticancer, anti-bacterial activity, wound healing, anti-allergic, anti-inflammatory and antioxidant effects¹.

Although several compounds have been isolated and purified from the fingerroot extract, panduratin A (PA), pinostrobin (PS) and pinocembrin (PC) (**Figure.1**) are among the most abundantly found cyclohexenyl chalcone (Fig. 1A) and flavonoid derivatives (**Fig. 1B&C**), respectively.

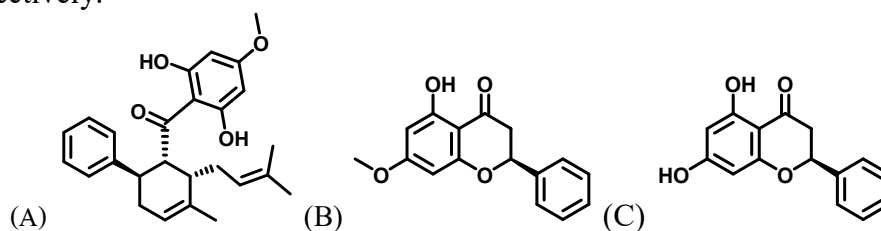


Figure 1. Chemical structure of isolated bioactive compounds from fingerroot; (A) Panduratin A, (B) Pinostrobin and (C) Pinocembrin.

Overproduction of reactive oxygen species (ROS) including superoxide, nitric oxide and hydroxyl radical has been implicated in the pathogenesis of several chronic diseases, including osteoarthritis (OA)^{2,3}. OA is one of the arthritic diseases that occurs with high prevalence in populations at age 65 years and above. Furthermore, several recent studies demonstrated that the active compounds from fingerroot enhance the antioxidant enzymes, e.g superoxide dismutase (SOD)⁴⁻⁶, and thereby might have a potential to attenuate the progression of OA. Thus, the present study aimed to evaluate the antioxidant activity of these active compounds by using various chemical assay systems.

MATERIALS AND METHODS

The bioactive compounds including PA, PS, and PC were extracted from fingerroot and provided by Department of Chemistry, Faculty of Science, Mahidol University, Thailand. All other reagents were purchased from Sigma Chemical Co. (St. Louis, MO). Panduratin A, pinostrobin, and pinocembrin in the concentration range of 0 to 125 μ M were tested using several chemically antioxidant assays to investigate the different antioxidant mechanisms occurring in biological processes.

DPPH radical assay: This assay was conducted as developed by Blois⁷. DPPH is a stable free radical, which produces a purple solution in methanol at its maximum absorption at 520 nm. DPPH reacts with antioxidant compound that can donate a hydrogen atom, then this gives rise to the corresponding pale yellow hydrazine. This assay, therefore, assesses the reduction in absorbance of DPPH (deep purple) as indicated by color changes from deep purple to decolorization (light yellow), which is correlates with the antioxidant capacity added to DPPH reagent solution. More the light yellow, more the free radical scavenging activity. All of the tested samples were dissolved in the absolute methanol (vehicle). Trolox was used as a positive control (standard antioxidant) and using methanol as blank. Briefly, 250 μ M DPPH were mixed with the solution of tested samples then incubated in dark at room temperature for 20 minutes. After the incubation, the absorbance was taken at 520 nm using a microplate reader (Varioskan™ Flash Multimode Reader, Thermo Scientific™). A percentages of scavenging activity (%SA) of DPPH radical were then calculated by using the following equation;

$$\%SA \text{ of DPPH} = [(A-B)/A] \times 100$$

where: A is the absorbance of blank (vehicle)
B is the absorbance of sample

FRAP assay: The assay was conducted as previously described by Benzie and Strain⁸, in which it can be used to measure antioxidant power by assess the ferric reducing ability at low pH causing a colored ferrous-tripyridyltriazine complex. FRAP values can be obtained by the measurement of the absorbance at 593 nm compared to the reaction mixture containing ferrous ions (Fe^{2+}) in known concentration. Briefly, samples were mixed with the FRAP reagent which containing 300 mM pH 3.6 acetate buffer, 10 mM 2,4,6-Tri(2-pyridyl)-s-triazine (TPTZ) in 40 mM HCl, and 200 mM ferric chloride ($\text{FeCl}_3 \cdot 6\text{H}_2\text{O}$) then incubated at room temperature for 10 minutes. After the incubation, the absorbance at 593 nm were then measured. The standard curve was plotted by using A_{593} against ferrous sulfate concentration to calculate the generated ferrous ion from the reactions with sample.

NO• scavenging assay: This assay was first described by Peter Griess⁹ to determine the ability of tested compound to scavenge nitrite ion (NO_2^-) which is an oxidize form of NO radical, a reactive species that involved in various pathological processes of several diseases. Typically, after the production of NO radical, it has a rapid half-life, which is then auto-oxidized to a nitrite ion (NO_2^-) (a more stable form). Griess' assay was used to assess the presence of NO_2^- in the reaction mixture, which can be converted back to the amount of NO. In brief, the tested samples or gallic acid (positive control) and 10 mM sodium nitroprusside (SNP; NO• generator) were incubated at room temperature in the presence of light for 30 minutes. After the incubation, 1% sulfanilamide in 5% phosphoric acid was added to the mixture and incubated at room temperature in dark for 10 minutes. Finally, 0.1% N-1-naphylethylenediamine dihydrochloride (NED) solution was added and incubated in dark at room temperature for 10 minutes, and the absorbance was measured within 30 minutes at 520 nm. The standard curve was plotted by using A_{520} against standard sodium nitrite (NaNO_2), which is used to calculate the concentration of NO_2^- that remains in the reactions.

O_2^- scavenging assay: To determine an ability of tests samples to scavenge the radical by using xanthine/xanthine oxidase method, which can be used to produce superoxide radical anion spontaneously¹⁰. Concisely, each sample was mixed with 0.4 U/mL of xanthine oxidase (in 2 M ammonium sulfate and 1 mM EDTA) using 75% MeOH as vehicles. This mixture was then mixed with the solution containing 0.4 mM xanthine and 0.25 mM NBT in 50 mM pH 10.2 sodium carbonate buffer with 0.1 mM EDTA. The absorbance was immediately determined every 30 second at 560 nm for 5 minutes. The absorbance per minutes (AU/min) were calculated using this equation;

$$\text{AU/min} = (\text{A}_{560} \text{ at } 5 \text{ min} - \text{A}_{560} \text{ at } 0 \text{ min})/5 \text{ min}$$

The percentage of O_2^- inhibition was calculated using AU/min of vehicles and sample.

RESULTS AND DISCUSSION

Antioxidant activities of these active compounds were assessed at the concentration up to 125 μM . The data are shown in Figure 2. DPPH assay showed that PA exhibited the highest ability to scavenge DPPH. Theoretically, 1 molecule of trolox donate 2 hydrogen atoms, therefore PA, which exhibited 50% activity of trolox, may donate 1 hydrogen atom rather than 2 hydrogen atoms due to steric hindrance of its structure (Figure 1A). Although PS and PC contain one and two hydroxyl groups, hydrogen donation activity was not observed.

None of tested compounds exhibited ferric reducing capacity and nitric oxide radical scavenging activity. However, superoxide radical scavenging capacity was observed in all of the tested compounds. Based on these findings, PA exhibited the highest antioxidant capacity, in which its activity might result from a hydrogen donating ability and superoxide scavenging activity, but without reducing capacity.

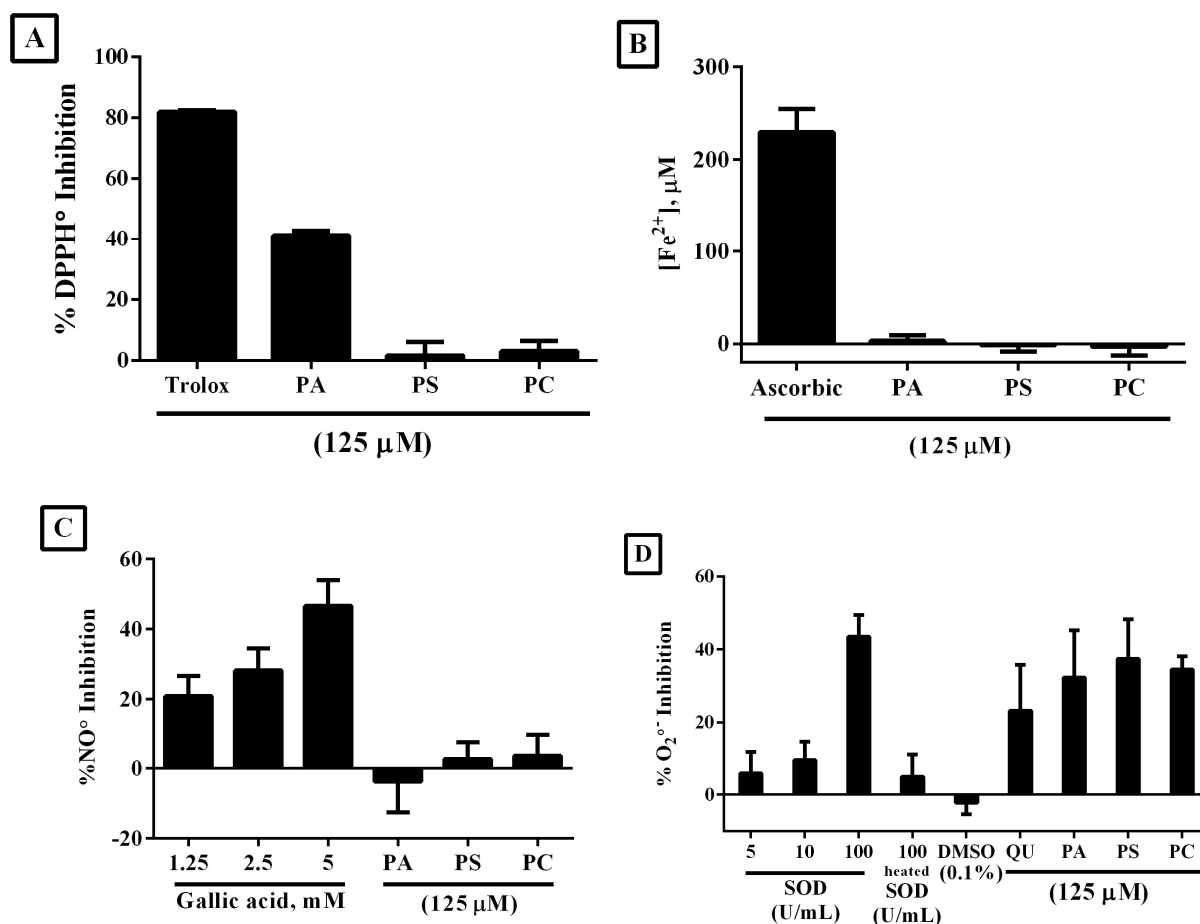


Figure 2. Antioxidant assays; (A) DPPH radical scavenging, (B) FRAP, (C) nitric oxide radical scavenging, and (D) superoxide radical scavenging assay. All values were conducted in triplicate and expressed as means \pm standard deviation (SD).

CONCLUSIONS

The present study demonstrated that only PA showed DPPH radical scavenging activity. However, all three active compounds present in the fingerroot exhibited the ability to scavenge $O_2^{\cdot-}$, which is the reactive oxygen species that are known to cause potentially harmful effects to chondrocytes and thus the progression of OA. However, further studies are required to investigate and confirm the antioxidant activity of these compounds in the oxidative-stress stimulated chondrocytes assays.

ACKNOWLEDGEMENTS

Mr. Chanathip Duangtha is thankful to the Science Achievement Scholarship of Thailand (SAST). This study was also supported in part by the Faculty of Science, Mahidol University. The authors would like to thank Prof. Dr. Patoomratana Tuchinda from Department of Chemistry, Faculty of Science, Mahidol University for providing active compounds in this study.

CONFLICT OF INTEREST

The authors declare that they have no conflicts of interest.

REFERENCES

1. Ongwisepaiboon O, Jiraungkoorskul W. Fingerroot, *Boesenbergia rotunda* and its Aphrodisiac Activity. *Pharmacogn Rev.* 2017;11(21):27-30.
2. Lepetos P, Papavassiliou AG. ROS/oxidative stress signaling in osteoarthritis. *Biochim Biophys Acta.* 2016;1862(4):576-91.
3. Poulet B, Beier F. Targeting oxidative stress to reduce osteoarthritis. *Arthritis Res Ther.* 2016;18:32.
4. Salama SM, Ibrahim IAA, Shahzad N, Al-Ghamdi S, Ayoub N, AlRashdi AS, et al. Hepatoprotectivity of Panduratin A against liver damage: In vivo demonstration with a rat model of cirrhosis induced by thioacetamide. *Apmis.* 2018;126(9):710-21.
5. Li C, Tang B, Feng Y, Tang F, Pui-Man Hoi M, Su Z, et al. Pinostrobin Exerts Neuroprotective Actions in Neurotoxin-Induced Parkinson's Disease Models through Nrf2 Induction. *J Agric Food Chem.* 2018;66(31):8307-18.
6. Shi L-l, Chen B-n, Gao M, Zhang H-a, Li Y-j, Wang L, et al. The characteristics of therapeutic effect of pinocembrin in transient global brain ischemia/reperfusion rats. *Life Sciences.* 2011;88(11):521-8.
7. Blois MS. Antioxidant Determinations by the Use of a Stable Free Radical. *Nature.* 1958;181(4617):1199-200.
8. Benzie IF, Strain JJ. The ferric reducing ability of plasma (FRAP) as a measure of "antioxidant power": the FRAP assay. *Analytical biochemistry.* 1996;239(1):70-6.
9. Griess P. Bemerkungen zu der Abhandlung der HH. Weselsky und Benedikt „Ueber einige Azoverbindungen“. *Berichte der deutschen chemischen Gesellschaft.* 1879;12(1):426-8.
10. Kuppasamy P, Zweier JL. Characterization of free radical generation by xanthine oxidase. Evidence for hydroxyl radical generation. *The Journal of biological chemistry.* 1989;264(17):9880-4.

PH-028

Pharmacoenhancing effect of piperine on disposition kinetics of oxyresveratrol in rats

Dhirarin Junsang¹, Tosapol Anukunwithaya¹, Phanit Songvut¹, Boonchoo Sritularak², Kittisak Likhitwitayawuid² and Phisit Khemawoot^{1,3,4}

¹ Department of Pharmacology and Physiology, Faculty of Pharmaceutical Sciences, Chulalongkorn University, Bangkok, Thailand.

² Department of Pharmacognosy and Pharmaceutical Botany, Faculty of Pharmaceutical Sciences, Chulalongkorn University, Bangkok, Thailand.

³ Department of Biochemistry and Microbiology, Faculty of Pharmaceutical Sciences, Chulalongkorn University, Bangkok, Thailand.

⁴ Preclinical Pharmacokinetics and Interspecies Scaling for Drug Development Research Unit, Chulalongkorn University, Bangkok, Thailand.

Corresponding author

E-mail address: phisit.k@chula.ac.th (P. Khemawoot).

ABSTRACT

INTRODUCTION: Oxyresveratrol from the heartwood of *Artocarpus lacucha* is a major bioactive compound with several biological activities. However, this compound has poor pharmacokinetic profile because of its low bioavailability. The purpose of this study was to examine the pharmacokinetic profiles of oxyresveratrol alone and in combination with piperine as a bioenhancer in rats.

METHODS: This study determined the pharmacokinetics of oxyresveratrol 10 mg/kg, oxyresveratrol 10 mg/kg co-administration with piperine 1 mg/kg by intravenous or oxyresveratrol 100 mg/kg, oxyresveratrol 100 mg/kg combined with piperine 10 mg/kg by oral gavage in male Wistar rats. Plasma, internal organs, urine and feces were collected and analyzed by LC-MS/MS to determine oxyresveratrol and oxyresveratrol glucuronide levels. Non compartmental analysis was used to calculate PK parameters, and statistical analysis by non-parametric method was conducted to determine significant difference between groups ($p < 0.05$).

RESULTS: Piperine could enhance oral bioavailability of oxyresveratrol approximately 2 folds with significantly higher maximum concentration in plasma. After intravenous or oral administration, oxyresveratrol distributed to several tissues and internal organs with a tissue to plasma ratio of 10–100 folds within 5 min after dosing. The major route of excretion of oxyresveratrol alone and in combination with piperine was urinary excretion as oxyresveratrol glucuronide within 24 h.

CONCLUSIONS: Piperine could improve the pharmacokinetic profiles of oxyresveratrol via both intravenous and oral combination. This pharmacokinetic data is beneficial for development of oxyresveratrol in combination with piperine as a phytopharmaceutical product.

Keywords: *Artocarpus lacucha*, Oxyresveratrol, Piperine, Bioenhancer, Pharmacokinetics

INTRODUCTION

Oxyresveratrol (2,4,3',5'-tetrahydroxystilbene) is a major bioactive substance found in the heartwood of *Artocarpus lacucha* Buch.–Ham. This compound has several pharmacological effects including skin whitening effect^{1–3}, antioxidant⁴, anti-inflammatory^{5,6}, antiviral^{7,8}, and neuroprotective effect⁹. Accordingly, oxyresveratrol could be developed as a phytopharmaceutical product for clinical use. Chen *et al.*¹⁰ investigated a pharmacokinetic study of oxyresveratrol after oral dosing at 100–400 mg/kg in rats and reported absolute oral bioavailability approximately 10–15%, with a rapid T_{max} occurring at approximately 15 min after dosing. Breuer *et al.*¹¹ focused on the tissue distribution of oxyresveratrol at 40 mg/kg after intraperitoneal administration in rats. The result showed that oxyresveratrol primarily resided in plasma, and there was solely a negligible concentration reached the brain. Mei *et al.*^{12,13} demonstrated that oxyresveratrol was biotransformed by phase II conjugation, particularly glucuronidation, with the majority of metabolites excreted in urine within 12 h after dosing.

Recently, scientists have attempted to improve the pharmacokinetic parameters of oxyresveratrol by adding bioenhancers. In a study by Johnson *et al.*¹⁴, a combination of resveratrol and piperine could increase the pharmacokinetic profile of resveratrol. Oxyresveratrol has its chemical structure resemble to resveratrol¹⁵; hence, piperine might enhance the pharmacokinetic profile of oxyresveratrol. Moreover, Suresh and Srinivasan¹⁶ demonstrated that piperine reduced the hepatic microsomal activity of UGT *in vitro*. Similarly, Atal *et al.*¹⁷ showed that piperine at doses of 10 and 25 mg/kg could decrease *in vivo* UGT activity by 36% and 55%, respectively. Piperine not only decreased UGT activity but also inhibited P-glycoprotein, a major efflux transporter found in the hepatobiliary system and enterocytes.¹⁸ The purpose of the present study is to investigate the pharmacokinetic profiles of oxyresveratrol alone and in combination with piperine in male Wistar rats. The pharmacokinetic data obtained from the present study would provide useful information for appropriate strategies to develop oxyresveratrol as a phytopharmaceutical product.

METHODS

Oxyresveratrol (purity >98%) and piperine (purity >98%) were supplied by Professor Kittisak Likhitwitayawuid from the Department of Pharmacognosy and Pharmaceutical Botany, Faculty of Pharmaceutical Sciences, Chulalongkorn University. Eight weeks old male Wistar rats were purchased from Nomura Siam International Co., Ltd. The rats were accommodated at $24 \pm 2^\circ\text{C}$ and humidity ranged from 40–60%, under a 12-h dark–light cycle. All rats were allowed to access food and water *ad libitum*. The animal protocol was approved by the Institutional Animal Care and Use Committee of the Faculty of Pharmaceutical Sciences, Chulalongkorn University (approval no. 17–33–002, approved March 8, 2017). The rats were divided randomly into four groups ($n = 6$ in each): oxyresveratrol 100 mg/kg p.o., oxyresveratrol 100 mg/kg plus piperine 10 mg/kg p.o., oxyresveratrol 10 mg/kg i.v., and oxyresveratrol 10 mg/kg plus piperine 1 mg/kg i.v. All rats were anaesthetized with isoflurane during drug administration, blood and tissue collection. For blood collection, blood sample approximately 300 μL was collected at 0, 0.083 (5 min), 0.25 (15 min), 0.5 (30 min), 1, 2, 4, 8, 16 and 24 h after dosing. The collected blood samples were centrifuged at $5000 \times g$ for 10 min to acquire plasma. Urine and feces from each rat were separately collected at 0–24 h and 24–48 h after dosing. Urine was centrifuged at $5000 \times g$ for 10 min, 100 μL of urine supernatant was collected and diluted 10 folds with methanol. Feces was collected and mixed with methanol up to 10 mL. For internal organ collection, brain, heart, lungs, liver, stomach, small intestine, kidneys and spleen were collected at 0.083 (5 min), 1, 2 and 4 h after dosing. Tissue samples were washed in cold normal saline solution to remove blood from the tissue. All samples were stored at -20°C until analysis.

The protein precipitation method was used for sample preparation. Briefly, 200 μL of methanol containing 10 ng of glycyrrhetic acid as an internal standard (IS) was added into 50 μL of plasma or urine. After that the mixture was centrifuged at $10,000 \times g$ for 10 min. Feces or tissue samples (50 mg) were mixed with 200 μL of methanol containing 10 ng of IS. The sample was homogenized on ice and then centrifuged at $10,000 \times g$ for 10 min. Identification of oxyresveratrol glucuronide was performed. In brief, all samples were incubated with 2000 units of glucuronidase in phosphate buffer (pH 6.8) at 37°C for 15 min. Then, the reaction was stopped by adding 1000 μL of methanol containing 50 ng of IS. The mixture was mixed and centrifuged at $10,000 \times g$ for 10 min. 150 μL of supernatant from each sample was collected and injected into the LC–MS/MS. Quantification of oxyresveratrol and piperine concentrations were conducted following the methods described by Huang *et al.*¹⁹ and Basu *et al.*²⁰, respectively. In brief, Nexera Ultra High–Performance Liquid Chromatography and 8060 triple quadrupole mass spectrometer (Shimadzu Co., Ltd.) was used in LC–MS/MS analysis. Synergi Fusion–RP C18 column (Phenomenex Inc.) with an oven temperature of 40°C was applied as the stationary phase. The gradient for the mobile phase was 0.2% formic acid in water and 100% methanol. The gradient started with 50% methanol for 0.50 min, increased to 90% methanol and maintained from 1.50 to 3.00 min, decreased to 50% methanol and *maintained at 50% methanol* from 4.00 to 5.00 min. The retention times for oxyresveratrol, piperine and glycyrrhetic acid were 0.51, 1.81 and 2.30 min, respectively. The lower limits for quantification of oxyresveratrol and piperine were 6.10 and 0.61 $\mu\text{g/L}$, respectively. The calibration curve for oxyresveratrol showed a good linearity range from 6.10–12,500 $\mu\text{g/L}$, and piperine had a good linearity range from 0.61–1250 $\mu\text{g/L}$ ($R^2 > 0.99$). The accuracy and precision of oxyresveratrol and piperine were within $\pm 10\%$, and the recovery percentage of the extraction method for oxyresveratrol and piperine was exceed more than 70%.

The pharmacokinetic parameters were determined by a non–compartmental analysis using PK Solution 2.0 software (Summit Research Service), and presented as mean \pm standard deviation (S.D.). All statistical analyses were carried out by SPSS version 16 (SPSS, Inc.). Statistical significances between oxyresveratrol alone and in combination with piperine were compared by a non–parametric method, with a p –value less than 0.05.

RESULTS

All male Wistar rats administered with oxyresveratrol alone or in combination with piperine demonstrated a good tolerability. Liver markers (aspartate transaminase (AST) and alanine transaminase (ALT)), and kidney markers (creatinine) were not significantly difference between predose and postdose among groups. All values were within the normal range as illustrated in Table 1.

As shown in Figure 1, the mean plasma concentration–time profiles of co–administration of oxyresveratrol and piperine generated a higher oxyresveratrol levels in plasma, after intravenous and oral dosing. The oral combination with piperine led to a significantly higher C_{max} and shorter T_{max} values of oxyresveratrol (Table 2). Similarly, all AUC parameters of oxyresveratrol in combination groups were superior than oxyresveratrol alone groups ($p < 0.05$). The mean residence time in combination groups likely to be longer, particularly when administered orally (11.66 vs. 7.25 h). The combination with piperine could enhance oral bioavailability of oxyresveratrol for approximately 2 folds.

The tissue to plasma ratio (K_p) of oxyresveratrol alone and in combination with piperine was presented in Figure 2. Oxyresveratrol could penetrate to most of the internal organs with a K_p of approximately 10–100 folds within 5 min, and slowly decreased at 1, 2 and 4 h after intravenous administration. For oral administration, the organs that displayed the high K_p were the stomach and small intestine from 5 min to 4 h. Following oral gavage, the tissue to plasma ratios of oxyresveratrol in other internal organs were approximately 1–100 folds from 5 min to 4 h.

Table 1. Tolerability of oxyresveratrol alone and in combination with piperine.

Parameters	Intravenous				Oral			
	OXY (10 mg/kg)		OXY + PIP (10 + 1 mg/kg)		OXY (100 mg/kg)		OXYI + PIP (100 + 10 mg/kg)	
	Predose (0 h)	Postdose (24 h)	Predose (0 h)	Postdose (24 h)	Predose (0 h)	Postdose (24 h)	Predose (0 h)	Postdose (24 h)
AST (U/L)	42.00 ± 7.15	45.40 ± 3.78	34.60 ± 17.03	46.75 ± 5.57	32.40 ± 16.47	40.83 ± 22.39	17.66 ± 13.50	23.66 ± 17.32
ALT (U/L)	5.00 ± 0.00	5.80 ± 1.09	9.40 ± 1.67	7.50 ± 2.88	9.40 ± 9.28	6.83 ± 3.25	7.00 ± 2.28	11.40 ± 11.63
Creatinine (mg/dL)	0.25 ± 0.15	0.32 ± 0.08	0.22 ± 0.03	0.24 ± 0.08	0.17 ± 0.01	0.17 ± 0.01	0.22 ± 0.03	0.20 ± 0.01

Data are presented as mean ± S.D. (n = 6). * $p < 0.05$ for predose vs postdose.

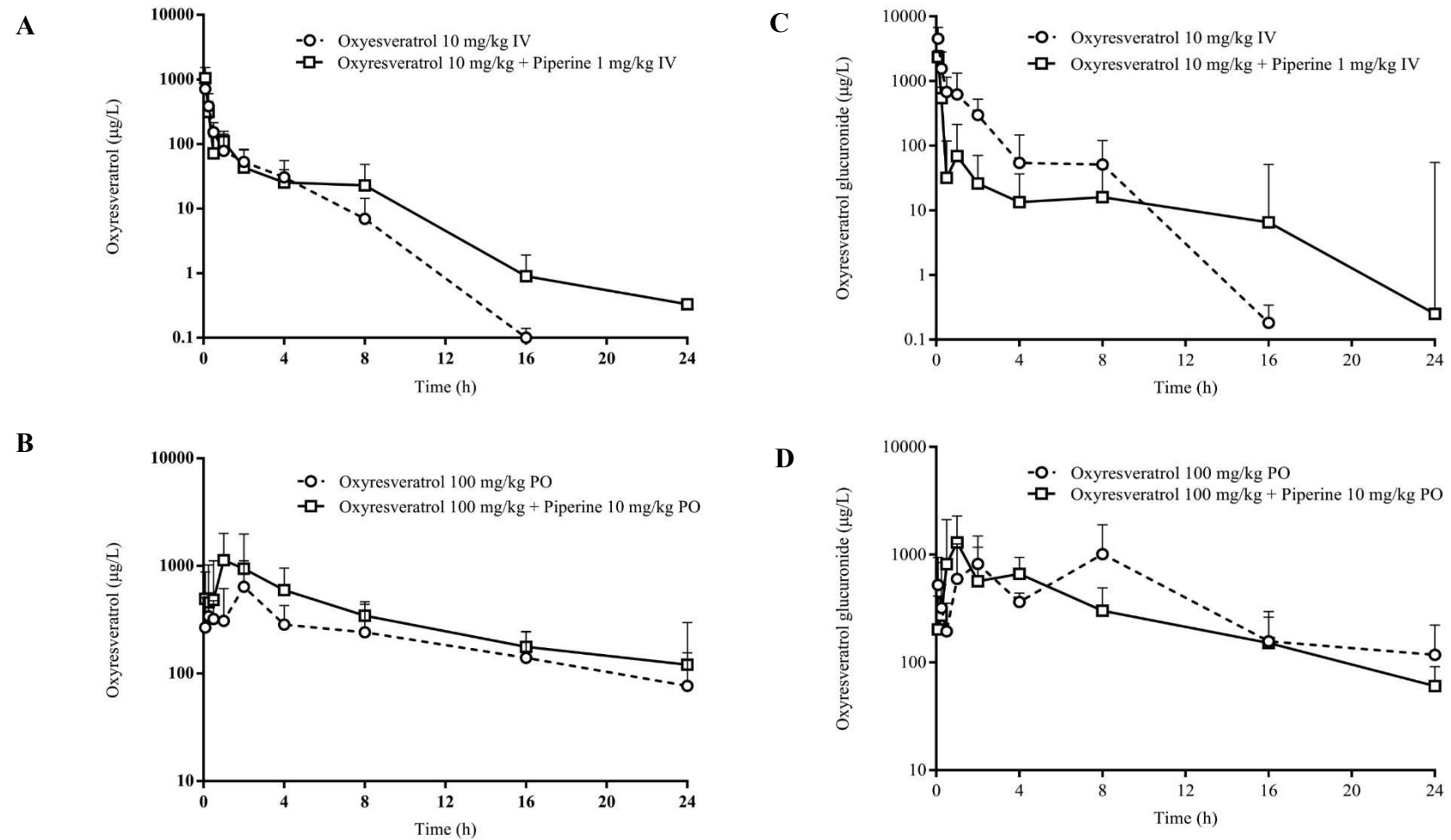


Figure 1. Plasma concentration–time profile of oxyresveratrol after intravenous dose (A); after oral dose (B) and plasma concentration–time profile of oxyresveratrol glucuronide after intravenous dose (C); after oral dose (D)

Table 2. Pharmacokinetic parameters of oxyresveratrol alone and in combination with piperine.

Parameters	Intravenous		Oral	
	OXY (10 mg/kg)	OXY + PIP (10 + 1 mg/kg)	OXY (100 mg/kg)	OXY + PIP (100 + 10 mg/kg)
Oxyresveratrol				
C_{max} ($\mu\text{g/L}$)	N/A	N/A	977.99 \pm 649.59	1,580.99 \pm 674.31*
T_{max} (h)	N/A	N/A	2.08 \pm 1.11	1.30 \pm 0.67
AUC _{0-t} ($\mu\text{g}\cdot\text{h/L}$)	825.60 \pm 545.26	1,455.90 \pm 1,953.48	5,133.32 \pm 1,227.78	7,837.18 \pm 2,603.81*
AUC _{0-inf} ($\mu\text{g}\cdot\text{h/L}$)	825.80 \pm 545.18	1,471.00 \pm 1,945.62	5,431.21 \pm 1,022.82	9,375.27 \pm 1,974.32*
MRT (h)	1.40 \pm 0.29	1.60 \pm 0.42	7.25 \pm 4.07	11.66 \pm 8.11
V_d (L/kg)	47.30 \pm 42.97	68.60 \pm 60.02	105.10 \pm 73.82	138.10 \pm 112.83
CL (L/h/kg)	16.90 \pm 9.30	14.60 \pm 8.57	19.05 \pm 4.06	11.09 \pm 2.52
$T_{1/2}$ (h)	1.70 \pm 0.77	2.80 \pm 1.60	3.72 \pm 1.95	8.67 \pm 6.55
Relative bioavailability (%)	100	178	100	173
Oxyresveratrol glucuronide				
AUC _{0-t} ($\mu\text{g}\cdot\text{h/L}$)	20,875.50 \pm 19,742.93	1,190.60 \pm 231.25	10,518.33 \pm 6,239.13	6,977.34 \pm 811.94
AUC _{0-inf} ($\mu\text{g}\cdot\text{h/L}$)	20,875.80 \pm 19,742.99	1,640.00 \pm 743.29	10,993.61 \pm 6,140.74	7,491.24 \pm 522.99
Ratio of AUC _{oxyresveratrol glucuronide} /AUC _{oxyresveratrol}	25.28	1.11	2.02	0.80*

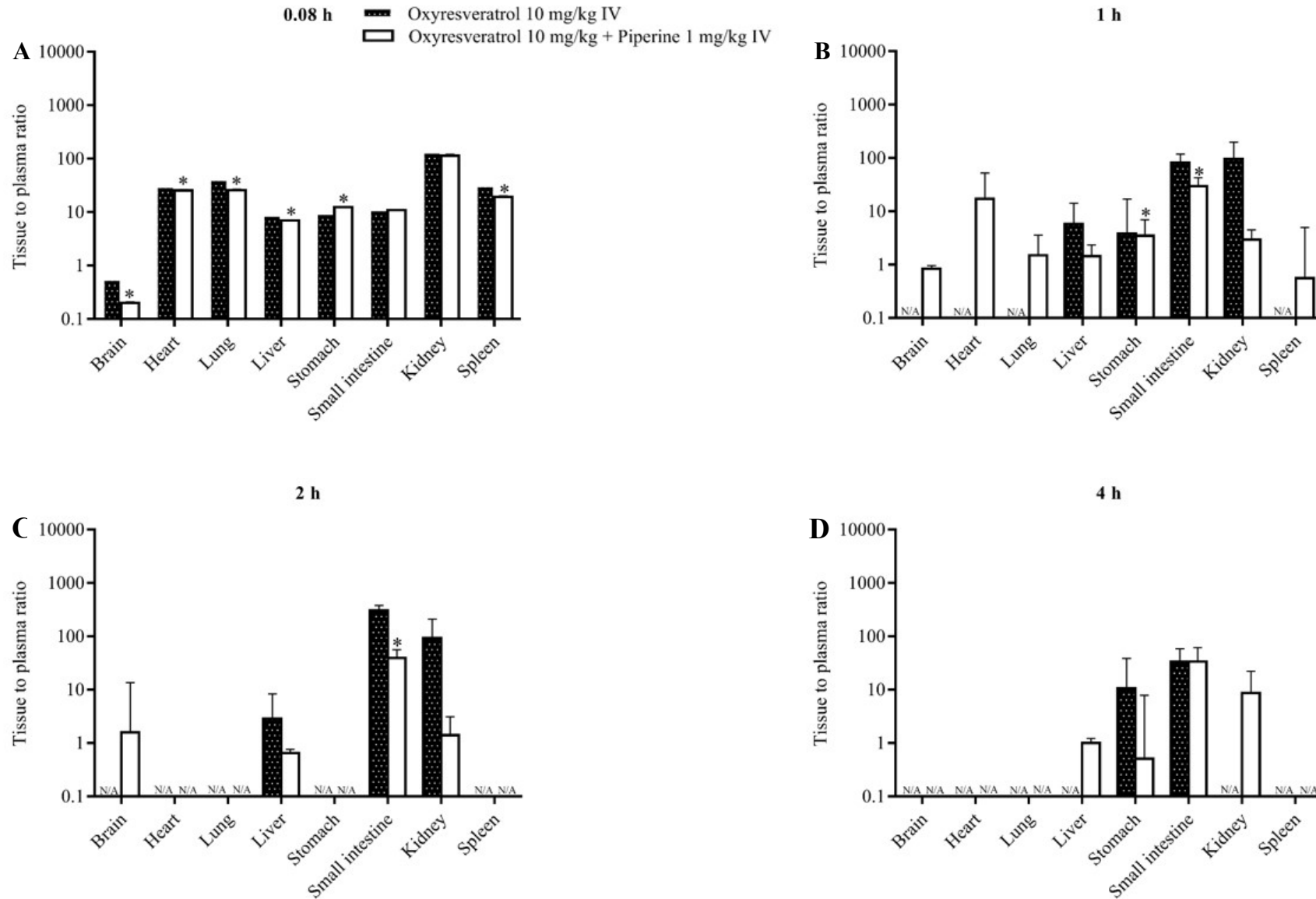
Data are presented as mean \pm S.D. (n = 6), * p <0.05 for oxyresveratrol alone vs oxyresveratrol + piperine.

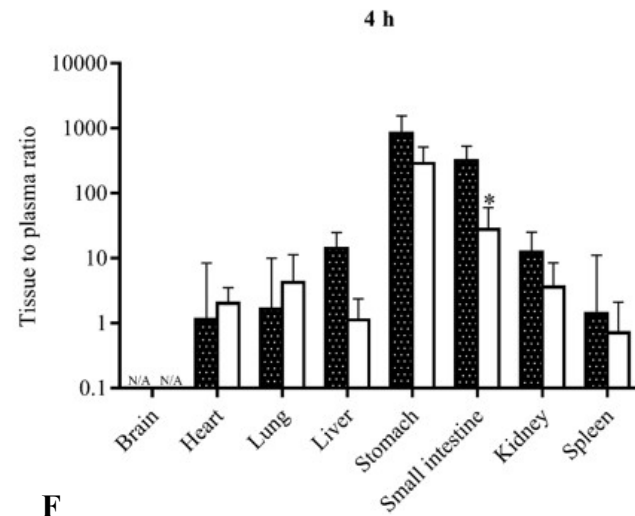
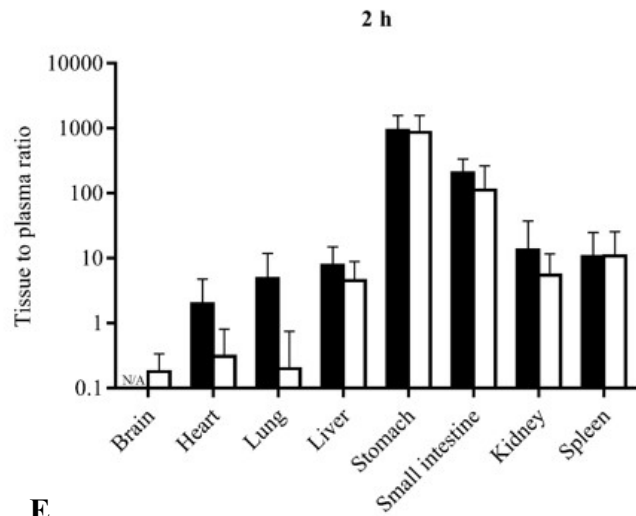
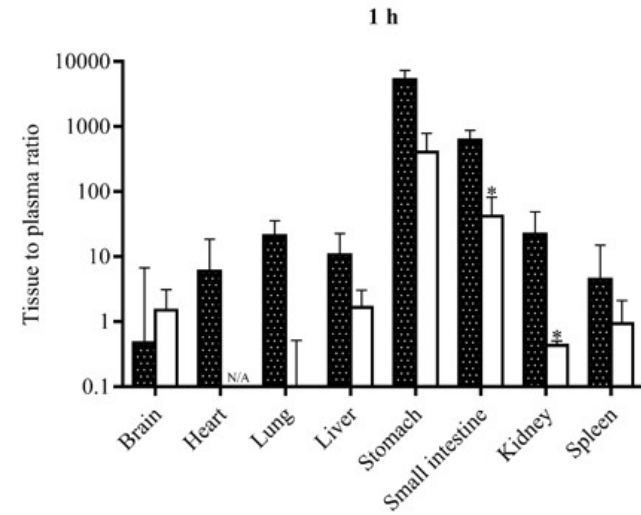
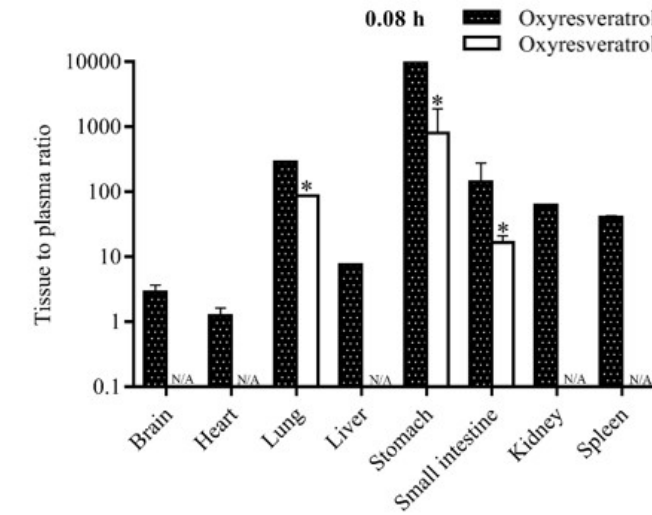
Table 3. Percent recovery of oxyresveratrol alone and in combination with piperine.

Recovery (%)	Intravenous		Oral	
	Oxyresveratrol (10 mg/kg)	Oxyresveratrol + piperine (10 + 1 mg/kg)	Oxyresveratrol (100 mg/kg)	Oxyresveratrol + piperine (100 + 10 mg/kg)
Unchanged Oxyresveratrol				
Urine 0-24h	8.51 ± 7.07	5.06 ± 3.22	3.70 ± 3.41	0.88 ± 0.46
Urine 24-48h	2.87 ± 1.34	1.78 ± 1.33	0.32 ± 0.08	0.27 ± 0.18
Feces 0-24h	0.23 ± 0.20	0.17 ± 0.53	0.21 ± 0.17	0.24 ± 0.43
Feces 24-48h	0.17 ± 0.16	0.11 ± 0.01	0.11 ± 0.06	0.10 ± 0.03
Oxyresveratrol glucuronide				
Urine 0-24h	29.44 ± 28.07	10.55 ± 9.71	9.89 ± 6.90	7.81 ± 6.68
Urine 24-48h	1.39 ± 0.73	0.71 ± 0.57	3.07 ± 2.69	0.09 ± 0.05*
Feces 0-24h	0.20 ± 0.16	0.63 ± 0.58	0.19 ± 0.16	0.10 ± 0.08
Feces 24-48h	0.30 ± 0.29	0.18 ± 0.01	0.20 ± 0.18	0.14 ± 0.06

Data are presented as mean ± S.D. (n = 6), * $p < 0.05$ for oxyresveratrol alone vs oxyresveratrol + piperine.

Figure 2. Tissue to plasma ratios of oxyresveratrol alone (black bars) and in combination with piperine (white bars) after intravenous dosing (A, B, C, D), or after oral dosing (E, F, G, H).





E

F

Interestingly, the tissue to plasma ratio of oxyresveratrol in the brain was slightly increased when administered with piperine.

The plasma concentration–time profile of oxyresveratrol glucuronide was shown in Figure 1. The conversion ratio of oxyresveratrol was approximately 2.02 folds with oral administration of oxyresveratrol alone, which was significantly lower to 0.80 folds when combined with piperine. For intravenous administration, the conversion ratio of oxyresveratrol glucuronide also declined after combination with piperine as shown in Table 2. The percentage recovery of unchanged oxyresveratrol in urine was found to be approximately 5–10% of the intravenous dose. A significant amount of oxyresveratrol glucuronide, ranging from 10–30%, was found in urine from 0–48 h after intravenous administration. Less than 1% of unchanged oxyresveratrol and oxyresveratrol glucuronide were detected in feces from 0–48 h after oral or intravenous dosing as illustrated in Table 3.

DISCUSSION

The previous studies demonstrated that oxyresveratrol has many pharmacological activities with low toxicity. It has been widely known that the problem of lead compounds from most of natural resources showed the poor pharmacokinetic profiles.^{10,13,21} The objective of this study was, therefore, to investigate pharmacokinetic profiles of oxyresveratrol that might be improved by the combination with piperine, which performed as a bioenhancer in rats. During the study, the results indicated that all rats showed good tolerability to the given doses.

According to the result of combination oxyresveratrol and piperine after intravenous administration, the plasma concentration–time profile showed that piperine could increase the plasma level of oxyresveratrol when considering the elimination phase during 8 to 24 h. Similarly, the oral combination revealed a similar pattern with higher levels of oxyresveratrol during the absorption, distribution and elimination phases compared to oxyresveratrol alone. Improvement of intravenous combination might be mainly due to UGT inhibition, meanwhile oral combination could be described by the inhibition of both efflux transporters and UGT enzyme. This result demonstrated that piperine enhanced the plasma concentration of oxyresveratrol both intravenous and oral administration. It was clearly observed that piperine could prolong the MRT of oxyresveratrol after oral dosing. Moreover, C_{\max} and AUC levels were significantly increased which approximately 1.5 folds, with a shorter T_{\max} from 2.08 to 1.30 h. Similar to the study by Johnson *et al.*¹⁴, piperine could improve the concentration of resveratrol with the increase in both C_{\max} and AUC by up to 229% and 1544%, respectively. Resveratrol has a similar structure with oxyresveratrol with less than one hydroxyl group. However, this compound is well known for its pharmacokinetic problems, which is extensively biotransformed by phase II metabolism.^{22–25} Piperine possessed various mechanisms to act as a bioenhancer, for instance, by decreasing UGT metabolism, inhibiting the efflux of P-glycoprotein and increasing the permeation in enterocytes.^{14,18,26,27,28} Interestingly, our data showed a shorter T_{\max} and higher C_{\max} for oxyresveratrol in both formulae compared with other pharmacokinetic studies of oxyresveratrol. A possible explanation for this might be the result of the test formulation used in present study was a clear solution, which would be more readily absorbed than the suspensions used by other studies. The relative bioavailability of oxyresveratrol was also increased up to 173% after the combination with piperine. This is in accordance with Sangsen *et al.*²⁹ that showed self-microemulsifying drug delivery system (SMEDDS) could improve the relative bioavailability of oxyresveratrol by 7.9 folds. Physical modifications by SMEDDS and an addition of bioenhancers showed superior pharmacokinetic profiles of oxyresveratrol than conventional formulation alone.

For tissue distribution, the test compound could penetrate extensively based on the value of V_d at approximately 50 L/kg after intravenous administration. This may be explained by molecular weight of oxyresveratrol of 224.07 Da and with the high lipophilic property of this compound (XLogP 2.8). Moreover, oxyresveratrol was rapidly distributed in to internal

organ since 5 min after administration with a K_p of 10–100, except for the brain. The oxyresveratrol levels in the brain was low at 1, 2, and 4 h after intravenous administration, suggesting that oxyresveratrol has limited deposition in brain tissues. Interestingly, the combination with piperine could slightly increase oxyresveratrol levels in brain tissues particularly at 1–2 h after administration. This result is supported by the study of Mei *et al.*¹³. Oxyresveratrol is a substrate of P-glycoprotein, an efflux transporter located at the blood brain barrier. It is possible that minimal amount of oxyresveratrol in the brain tissues might be due to the restricted xenobiotic penetration and efflux transport of oxyresveratrol from the brain tissues into the circulation. The addition of piperine could improve oxyresveratrol levels in the brain tissues, especially in intravenous administration.

Regarding the excreta, previous studies demonstrated that glucuronidation reaction is the major metabolic pathway for oxyresveratrol. This compound was promptly excreted in urine 0–12 h after administration.^{12,13} Our data is consistent with previous reports that the main route of oxyresveratrol excretion is the urinary system when considering the percentages of unchanged oxyresveratrol and oxyresveratrol glucuronide from 0–48 h after dosing. This result may be due to the fact that oxyresveratrol becomes more hydrophilic by biotransformation via metabolic conjugation to monoglucuronide oxyresveratrol. After intravenous dosing of oxyresveratrol alone, the conversion ratio of oxyresveratrol to glucuronide metabolites was 25.28. The conversion ratio was declined to 1.11 after intravenous dosing and 0.80 after oral dosing in the combination with piperine. These results suggest that piperine could reduce the glucuronide reaction of oxyresveratrol.

CONCLUSIONS

The pharmacokinetic parameters of oxyresveratrol were improved by adding piperine as a bioenhancer in both intravenous and oral administration. For oral administration, C_{max} and AUC levels were significantly increased when combined with piperine. Oxyresveratrol in brain tissues was improved after intravenous administration. Regarding metabolites, piperine significantly decreased glucuronide metabolites of oxyresveratrol. Pharmacokinetic information obtained from this study could pave the way to the development of oxyresveratrol plus piperine as a phytopharmaceutical product.

REFERENCES

1. Sritularak B, De-Eknamkul W, Likhitwitayawuid K. Tyrosinase inhibitors from *Artocarpus lakoocha*. *Thai J Pharm Sci* 1998;22:149–55.
2. Likhitwitayawuid K, Sornsute A, Sritularak B, Ploypradith P. Chemical transformations of oxyresveratrol (2,4,3',5'-tetrahydroxystilbene) into a potent tyrosinase inhibitor and a strong cytotoxic agent. *Bioorg Med Chem Lett* 2006;16:5650–3.
3. Tengamnuay P, Pengrungruangwong K, Pheansri I, Likhitwitayawuid K. *Artocarpus lakoocha* heartwood extract as a novel cosmetic ingredient: evaluation of the in vitro anti-tyrosinase and in vivo skin whitening activities. *Int J Cosmet Sci* 2006;28:269–76.
4. Aftab N, Likhitwitayawuid K, Vieira A. Comparative antioxidant activities and synergism of resveratrol and oxyresveratrol. *Nat Prod Res* 2010;24:1726–33.
5. Ashraf MI, Shahzad M, Shabbir A. Oxyresveratrol ameliorates allergic airway inflammation via attenuation of IL-4, IL-5, and IL-13 expression levels. *Cytokine* 2010;76:375–81.
6. Chung KO, Kim BY, Lee MH, Kim YR, Chung HY, Park JH, Moon JO. In-vitro and in-vivo anti-inflammatory effect of oxyresveratrol from *Morus alba* L. *J Pharm Pharmacol* 2003;55:1695–700.

7. Galindo I, Hernáez B, Berná J, Fenoll J, Cenis JL, Escribano JM, Alonso C. Comparative inhibitory activity of the stilbenes resveratrol and oxyresveratrol on African swine fever virus replication. *Antiviral Res* 2011;91:57–63.
8. Lipipun V, Sasivimolphan P, Yoshida Y, Daikoku T, Sritularak B, Ritthidej G, Likhitwitayawuid K, Pramyothin P, Hattori M, Shiraki K. Topical cream-based oxyresveratrol in the treatment of cutaneous HSV-1 infection in mice. *Antiviral Res* 2011;91:154–60
9. Weber JT, Lamont M, Chibrikova L, Fekkes D, Vlug AS, Lorenz P, Kreutzmann P, Slemmer JE. Potential neuroprotective effects of oxyresveratrol against traumatic injury. *Eur J Pharmacol* 2012;680:55–62.
10. Chen W, Yeo SCM, Elhennawy MGAA, Lin HS. Oxyresveratrol: A bioavailable dietary polyphenol. *J Funct Foods* 2016;22:122–31.
11. Breuer C, Wolf G, Andrabi SA, Lorenz P, Horn TFW. Blood–brain barrier permeability to the neuroprotectant oxyresveratrol. *Neurosci Lett* 2006;393:113–8.
12. Huang HL, Zhang JQ, Chena G T, Lu ZQ, Sha N, Guo DA. Simultaneous determination of oxyresveratrol and resveratrol in rat bile and urine by HPLC after oral administration of *Smilax china* extract. *Nat Prod Commun* 2009;4:825–30.
13. Mei M, Ruan JQ, Wu WJ, Zhou RN, Lei JP, Zhao HY, Yan R, Wang YT. In vitro pharmacokinetic characterization of mulberroside A, the main polyhydroxylated stilbene in mulberry (*Morus alba* L.), and its bacterial metabolite oxyresveratrol in traditional oral use. *J Agric Food Chem* 2012;60:2299–308.
14. Johnson JJ, Nihal M, Siddiqui CO, Bailey HH, Mukhtar H, Ahmad N. Enhancing the bioavailability of resveratrol by combining it with piperine. *Mol Nutr Food Res* 2011;55:1169–76.
15. Sun Y, Xia ZY, Zheng JK, Qiu PJ, Zhang LJ, McClements DJ, Xiao H. Nanoemulsion-based delivery systems for nutraceuticals: Influence of carrier oil type on bioavailability of pterostilbene. *J Funct Foods* 2015;13:61–70.
16. Suresh D, Srinivasan K. Influence of curcumin, capsaicin, and piperine on the rat liver drug–metabolizing enzyme system in vivo and in vitro. *Can J Physiol Pharmacol* 2006;84:1259–65.
17. Atal CK, Dubey RK, Singh J. Biochemical basis of enhanced drug bioavailability by piperine: evidence that piperine is a potent inhibitor of drug metabolism. *J Pharmacol Exp Ther* 1985;232:258–62.
18. Bhardwaj RK, Glaeser H, Becquemont L, Klotz U, Gupta SK, Fromm MF. Piperine, a major constituent of black pepper, inhibits human P-glycoprotein and CYP3A4. *J Pharmacol Exp Ther* 2002;302:645–50.
19. Huang H, Chen G, Lu Z, Zhang J, Guo DA. Identification of seven metabolites of oxyresveratrol in rat urine and bile using liquid chromatography/tandem mass spectrometry. *Biomed Chromatogr* 2010;24:426–32.
20. Basu S, Patel VB, Jana S, Patel H. Liquid chromatography tandem mass spectrometry method (LC–MS/MS) for simultaneous determination of piperine, cinnamic acid and gallic acid in rat plasma using a polarity switch technique. *Anal Methods* 2013;5:967–76.
21. Hu N, Mei M, Ruan J, Wu W, Wang Y, Yan R. Regioselective glucuronidation of oxyresveratrol, a natural hydroxystilbene, by human liver and intestinal microsomes and recombinant UGTs. *Drug Metab Pharmacokinet* 2014;29:229–36.
22. aur JA, Sinclair DA. Therapeutic potential of resveratrol: the in vivo evidence. *Nat Rev Drug Discov* 2006;5:493–506.
23. Das S, Lin HS, Ho PC, Ng KY. The impact of aqueous solubility and dose on the pharmacokinetic profiles of resveratrol. *Pharm Res* 2008;25:2593–600.
24. Marier JF, Vachon P, Gritsas A, Zhang J, Moreau JP, Ducharme MP. Metabolism and disposition of resveratrol in rats: Extent of absorption, glucuronidation,

- and enterohepatic recirculation evidenced by a linked-rat model. *Journal of Pharmacology and Experimental Therapeutics* 2002;302:369–73.
25. Ndiaye M, Kumar R, Ahmad N. Resveratrol in cancer management: where are we and where we go from here? *Annals of the New York Academy of Sciences* 2011;1215:144–9.
 26. Shoba G, Joy D, Joseph T, Majeed M, Rajendran R, Srinivas PS. Influence of piperine on the pharmacokinetics of curcumin in animals and human volunteers. *Planta Medica* 1998;64:353–6.
 27. Lambert JD, Hong J, Kim DH, Mishin VM, Yang CS. Piperine enhances the bioavailability of the tea polyphenol [–]–epigallocatechin-3-gallate in mice. *Journal of Nutrition* 2004;134:1948–52.
 28. Reen RK, Jamwal DS, Taneja SC, Koul JL, Dubey RK, Wiebel FJ, Singh J. Impairment of UDP–glucose dehydrogenase and glucuronidation activities in liver and small intestine of rat and guinea pig in vitro by piperine. *Biochemical Pharmacology* 1993;46:229–38.
 29. Sangsen Y, Sooksawate T, Likhitwitayawuid K, Sritularak B, Wiwattanapatapee R. A self-microemulsifying formulation of oxyresveratrol prevents amyloid beta protein-induced neurodegeneration in mice. *Planta Medica* 2018;84:830–28.

PH-029

Interspecies differences in pharmacokinetic and metabolic profiles of triterpenoid glycosides in standardized extract of *Centella asiatica*, ECa 233

Phanit Songvut¹, Tosapol Anukunwithaya¹, Pajaree Chariyavilaskul²,
Mayuree H. Tantisira³ and Phisit Khemawoot^{1,4,5}

¹ Department of Pharmacology and Physiology, Faculty of Pharmaceutical Sciences, Chulalongkorn University, Bangkok, Thailand.

² Clinical Pharmacokinetics and Pharmacogenomics Research Unit, Department of Pharmacology, Faculty of Medicine, Chulalongkorn University, Bangkok, Thailand.

³ Faculty of Pharmaceutical Sciences, Burapha University, Chonburi, Thailand.

⁴ Preclinical Pharmacokinetics and Interspecies Scaling for Drug Development Research Unit, Chulalongkorn University, Bangkok, Thailand.

⁵ Department of Biochemistry and Microbiology, Faculty of Pharmaceutical Sciences, Chulalongkorn University, Bangkok, Thailand.

ABSTRACT

INTRODUCTION: ECa 233, a well-characterized standardized extract of *Centella asiatica*, demonstrated favorable safety profiles and pharmacological benefits in preclinical evaluations, particularly in term of improving cognitive impairment. To indicate this newly developed ECa 233 could be potentially useful in human, understanding of interspecies pharmacokinetics and its metabolic profiles should be verified in the initial steps for its development as phytopharmaceutical products.

OBJECTIVES: The aims of this study were to investigate the species differences in pharmacokinetic profiles and metabolic pathways of triterpenoid glycosides in ECa 233, especially comparison between rodents and humans following single and repeated oral administrations.

METHODS: In order to explicate the plasma concentration-time profiles of metabolites across species, this study carried out pharmacokinetics in Wistar rats and healthy Thai volunteers. The modified and validated LC-MS/MS method was used to simultaneously determine the concentration of all major bioactive compounds in plasma samples and the pharmacokinetic parameters were calculated using non-compartmental analysis.

RESULTS: Considering the metabolic pathway of ECa 233, the two major parent compounds which are triterpenoid glycosides, madecassoside and asiaticoside, have biotransformed to the two mainly active metabolites, madecassic acid and asiatic acid, respectively. Interestingly, plasma concentrations of those two metabolites in healthy volunteers are much higher when compared to the concentrations of their respective parent compounds. These results are contrary to the pharmacokinetic findings in rats, where the parent compounds were obviously observed in rat plasma while their metabolites could not be detected even in plasma concentration-time profiles. This discrepancy between rodents and humans suggests that there may be species differences in the biotransformation of triterpenoid glycoside in ECa 233, which could be due to the influence of human gut microbiota or to enzymes associated with glycosides hydrolysis. The safety assessment of ECa 233 was well tolerated in rats and also healthy volunteers whether it was administered as single or multiple doses. There were no significant changes in laboratory testing or any physical appearances throughout the dose escalation studies both in animals and humans.

CONCLUSIONS: The overall results of oral metabolic profiles showed strongly interspecies differences; however, the corresponding safety profiles across species were similar. This newly developed ECa 233 could be considered as a candidate for phytopharmaceutical product in human use.

Keywords: *Centella asiatica*, metabolic profiles, pharmacokinetics, triterpenoid glycosides, triterpenic acid

INTRODUCTION

Cognitive impairment is defined as difficulty in processing thoughts that leads to memory loss and decline in learning ability [1]. Based on several preclinical pharmacology evaluations, there is increased interest in the efficacy of *Centella asiatica* (Linn.), especially in terms of ameliorating learning and memory deficit [2, 3]. Thus, researchers at the Faculty of Pharmaceutical Sciences, Chulalongkorn University, have developed a standardized extract of *C. asiatica* named 'ECa 233' containing triterpenoid glycosides not less than 80% [4], which has a consistent ratio of madecassoside (MDS) and asiaticoside (ASS) within $1.5 \pm 0.5:1$ [5]. To comply with regulations on developing products for medical use in humans, preclinical pharmacokinetics are required in the initial steps of this study. Therefore, the pharmacokinetics of ECa 233 was first investigated in rats. The study demonstrated that when ECa 233 was orally given at doses of 50 to 200 mg/kg, MDS and ASS were rapidly but not completely absorbed from the gastrointestinal tract. Their highest concentration in plasma could be detected within 5-15 minutes; however, those parent compounds had poor oral bioavailability after oral administration in rats [6]. The accumulation of MDS and ASS could be observed in rodent tissues, especially in hippocampus after multiple oral dosing in rats. In addition, ECa 233 also showed excellent efficacy and good tolerability in rat models with defect in memory and learning ability. It could consider that ECa 233 has potential benefits to develop as phytopharmaceutical products for cognitive impairment in human use.

For the first time medicinal product is administered to humans, the additional pharmacokinetics of ECa 233 in different species should be verified, particularly in metabolic pathway of major components of the test compound. This study, therefore, focuses on the differences in metabolic profiles of triterpenoid glycosides in ECa 233 between rats and humans.

MATERIALS AND METHODS

Chemicals and Reagents

Standardized extract of *Centella asiatica*, ECa 233, as a raw material was provided by Siam Herbal Innovation Co., Ltd. (Lot number MRA 0816001, madecassoside 49.33%, asiaticoside 43.12%). The newly developed ECa 233 capsules were formulated by Pharma Neuva Co., Ltd. (101.8% label amount of total triterpene derivatives, Lot number K17EC003002/1) in accordance with an approval quality standard of Good Manufacturing Practice. Analytical standards of asiaticoside (purity > 98.5%) and asiatic acid (purity > 97.0%) were purchased from Sigma-Aldrich Corp.; madecassoside (purity > 96.7%) and madecassic acid (purity > 97.5%) were purchased from Chromadex Corp. The glycyrrhizin (purity > 90.0%) and glycyrrhetic acid (purity > 98.0%) used as the internal standard were obtained from Wako Pure Chemical Industries, Ltd.

Animals Pharmacokinetic Study

The protocol was reviewed and approved by the Institutional Animal Care and Use Committee, IACUC of the Faculty of Pharmaceutical Sciences, Chulalongkorn University (approval number 13-33-007, approval date: March 4, 2013). Male Wistar rats, aged 15-30 weeks, were housed in a controlled environment at temperature 22 ± 1 °C and under 12:12 h light-dark cycle, with free access to food and water. At least 10 h prior to the beginning of pharmacokinetic study, rats were kept in metabolic cages without any food provided, but with water still available *ad libitum*. The formulation of ECa 233 was freshly prepared in 20% v/v DMSO/NSS solution and was then given to randomized rats at 100 mg/kg by oral administration. For multiple dosing, rats received 100 mg/kg of ECa 233 solution for seven consecutive days. 300 μ L of blood samples were taken from the lateral tail vein at 0 (pre-dose), 5, 15, 30 min, and 1, 2, 4, 8, 16, 24 h after dosing. All serial blood samples were kept in heparinized tubes, then the plasma was separated from the samples using centrifugation at $1,500 \times g$ for 10 min and stored at -70 °C until analysis.

Healthy Thai Volunteers Pharmacokinetic Study

The safety and pharmacokinetic study of ECa 233 in healthy Thai volunteers was designed as an open-labeled, orally single and multiple dosing study under fasting conditions. The study protocol was approved by the Institutional Review Board, IRB of the Faculty of Medicine, Chulalongkorn University and Thai Clinical Trials Registry (TCTR 20171107002, approval date: November 6, 2017). All clinical procedures were performed in compliance with the International Conference on Harmonization-Good Clinical Practice and the Declaration of Helsinki.

Twelve healthy Thai volunteers were enrolled in this study. They were aged 18-50 years old, with a body mass index of 18-25 kg/m². For the single dose, all volunteers were assigned to take one capsule, 250 mg of ECa 233. Venous blood samples were collected at pre-dose and 0.25, 0.50, 1, 2, 4, 8 and 24 h post-dose via a forearm vein catheter. For multiple dosing, all subjects were administered one capsule of ECa 233 every morning for the following seven consecutive days. After a three-week washout period, a 500 mg dose was administered in the same group of subjects, using the same pharmacokinetic blood sampling time points. Blood samples were then centrifuged at 1,500 × g for 10 min and plasma samples were kept at -70 °C until further analysis.

Bioanalysis of ECa 233 Bioactive Compounds in Plasma

The plasma concentration of all major components were determined according to a modification of the previously published liquid chromatography tandem mass spectrometry method [6] developed at the Department of Pharmacology and Physiology, Faculty of Pharmaceutical Sciences, Chulalongkorn University. This LC-MS/MS method was validated according to the International Conference on Harmonization (ICH) Guidelines “Validation of Analytical Procedures” [7].

Sample preparation was performed by protein precipitation in the presence of internal standards. Briefly, 50 µL of plasma samples were extracted with 200 µL of methanol containing internal standards. After vortex mixing for approximately 10 min, the mixtures were then centrifuged at 12,000 × g and 4 °C for 10 min. The supernatants were injected into the LC-MS/MS system which was performed using LCMS-8060 (Shimadzu Corp.) equipped with a triple quadrupole mass spectrometer. The electrospray ionization was conducted in the negative ion mode and the multiple-reaction monitoring mode was used for quantification. The samples were separated on C18 reversed phase column, model Phenomenex Synergi Fusion-RP with Guard C18 column (Phenomenex, Inc.) using mobile phase consisting of 100% methanol and 0.2% formic acid in water with a gradient system (0.0–0.5 min 10% methanol, 0.5–3.0 min 90% methanol, 3.0–5.0 min 10% methanol) at a flow rate of 0.5 mL/min and 10 µL injection volume. The precursor/product ion transitions of madecassoside, asiaticoside, madecassic acid, asiatic acid, glycyrrhizin, and glycyrrhetic acid were 973.40/503.30, 957.40/469.20, 503.25/437.15, 487.30/409.45, 821.25/350.90, and 469.35/409.40, respectively.

Pharmacokinetic Analysis

Pharmacokinetic parameters were determined by non-compartmental analysis using PK solutions software, version 2.0 (Summit Research Services). The maximum concentration of target compounds (C_{max}) and the time to reach maximum concentration (T_{max}) were taken directly from the individual plasma concentration versus time profile. The area under the curve from time zero to the last sampling time (AUC_{0-t}) was estimated using the linear trapezoidal rule.

RESULTS

Rodent Pharmacokinetic Profiles

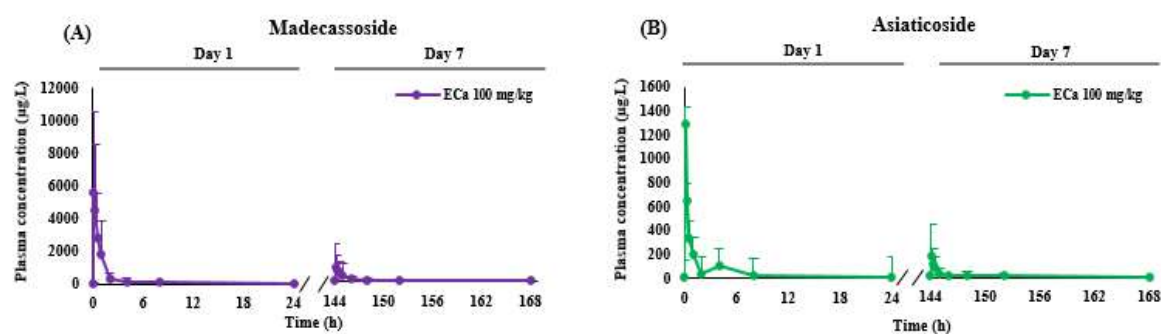


Figure 1. Rats plasma concentration versus time profiles of (A) madecassoside and (B) asiaticoside after single or multiple oral dosing 100 mg/kg of ECa 233. Data are presented as means \pm SD ($n = 9$). The levels of madecassic acid and asiatic acid were below LLOQ.

Table 1. Pharmacokinetic parameters of madecassoside and asiaticoside after oral dosing of ECa 233 (100 mg/kg/day) on days 1 and 7.

Pharmacokinetic parameters	Parent compounds (Triterpenoid glycosides)			
	Madecassoside		Asiaticoside	
	Day 1	Day 7	Day 1	Day 7
	ECa 233 100 mg/kg	ECa 233 100 mg/kg	ECa 233 100 mg/kg	ECa 233 100 mg/kg
C_{max}^a ($\mu\text{g/L}$)	5713.00 ± 5069.38	$948.03 \pm 1449.37^*$	1281.60 ± 407.48	$209.62 \pm 250.74^*$
T_{max}^a (h)	0.17 ± 0.14	1.30 ± 2.72	0.08 ± 0.00	1.50 ± 3.19
AUC^a ($\mu\text{g}\cdot\text{h/L}$)	7361.88 ± 4195.27	$1604.40 \pm 2066.20^*$	11.498 ± 713.29	$306.78 \pm 234.37^*$

Notes: ^adata are expressed as mean \pm SD ($n = 9$); * $p < 0.05$ pharmacokinetic parameters on day 1 vs. day 7.

Abbreviations: C_{max} , maximum plasma concentration; T_{max} , time to reach C_{max} ; AUC, area under the plasma concentration–time curve from time zero to the last measurable concentration.

Table 2. Pharmacokinetic parameters of madecassic acid and asiatic acid after oral administration of ECa 233 capsules in healthy volunteers, comparing single and multiple doses.

Pharmacokinetic parameters	Active metabolites (Triterpenic acid)							
	Madecassic acid				Asiatic acid			
	Day 1		Day 7		Day 1		Day 7	
	250 mg ($n = 11$)	500 mg ($n = 10$)	250 mg ($n = 11$)	500 mg ($n = 10$)	250 mg ($n = 11$)	500 mg ($n = 10$)	250 mg ($n = 11$)	500 mg ($n = 10$)
C_{max}^a ($\mu\text{g/L}$)	40.92 ± 25.78	52.14 ± 18.67	42.71 ± 21.06	80.79 ± 27.76	38.02 ± 12.21	$84.08 \pm 33.91^*$	51.28 ± 17.91	$116.62 \pm 32.26^*$
T_{max}^a (h)	2.09 ± 2.02	1.70 ± 0.95	2.18 ± 2.14	1.5 ± 0.53	3.00 ± 3.22	1.05 ± 0.37	2.18 ± 2.14	1.65 ± 2.24
AUC^a ($\mu\text{g}\cdot\text{h/L}$)	348.44 ± 362.47	357.20 ± 116.65	412.66 ± 375.88	681.05 ± 413.17	434.13 ± 195.72	$724.75 \pm 259.98^*$	624.97 ± 277.14	$1202.29 \pm 293.37^*$

Notes: ^adata are expressed as mean \pm SD; * $p < 0.05$ for significant differences.

Abbreviations: C_{max} , maximum plasma concentration; T_{max} , time to reach C_{max} ; AUC, area under the plasma concentration–time curve from time zero to the last measurable concentration.

Human Pharmacokinetic Profiles

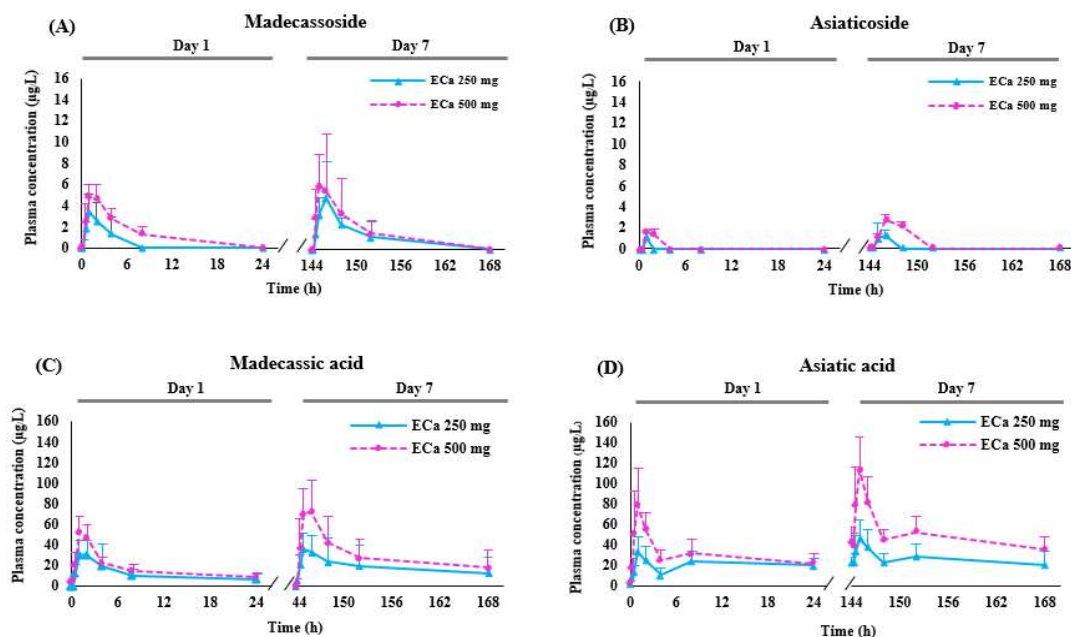


Figure 2. Plasma concentration versus time profiles of (A) madecassoside, (B) asiaticoside, (C) madecassic acid, and (D) asiatic acid after single or multiple dose oral administration of 250 mg or 500 mg ECa 233 capsules. Data are presented as means \pm SD ($n = 10-11$).

DISCUSSION

The pharmacokinetic parameters of ECa233 oral administration in rats and human are listed in Table 1 and 2, respectively. The results in human pharmacokinetic study (Figure 2) showed that the plasma concentrations of metabolites, madecassic acid (2C) and asiatic acid (2D), were higher than the concentrations of their respective parent compounds, madecassoside (2A) and asiaticoside (2B), in both single and multiple dosing. These data support the previous hypothesis that the two major parent compounds have been biotransformed into active metabolites in the human body [8, 9]. This finding in human pharmacokinetics seems contrary to the results of pharmacokinetics in rats (Figure 1). The parent compounds were mainly observed while their metabolites could not be detected in the plasma concentration-time curve of rats [6, 10]. These different findings in the metabolic profiles of humans and rats suggest that there may be a species difference in the metabolic profiles of triterpenoid glycosides in ECa 233. According to previous report, human gut microbiota had an influence on the biotransformation of the major parent compound (madecassoside and asiaticoside) and contributed higher plasma concentration of triterpenic acid metabolites (madecassic acid and asiatic acid) [9]. Physical and biochemical profiles of rats and subject demographics of healthy volunteers are shown in Table 3 and 4, respectively. ECa 233 were safe and well tolerated in both species since there were no significant changes in vital signs, physical examinations, or any clinical biochemical laboratory tests.

Considering the current understanding in disposition kinetics of ECa 233, MDS and ASS are not easily absorbed from the gastrointestinal tract since they are glycosides, which contain large hydrophilic sugars. They are also resistant to gastric acid or any digestive enzymes [11], so they are mostly retained in the GI tract. Thus, these glycosides can pass through the upper intestinal tract then continue to exist in the lower tract, where numerous anaerobes are present as resident microbiota. Consequently, these unabsorbed glycosides, madecassoside and asiaticoside are hydrolyzed to aglycones, madecassic acid and asiatic acid, by enzymes produced by intestinal bacteria; this is probably *Eubacterium* spp., which can produce β -glycosidase, an enzyme responsible for hydrolyzing glycosides [9, 11]. Based on

the human plasma concentration-time profiles observation, the accumulation of asiatic acid after repeated doses is highly suggestive. This accumulation might be associated with a recirculation of metabolite profiles, as mentioned in a previous study [8].

Safety and tolerability assessments in rats and healthy volunteers

Table 3. Physical and biochemical profiles of rats pre- and post-treatment with oral dosing of ECa 233 (100 mg/kg/day) for 7 consecutive days.

Demographic data	Baseline	ECa 233, 100 mg/kg
Physical appearance	Normal	Normal
Clinical laboratory screening ^a		
Creatinine (mg/dL)	0.21 ± 0.03	0.22 ± 0.04
SGOT, AST (U/L)	61.56 ± 11.45	74.11 ± 35.94
SGPT, ALT (U/L)	18.67 ± 7.53	22.00 ± 7.27

^aData expressed as mean ± SD, (n = 9).

Table 4. Demographic and baseline characteristic data of participants administered 250 and 500 mg ECa 233 capsules.

Demographic data	Baseline	ECa 233, 250 mg	ECa 233, 500 mg
Gender, % (n)			
Female		36% (n=4)	40% (n=4)
Male		64% (n=7)	60% (n=6)
Age at enrollment ^b (year)		31.3 ± 8.79	30.55 ± 8.71
Body mass index ^{a,b} (kg/m ²)		22.15 ± 1.94	21.93 ± 1.98
Systolic blood pressure (mmHg)	118 ± 10	112 ± 9	115 ± 13
Diastolic blood pressure (mmHg)	66 ± 8	65 ± 12	65 ± 12
Body temperature (°C)	36.7 ± 0.3	36.5 ± 0.2	36.6 ± 0.2
Clinical laboratory screening ^b			
White blood cell (x10 ³ /μL)	7.37 ± 1.67	6.76 ± 1.42	6.16 ± 1.42
Red blood cell (x10 ⁶ /μL)	5.31 ± 0.36	5.15 ± 0.40	4.99 ± 0.40
Hemoglobin (g/dL)	13.8 ± 1.3	13.3 ± 1.2	13.0 ± 1.3
Platelet (x10 ³ /μL)	270 ± 40	277 ± 66	274 ± 58
Fasting blood glucose (mg/dL)	87.36 ± 6.36	85.09 ± 5.92	83.50 ± 5.84
Blood urea nitrogen (mg/dL)	12 ± 4	13 ± 4	14 ± 4
Creatinine (mg/dL)	0.81 ± 0.15	0.85 ± 0.19	0.86 ± 0.14
Albumin (g/dL)	4.33 ± 0.25	4.26 ± 0.24	4.26 ± 0.23
Total bilirubin (mg/dL)	0.72 ± 0.35	0.59 ± 0.23	0.62 ± 0.30
SGOT, AST (U/L)	21 ± 7	20 ± 6	20 ± 8
SGPT, ALT (U/L)	25 ± 17	22 ± 11	22 ± 12
Alkaline phosphatase (U/L)	64 ± 21	58 ± 17	60 ± 18
Total cholesterol (mg/dL)	179 ± 25	189 ± 25	178 ± 27
Triglycerides (mg/dL)	92 ± 47	78 ± 32	72 ± 17
HDL cholesterol (mg/dL)	57 ± 8	53 ± 7	54 ± 8
LDL cholesterol (mg/dL, calculated)	103 ± 24	120 ± 24	110 ± 26
Sodium (mmol/L)	139 ± 1	139 ± 1	142 ± 1
Chloride (mmol/L)	105 ± 2	106 ± 3	107 ± 2
Potassium (mmol/L)	4.2 ± 0.2	4.3 ± 0.3	4.1 ± 0.2
Calcium (mg/dL)	9.5 ± 0.3	9.5 ± 0.3	9.2 ± 0.3
Magnesium (mg/dL)	2.4 ± 0.2	2.5 ± 0.1	2.4 ± 0.2
Phosphorus (mg/dL)	3.5 ± 0.5	3.6 ± 0.5	3.8 ± 0.5

^aBMI was defined as the [body mass](#) divided by the [square](#) of the [body height](#).

^bData expressed as mean ± SD, (n = 10-11).

Decimal numbers were reported according to laboratory standard of Chula Clinical Research Laboratory, Chula Clinical Research Center, Faculty of Medicine, Chulalongkorn University.

Actually, ASS seems to be mostly biotransformed by microflora to become ASA [12], leading to the availability of metabolite profile, and in turn to the increased asiatic acid in blood circulation that occurred in humans but not in rats. This difference indicates an interspecies variation in the metabolic profiles of triterpenoid glycosides in ECa 233.

CONCLUSIONS

In summary, there were species differences in metabolic profiles of active components in standardized extract of *C. asiatica*, ECa 233. The parent triterpenoid glycosides were mainly observed in rat plasma, meanwhile metabolite triterpenic acids were major components in humans after oral dosing of ECa 233. Both species were well tolerated to this extract even at repeated dose or high dosage regimen, 100 mg/kg/day in rats and 500 mg/day in healthy volunteers. These new findings support for further strategies of phytopharmaceutical product development from *Centella asiatica*.

REFERENCES

1. Kelley BJ, Petersen RC. Alzheimer's disease and mild cognitive impairment. *Neurol Clin* 2007; 25: 577.
2. Singh RH, Narsimhamurthy K, Singh G. Neuronutrient impact of Ayurvedic Rasayana therapy in brain aging. *Biogerontology* 2008; 9: 369-74.
3. Veerendra Kumar MH, Gupta YK. Effect of different extracts of *Centella asiatica* on cognition and markers of oxidative stress in rats. *J Ethnopharmacol* 2002; 79: 253-60.
4. Saifah E, Suttisri R, Patarapanich C, Laungchonlatan S, Tantisira MH, Tantisira B. Preparation methods of colorless mixture between madecassoside and asiaticoside from *Centella asiatica*. In: Department of Intellectual Property MoC ed. C07H 1/00 ed. Bangkok, Thailand: Chulalongkorn University; 2009.
5. Tantisira MH. Research and development of standardized extract of *Centella asiatica* ECa 233. The International Conference on Herbal and Traditional Medicine KhonKaen, Thailand; 2015.
6. Anukunwithaya T, Tantisira MH, Tantisira B, Khemawoot P. Pharmacokinetics of a standardized extract of *Centella asiatica* ECa 233 in rats. *Planta Med* 2017; 83: 710-7.
7. International Conference on Harmonisation of Technical Requirements for Registration of Pharmaceuticals for Human Use. Validation of analytical procedures: text and methodology Q2 (R1). In, International Conference on Harmonization, Geneva, Switzerland; 2005: 11-2.
8. Leng DD, Han WJ, Rui Y, Dai Y, Xia YF. *In vivo* disposition and metabolism of madecassoside, a major bioactive constituent in *Centella asiatica* (L.) Urb. *J Ethnopharmacol* 2013; 150: 601-8.
9. Rush WR, Murray GR, Graham DJ. The comparative steady-state bioavailability of the active ingredients of madecassol. *Eur J Drug Metab Pharmacokinet* 1993; 18: 323-6.
10. Hengjumrut P, Anukunwithaya T, Tantisira MH, Tantisira B, Khemawoot P. Comparative pharmacokinetics between madecassoside and asiaticoside presented in a standardised extract of *Centella asiatica*, ECa 233 and their respective pure compound given separately in rats. *Xenobiotica* 2018; 48: 18-27.
11. Kobashi K, Akao T. Relation of intestinal bacteria to pharmacological effects of glycosides. *Bioscience and Microflora* 1997; 16: 1-7.
12. Bone K, Mills S. Principles and practice of phytotherapy: modern herbal medicine, 2nd edition. Saint Louis: Churchill Livingstone; 2013.

PH-032

Tape stripping technique in rat skin model for the determination of substance penetration into the dermisSuteera Pumpakdee^{*1} and Suree Jianmongkol^{**2}

¹ *Inter-Department Program of Pharmacology, Graduate School, Chulalongkorn University, Bangkok 10330, Thailand.*

² *Department of Pharmacology and Physiology, Faculty of Pharmaceutical Sciences, Chulalongkorn University, Bangkok 10330, Thailand.*

ABSTRACT

INTRODUCTION: Topical medications deliver drug dermally or transdermally. After application, drug needs to penetrate the stratum corneum (SC), which is the outermost skin layer into the dermis. In the development of new topically administered drugs, particularly those with dermis as their primary site of action, rat model is suitable for pharmacokinetic (PK) and pharmacodynamic (PD) assessment. Thus, epidermal-dermal separation is a technique required for determining drug penetration into the dermis. Among several available separation techniques, tape stripping is a non-invasive method for the removal of epidermal layer. However, there are no well-established protocols when rat skin is employed as the model.

OBJECTIVES: In this study, we validated the tape stripping technique for epidermal-dermal separation in male Sprague Dawley rat skin.

METHODS: We applied constant weight of 700 g on the rat skin surface (1 x 2 cm) covered by 3M™ Transpore™ surgical tape for 30 s per tape before tape detachment. Then the skin was fixed in 4% paraformaldehyde, 30% sucrose prior to cross sectioned and stained with *hematoxylin and eosin*. The thickness of epidermis layer was evaluated under light microscope.

RESULTS: Our results demonstrated that the SC was completely removed without any morphological damages to the skin after 4 consecutive cycles of adhesive tape application and removal.

CONCLUSION: Our procedure offers an easy, effective and cheap method with better outcome that can be applied in PK and PD studies of topical drugs.

Keywords: Rat skin model, tape stripping techniques, epidermal-dermal separation, topical drug.

INTRODUCTION

Animal models such as monkey, rabbit, pig and rat have been used for decades in drug discovery and development. Rat model is the most popular and suitable for pharmacokinetic (PK) and pharmacodynamic (PD) assessment. Topical medications deliver drug dermally or transdermally. After application, drug needs to penetrate the stratum corneum (SC), which is the outermost skin layer, into the dermis and blood circulation. In the development of new topically administered drugs, particularly those with dermis as their primary site of action, the amount of drug retained in the dermis should be accurately quantified to establish PK/PD in skin.

Epidermal-dermal separation is a basic principle technique required for removal of residual drug in SC from that penetrated into the deeper skin layers. There are several

separation techniques such as heat, enzymes, chemicals and mechanical methods.¹⁻³ Among the available separation techniques, tape stripping is a non-invasive method for the removal of epidermal layer.⁴ With this technique, SC is trapped into adhesive tapes and easily removed from the skin. Various protocols of tape stripping techniques have been reported.⁵ However, there are no well-established protocols when rat skin is employed as the model.

In this study, we validated the tape stripping technique for SC removal in male Sprague Dawley rat skin. With the help of constant weight of 700 g per 2 cm² skin area for 30 s per tape, the epidermis layer was completely removed without any morphological damages to the skin after 4 consecutive cycles of adhesive tape application and detachment. Our procedure offers an easy, effective and cheap method with better outcome that can be applied in PK and PD studies of topical drugs.

METHODS

Rat skin

Skins of Sprague Dawley male rats 3-5-weeks of age were donated from Laboratory Animal Center, faculty of Pharmaceutical Sciences, Chulalongkorn University. Whole skin from the back (dorsal) of each rat was shaved and collected at the area of 2 cm² (1 x 2 cm).

Determination the thickness of epidermis layers

Skin samples were fixed in 4% paraformaldehyde for 3 days followed by in 30% sucrose for 1 day. Then the skin tissues were cross-sectioned by a CM1800 cryostat microtome (Leica, Baden-Württemberg, Germany) at -20°C. Each skin section (30 µm) was transferred to a microscope glass slide and stained with *hematoxylin and eosin (H&E)* for 2 days. The stained samples were evaluated under a *Nikon Eclipse E600 light microscope* (Nikon corporation, Tokyo, Japan) equipped with ImageJ program version k 1.45 (U.S. National Institutes of Health, MD, USA). The visual observation was carried out at 10x magnification.

Tape stripping procedure

The adhesive transpore surgical tape (3M™ Transpore™, 3M health care company, MN, USA) was applied covering the skin area of 2 cm². As shown in figure 1, the constant 700 g weight was pressed onto the skin surface for 30 s per tape before tape detachment. This process was repeated up to 15 consecutive cycles of adhesive tape application and removal. The skin was fixed and assessed visually under light microscope as abovementioned.

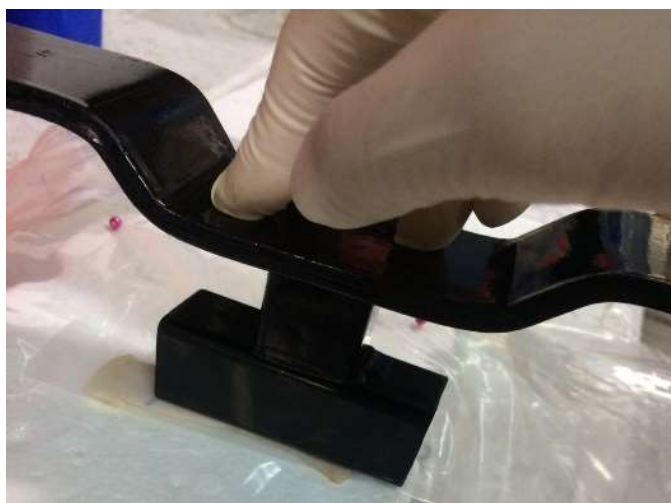


Figure 1. The constant weight used in tape stripping procedure.

RESULTS AND DISCUSSION

The outermost skin layer SC is the initial exposure site of topical administered drugs prior to percutaneous penetration to the deeper region. Figure 2 depicts normal rat skin (3-5 weeks rats) with epidermis and dermis layers. The average epidermal thickness of Sprague Dawley rat skins in this study was $37.584 \pm 1.79 \mu\text{m}$ ($n = 5$). Apparently, the epidermal skin layer of Sprague Dawley rats was slightly thicker than that of hairless male rats ($30.81 \pm 2.83 \mu\text{m}$).⁶ It was reported that the thickness of human and porcine ear epidermal layers was 43 and 60 μm , respectively.

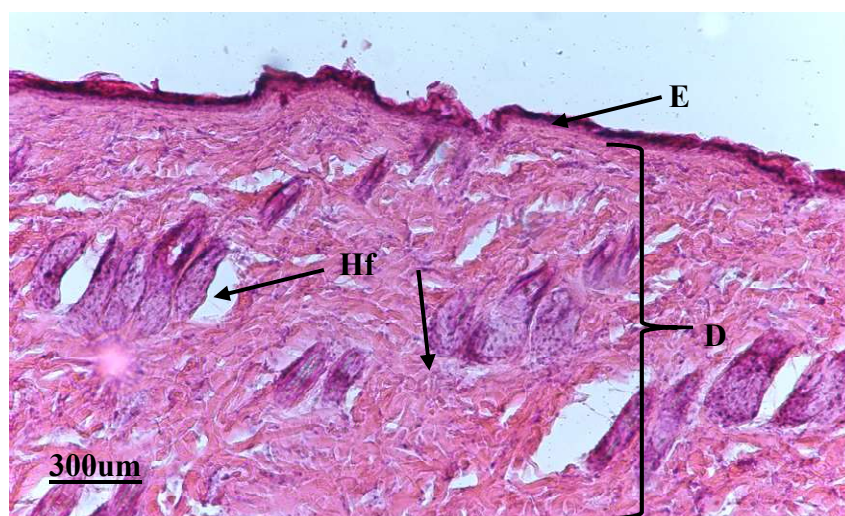


Figure 2. Microscopic anatomy of normal rat skin stained with H&E dye, 10x magnification. Epidermis (E), dermis (D), hair follicles (Hf).

Epidermal-dermal separation is an important step for quantification of drug retained in either epidermis or dermis layers. Tape stripping of SC is a non-invasive procedure to isolate epidermis from other skin layers. With this technique, both epidermis and dermis layers can be collected to further determine drug absorption in skin.⁷ Different protocols of tape stripping method have been reported.⁵ In this study, rat skin was tape stripped with the pressure of constant 700 g weight on 2 cm² shaved skin area for 30 s at various consecutive cycles of adhesive tape application and removal. Figure 3 shows the effect of the number of tape stripping cycles (1-15 times) on SC removal. Our results demonstrated that the SC was completely removed without any morphological damages to the skin after 4 consecutive cycles (Figure 3A-F, Table 1). The number of tape stripping cycles may vary depending on several factors including skin condition, the thickness of epidermal layer, the types of adhesive tape and the pressure applied on skin.⁸ It was reported that porcine ear skin with 60 μm thickness needed 15 tape stripping cycles with the adhesive tape (Scotch®; 3M, S. Paulo, Brazil) under the pressure of 2 kg weight (349.3 g per 1 cm²) for 30 s.⁹ In this study, we introduced the constant weight to enhance SC trapping into the adhesive tapes. This procedure should provide better consistency in application of pressure and SC removal than the use of finger pressure reported elsewhere.⁵

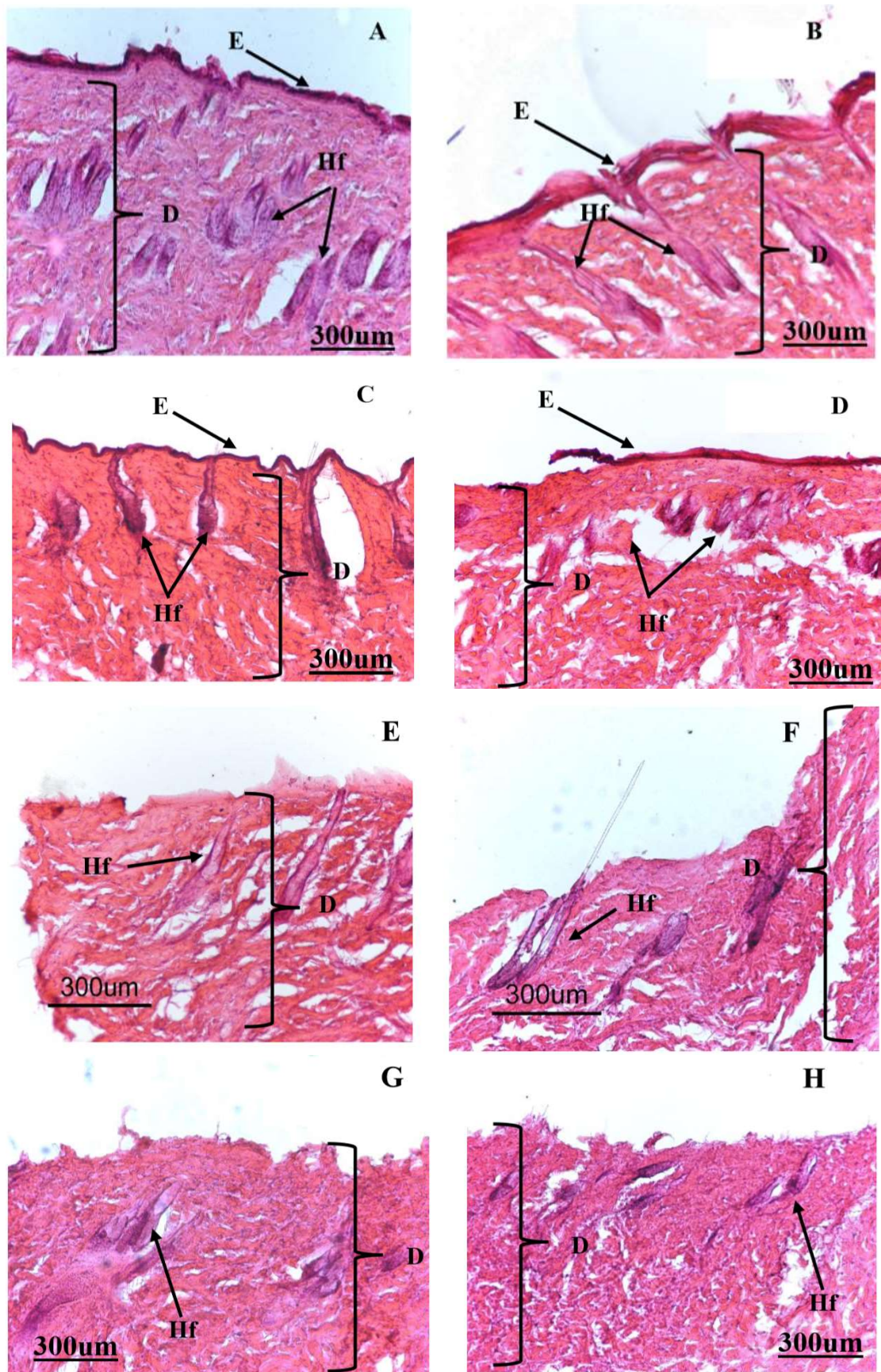


Figure 3. Effects of tape stripping on SC removal in normal rat shaved skin.

Microscopic anatomy before tape stripping (A) and after tape stripping 1, 2, 3, 4, 5, 10 and 15 times (B-H) (n=5), 10x magnification. Epidermis (E), dermis (D), hair follicles (Hf).

Table 1. Epidermal thickness before and after tape stripping

Number of strips	Epidermal thickness ($\mu\text{m} \pm \text{SD}$)	% of control
0	37.584 \pm 1.79	100
1	13.182 \pm 3.02	35.07
2	9.173 \pm 1.94	24.41
3	7.248 \pm 1.19	19.28
4	N/A	N/A
5	N/A	N/A
10	N/A	N/A
15	N/A	N/A

CONCLUSIONS

Tape stripping is a simple and non-invasive technique for epidermal-dermal separation. Epidermal removal efficiency for rat skin (2 cm² area) could be obtained at 4 consecutive cycles of adhesive tape application (with constant 700 g pressure) and removal.

ACKNOWLEDGEMENT

This work was supported by the Thailand Research Fund (RDG6050028).

REFERENCES

1. Zou Y and Maibach HI. Dermal–epidermal separation methods: research implications. *Archives of dermatological research* 2018;310(1):1-9.
2. Wilkinson DI and Walsh JT. Effect of various methods of epidermal-dermal separation on distribution of ¹⁴C–acetate-labeled polyunsaturated fatty acids in skin compartments. *Journal of investigative dermatology* 1974;62(5): 517-21.
3. Snorradóttir BS, Gudnason PI, Thorsteinsson F, Másson M. Experimental design for optimizing drug release from silicone elastomer matrix and investigation of transdermal drug delivery. *European Journal of Pharmaceutical Sciences* 2011;42(5):559-67.
4. Cambon M, Issachar N, Castelli D, Robert C. An in vivo method to assess the photostability of UV filters in a sunscreen. *Journal of Cosmetic Science* 2001;52(1):1–11.
5. Lademann J, Jacobi U, Surber C, Weigmann HJ, Fluhr JW. The tape stripping procedure--evaluation of some critical parameters. *European Journal of Pharmaceutics and Biopharmaceutics* 2009;72(2):317-23.
6. Monti D, Tampucci S, Burgalassi S, Chetoni P, Lenzi C, Pirone A, Mailland F. Topical formulations containing finasteride. Part I: in vitro permeation/penetration study and in vivo pharmacokinetics in hairless rat. *Journal of pharmaceutical sciences* 2014;103(8):2307-14.
7. Nair A, Jacob S, AlDhubiab B, Attimarad M, Harsha S. Basic considerations in the dermatokinetics of topical formulations. *Brazilian Journal of Pharmaceutical Sciences* 2013;49(3): 423-34.
8. Bashir SJ, Chew AL, Anigbogu A, Dreher F, Maibach HI. Physical and physiological effects of stratum corneum tape stripping. *Skin research and technology* 2001;7(1):40-8.
9. Praça FSG, Medina WSG, Eloy JO, Petrilli R, Campos PM, Ascenso A, Bentley MVLB. Evaluation of critical parameters for in vitro skin permeation and penetration studies using animal skin models. *European Journal of Pharmaceutical Sciences* 2018;111:121-32.

PH-033

Plumbagin exerts anticancer activity by suppressing HIF-1 α expression under hypoxic condition in MCF-7 breast cancer cells

Supawan Jampasri¹, Somrudee Reabroi¹, Duangjai Tungmunnithum², Warisara Parichatikanond³, Pornnipa Korprasertthaworn¹ and Darawan Pinthong^{1*}

¹ Department of Pharmacology, Faculty of Science, Mahidol University, Bangkok 10400, Thailand.

² Department of Pharmaceutical Botany, Faculty of Pharmacy, Mahidol University, Bangkok 10400, Thailand.

³ Department of Pharmacology, Faculty of Pharmacy, Mahidol University, Bangkok 10400, Thailand.

ABSTRACT

INTRODUCTION: Human breast cancers contain hypoxic regions and adapt to low oxygen availability (hypoxic conditions) by increasing the expression of hypoxia-inducible factor-1 α (HIF-1 α). A high level of HIF-1 α is associated with an increased risk of tumor metastasis and poor clinical prognosis in cancer patients. Plumbagin (5-hydroxy-2-methyl-1, 4-naphthoquinone) isolated from *Plumbago indica* L. exerts several pharmacological properties especially anticancer effects on many cancer cell types including breast cancer cells. However, the effect of plumbagin under hypoxic condition in MCF-7 breast cancer cells has never been investigated.

OBJECTIVES: To investigate the anticancer effect of plumbagin on MCF-7 cell viability and HIF-1 α expression under normoxia and hypoxia mimicking conditions.

METHODS: MCF-7 cells were treated with plumbagin at the concentrations between 0.5 to 5 μ M for 24, 48, and 72 h. Cobalt chloride (CoCl₂) at the concentration of 150 μ M was used to mimic hypoxic condition. The effect of plumbagin on MCF-7 cell viability under normoxic and hypoxic conditions were determined by MTT assay. The mRNA, protein expression of HIF-1 α and target genes was analyzed by quantitative real-time PCR (qRT-PCR) and western blotting, respectively.

RESULTS: Plumbagin decreased cell viability in MCF-7 cell line. The IC₅₀ values of plumbagin are 2.63 \pm 0.01 μ M, 2.86 \pm 0.01 μ M and 2.76 \pm 0.01 μ M at 24, 48 and 72 h, respectively, under normoxic condition. The results of qRT-PCR and western blotting showed that CoCl₂ significantly induced the expression of HIF-1 α mRNA and protein, respectively. Interestingly, in the presence of plumbagin, HIF-1 α mRNA, protein expression levels and HIF-1 α target genes were down-regulated under CoCl₂-induced hypoxia in MCF-7 cells in a concentration-dependent manner.

CONCLUSIONS: Plumbagin inhibited MCF-7 cell growth and suppressed mRNA and protein expression of HIF-1 α and target genes under hypoxic condition. Therefore, this study provides the mechanistic basis for potential anticancer effect of plumbagin.

Keywords: plumbagin, hypoxia-inducible factor-1 α (HIF-1 α), MCF-7 cell, breast cancer

INTRODUCTION

Breast cancer (BC) is one of the most common type of cancer in women worldwide¹ and is also one of the cancer burden in Thailand among breast, liver, lung, cervix, and colorectal cancers.² The poor prognosis of breast cancer are directly associated with tumor hypoxia³

which is a common phenomenon in solid tumors. Hypoxia refers to a low oxygen available stage at tissue level (less than 1–2% oxygenation compared with 21% oxygenation under normoxia) due to the impaired vascular function and results in an inadequate blood supply.⁴ Many cellular responses adapt to low oxygen availability (hypoxic conditions) by increasing the expression of hypoxia-inducible factor-1 α (HIF-1 α). Activation of HIF-1 α causes transcription process of many genes including pro-angiogenic factors that are critically involved in tumor aggression. Vascular endothelial growth factor A (VEGF-A) is one of the most important regulators of tumor-associated angiogenesis.⁵ Consequently, a high level of HIF-1 α is associated with an increased risk of tumor metastasis and poor clinical prognosis in cancer patients.⁶ Since HIF-1 α is a key regulator in the malignant solid tumor progression, therefore, HIF-1 α is an attractive target for anticancer treatment.

Plumbagin (5-hydroxy-2-methyl-1, 4-naphthoquinone), one phytochemical compounds from *Plumbago indica* L., has been used traditionally for the treatment of carminative, tonic elements, blood tonic, and anti-diarrhea agent.⁷ Plumbagin also exerts a variety of pharmacological properties such as anti-inflammatory, analgesic⁸, antimutagenicity and antioxidant activity.⁹ Under normoxic conditions, the anticancer effects on the inhibition of breast cancer cell growth,¹⁰ promotion of apoptosis¹¹ and suppression of invasion and migration¹² have been reported. However, the effect of plumbagin under hypoxic condition in MCF-7 breast cancer cells has never been investigated so far. Plumbagin may exert the anticancer activity by targeting HIF-1 α on the adaptation to hypoxic microenvironment in breast cancer cells. In this study, we investigated the anticancer role of plumbagin on MCF-7 cell viability, HIF-1 α expression and downstream target gene under normoxia and hypoxia mimetic conditions.

METHODS

Human breast cancer cell line (MCF-7) was obtained from the American Type Culture Collection (ATCC) and maintained in complete growth media Minimum Essential Medium (MEM) containing 10% Fetal Bovine Serum (FBS), 100 ug/ml penicillin, and 100 μ g/ml streptomycin (Invitrogen, Carlsbad, CA, USA). MCF-7 cells were cultured at 37°C in a humidified incubator with 5% CO₂. MCF-7 cells were plated at a density of 9×10^3 cells/well in 96-well plates and treated with plumbagin (Sigma-Aldrich, St. Louis, MO, USA) at various concentrations (0.5 to 5 μ M) for 24, 48, and 72 h. Under hypoxic conditions, MCF-7 cells were pre-treated with cobalt chloride (CoCl₂) (Sigma-Aldrich, St. Louis, MO, USA) at the concentration of 150 μ M for 6 h to mimic hypoxic condition followed by treatment with plumbagin for another 24 h. The effect of plumbagin on MCF-7 cell viability under normoxic and hypoxic conditions were determined by MTT assay. Data in each group were compared using a one-way ANOVA with Tukey's post-test. P-values < 0.05 were considered statistically significant. For qRT-PCR, total RNA was extracted from cell cultures using the TRIzol reagent (Invitrogen, Carlsbad, CA, USA) following the manufacturer's instructions. The purity of the RNA was determined using a NanoDrop™ One (Thermo Scientific). cDNAs were synthesized by using an iScript™ Reverse Transcription Supermix for qRT-PCR according to the manufacturer's protocol and stored at -20 °C until use. Real time PCR of HIF-1 α and VEGF-A was performed on equal amount of cDNA following the protocol provided with iTaq™ Universal SYBR® Green Supermix (Bio-Rad, Hercules, CA, USA) and analyzed with ABI PRISM7500 Sequence Detection System and analytical software (Applied Biosystems, Carlsbad, CA, USA). A panel of PCR primers were designed using NCBI/Primer-Blast follows: HIF-1 α , FW 5'-TTTTGGCAGCAACGACACAG-3' and RW 5'-TTTTCGTTGGGTGAGGGGAG-3'; VEGF, FW 5'-ACAACAAATGTGAATGCAGACCA-3' and RW 5'-TACCGGGATTCTTGCGCTT-3'; GAPDH, FW 5'-GACAGTCAGCCGCATCTTCT-3' and RW 5'-ACCAAATCCGTTGACTCCGA-3'. Samples were analyzed in triplicate and the expression ratio was normalized with GAPDH. For

protein analysis, total protein was lysed by using RIPA buffer supplemented with protease inhibitors (Bio-Rad, Hercules, CA, USA) and phosphatase inhibitor cocktail (Roche Diagnostic, Mannheim, Germany). The protein concentrations were determined by using the BCA protein assay kit (Bio-Rad, Hercules, CA, USA). Proteins were separated by 10% sodium dodecyl sulfate–polyacrylamide gel electrophoresis (SDS-PAGE) and transferred onto PVDF membranes. Blots were blocked with 5% nonfat dry milk and probed overnight at 4 °C with primary antibody: anti-HIF-1 α (H1alpha67) (Novus Biologicals, CO, USA); anti- β -actin (Cell Signaling Technology, Danvers, MA, USA). The membranes were then incubated with specific secondary antibodies. The detection of the bands was developed using ECL reagent (Millipore, Darmstadt, Germany) and imaged with ChemiDocTM Touch Imaging system (BioRad, Hercules, CA, USA). All statistical analysis was performed using GraphPad Prism 6 (GraphPad Software, San Diego, CA). Samples were analyzed in triplicates and the expression ratio was normalized with β -actin.

RESULTS

The effects of plumbagin on MCF-7 cell were examined by MTT assay. The cells were treated with plumbagin (1, 2 and 4 μ M) for 24, 48 or 72 h under normoxic and hypoxic conditions. Results showed that after treatment with plumbagin for 24 h, the cell viability of MCF-7 cells was reduced in a concentration-dependent manner in both conditions (Figure 1A and B.). The IC₅₀ values of plumbagin are 2.63 \pm 0.01, 2.86 \pm 0.01, and 2.76 \pm 0.01 μ M at 24, 48, and 72 h, respectively, under normoxic condition. Whereas, under hypoxic condition, plumbagin had a more potent inhibitory effect on cell viability (IC₅₀ = 2.30 \pm 0.02 μ M) (Table 1.). This result showed that plumbagin decreased cell viability in a concentration-dependent manner.

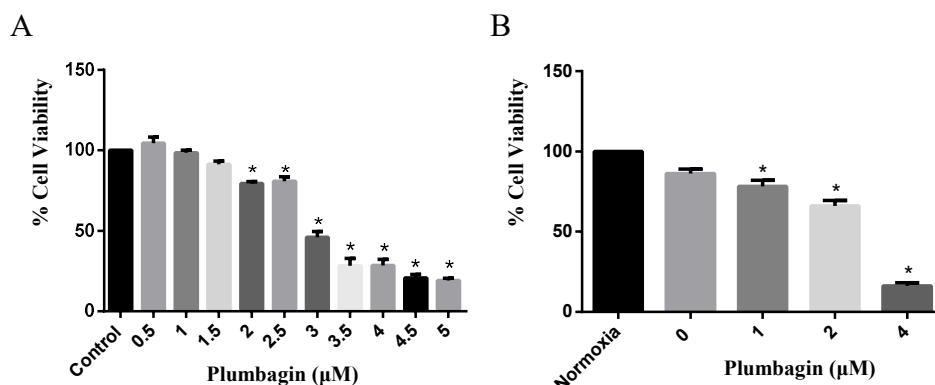


Figure 1. Plumbagin decreased cell viability in MCF-7 cell line at 24 h. Data are means \pm SEM compared with the vehicle control (n = 3) (*P < 0.05).

Table 1. IC₅₀ values (μ M) of Plumbagin in MCF-7 cell line at various time points.

Time	24 h	48 h	72 h
IC ₅₀ under normoxic condition	2.63 \pm 0.01	2.86 \pm 0.01	2.76 \pm 0.01
IC ₅₀ under hypoxic condition	2.30 \pm 0.02	-	-

To examine the effect of plumbagin on HIF-1 α protein expression under hypoxic conditions in MCF-7 cell line was determined by Western blotting. The cells were treated with various concentrations of plumbagin for 24 h under 150 μ M CoCl₂-induced hypoxic condition. These chemical mimics hypoxia via inhibits the hydroxylation by prolyl hydroxylase (PHDs) leading to HIF-1 α stabilization, accumulation and translocate into nucleus.¹³ The results

showed that CoCl₂ significantly induced the expression of HIF-1 α protein compared with normoxic group. Moreover, HIF-1 α protein expression level was significantly down-regulated by plumbagin at the concentration of 4 μ M (Figure 2A.). The relative quantity of HIF-1 α protein is shown in (Figure 2B.).

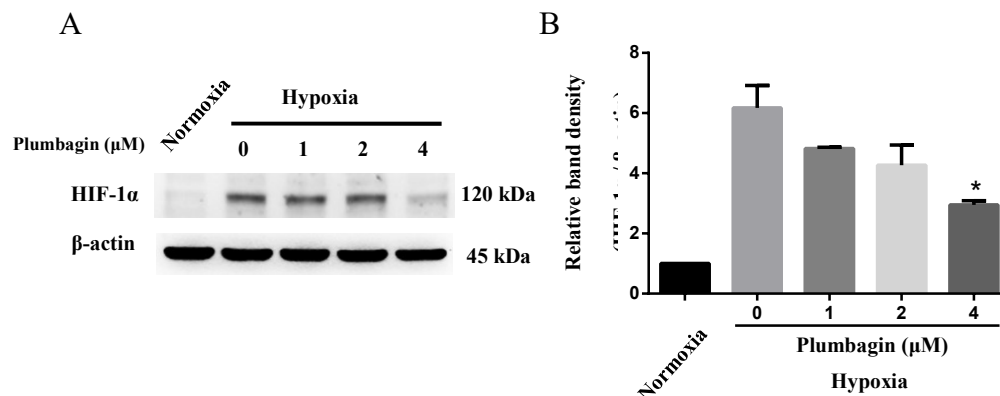


Figure 2. Plumbagin down-regulated HIF-1 α protein expression levels in MCF-7 cell line in hypoxic conditions. Data are means \pm SEM compared with the mimic hypoxia group without treatment (n = 3) (*P < 0.05).

To determine whether the reduction of HIF-1 α protein induced by plumbagin was attributable to the decrease in transcription, HIF-1 α mRNA expression levels were determined by qRT-PCR. The cells were treated with various concentrations of plumbagin for 24 h under 150 μ M CoCl₂-induced hypoxia. The results revealed that CoCl₂ significantly induced the expression of HIF-1 α mRNA compared to normoxic group. Furthermore, plumbagin at the concentration of 2 and 4 μ M significantly down-regulated HIF-1 α mRNA expression levels (Figure 3A.). In addition, plumbagin at the concentration of 4 μ M also significantly down-regulated the mRNA expression levels of HIF-1 α target genes, VEGF-A (Figure 3B.).

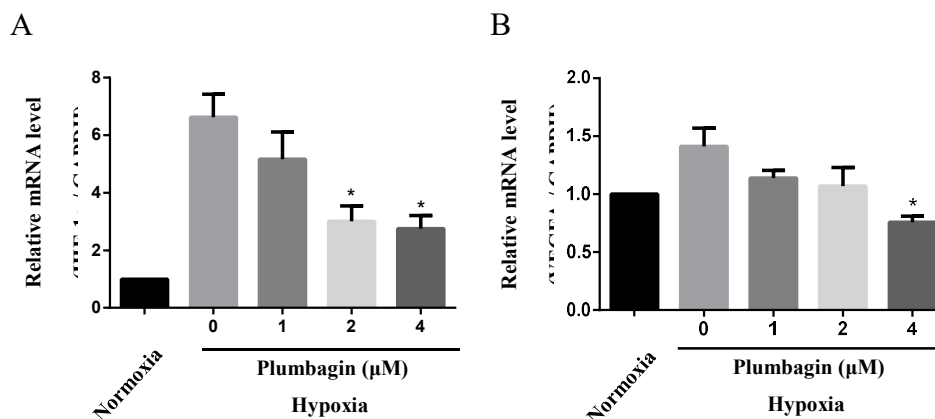


Figure 3. Plumbagin down-regulates HIF-1 α and VEGF-A mRNA expression levels in MCF-7 cell line under hypoxic condition. The relative mRNA expression was quantified and normalized with GAPDH. Data are means \pm SEM compared with the mimic hypoxia group without treatment (n = 3) (*P < 0.05).

DISCUSSION

Plumbagin has been reported to exert cytotoxicity against various cancer cell lines,^{10,14-15} and also exert antitumor and anti-angiogenic effects in several tumor cells through various mechanisms under normoxic condition.¹⁶⁻¹⁸ However, under hypoxic conditions, HIF-1 α

expression is induced and this event promotes tumor growth and angiogenesis. Therefore, the inhibition of HIF-1 α may be a promising target for breast cancer. In this study, we demonstrated that plumbagin reduced the viability of MCF-7 breast cancer cell lines. In particular, plumbagin down-regulates HIF-1 α mRNA, protein expression levels and HIF-1 α target gene (VEGF-A) under hypoxic condition. This result indicated that plumbagin acted as HIF-1 α inhibitor at mRNA and protein levels in MCF-7 breast cancer cells. However, the underlying mechanism by which plumbagin affects HIF-1 α expressions under hypoxic condition remains to be investigated.

CONCLUSIONS

In conclusion, plumbagin, a natural compound, exerts anticancer activity on MCF-7 cells by blocking HIF-1 α expressions. Plumbagin can be a promising HIF-1 α inhibitor targeted HIF-1 α overexpression in hypoxic environment of human breast cancers. This study provides new insights into anticancer mechanisms of plumbagin in breast cancer.

CONFLICT OF INTEREST

All authors declare no conflicts of interest.

REFERENCES

1. Fitzmaurice C, Allen C, Barber RM, Barregard L, Bhutta ZA, et al. Global, regional, and national cancer incidence, mortality, years of life lost, years lived with disability, and disability-adjusted life-years for 32 cancer groups, 1990 to 2015: a systematic analysis for the global burden of disease study. *JAMA Oncol* 2017;3(4):524-48.
2. Virani S, Bilheem S, Chansaard W, Chitapanarux I, Daoprasert K, Khuanchana S, et al. National and subnational population-based incidence of cancer in thailand: assessing cancers with the highest burdens. *Cancers* 2017;9(8):108.
3. Walsh JC, Lebedev A, Aten E, Madsen K, Marciano L, Kolb HC. The clinical importance of assessing tumor hypoxia: relationship of tumor hypoxia to prognosis and therapeutic opportunities. *Antioxid Redox Signal* 2014;21(10): 1516–54.
4. Armitage EG, Kotze HL, Williams KJ. Cancer hypoxia and the tumour microenvironment as effectors of cancer metabolism. *Correlation-based network analysis of cancer metabolism*. Springerbriefs in systems biology. London: Springer-Verlag New York; 2014. p. 7-14.
5. Ferrara N, Gerber HP, LeCouter J. The biology of VEGF and its receptors. *Nat Med* 2003;9:669-76.
6. Gilkes DM, Semenza GL. Role of hypoxia-inducible factors in breast cancer metastasis. *Future Oncol* 2013;9(11):1623-36.
7. สุดารัตน์ หอมหวล. เจตมูลเพลิงแดง [อินเทอร์เน็ต]. อุบลราชธานี: คณะเภสัชศาสตร์ มหาวิทยาลัยอุบลราชธานี; 2553 [เข้าถึงเมื่อ 1 มีนาคม 2561]. เข้าถึงได้จาก <http://www.thaicrudedrug.com/main.php?Action=viewpage&pid=174>
8. Luo P, Wong YF, Ge L, Zhang ZF, Liu Y, Liu L, et al. Anti-inflammatory and analgesic effect of plumbagin through inhibition of nuclear factor-B activation. *J Pharmacol Exp Ther* 2010;335(3):735-42.
9. Kumar S, Gautam S, Sharma A. Antimutagenic and antioxidant properties of plumbagin and other naphthoquinones. *Mutat Res* 2013;755(1):30-41.
10. Ahmad A, Banerjee S, Wang Z, Kong D, Sarkar FH. Plumbagin-induced apoptosis of human breast cancer cells is mediated by inactivation of NF-kappaB and Bcl-2. *J Cell Biochem* 2008;105(6):1461-71.

11. Zhang XQ, Yang CY, Rao XF, Xiong JP. Plumbagin shows anti-cancer activity in human breast cancer cells by the upregulation of p53 and p21 and suppression of G1 cell cycle regulators. *Eur J Gynaecol Oncol* 2016;37(1):30-5.
12. Yan W, Tu B, Liu YY, Wang TY, Qiao H, Zhai ZJ, et al. Suppressive effects of plumbagin on invasion and migration of breast cancer cells via the inhibition of STAT3 signaling and down-regulation of inflammatory cytokine expressions. *Bone Res* 2013;1(4):362-70.
13. Yuan Y, Hilliard G, Ferguson T, Millhorn DE. Cobalt inhibits the interaction between hypoxia-inducible factor- α and von Hippel-Lindau protein by direct binding to hypoxia-inducible factor- α . *J Biol Chem* 2003;278(18):15911-6.
14. Powolny AA, Singh SV. Plumbagin-induced apoptosis in human prostate cancer cells is associated with modulation of cellular redox status and generation of reactive oxygen species. *Pharm Res* 2008;25(9):2171-80.
15. Manu KA, Shanmugam MK, Rajendran P, Li F, Ramachandran L, Hay HS et al. Plumbagin inhibits invasion and migration of breast and gastric cancer cells by downregulating the expression of chemokine receptor CXCR4. *Mol Cancer* 2011;10:107.
16. Hsu YL, Cho CY, Kuo PL, Huang YT, Lin CC. Plumbagin (5-hydroxy-2-methyl-1,4-naphthoquinone) induces apoptosis and cell cycle arrest in A549 cells through p53 accumulation via c-Jun NH2-terminal kinase-mediated phosphorylation at serine 15 in vitro and in vivo. *J Pharmacol Exp Ther* 2006;318(2):484-94.
17. Sameni S, Hande MP. Plumbagin triggers DNA damage response, telomere dysfunction and genome instability of human breast cancer cells. *Biomed Pharmacother* 2016;82: 256-68.
18. Sinha S, Pal K, Elkhany A, Dutta S, Cao Y, Mondal G, et al. Plumbagin inhibits tumorigenesis and angiogenesis of ovarian cancer cells in vivo. *Int J Cancer* 2013;132(5):1201-12.

PH-036

Luteolin induces apoptosis in non-small cell lung cancer A549 cells

Wuttipong Masraksa¹, Supita Tanasawet² and Wanida Sukketsiri^{1*}

¹ Department of Pharmacology, Faculty of Science, Prince of Songkla University, Songkhla 90110, Thailand.

² Department of Anatomy, Faculty of Science, Prince of Songkla University, Songkhla 90110, Thailand.

ABSTRACT

INTRODUCTION: Lung cancer, non-small cell lung cancer subtype, is one of the major causes of death worldwide. Failure of current chemotherapeutic treatments leads to the cancer pathology recurrence and mortality in lung cancer patients. Luteolin (3',4',5,7-tetrahydroxyflavone) is a flavonoid compound that possesses anti-cancer effects. However, its effect on lung cancer is not well understood.

OBJECTIVES: The presents study aimed to investigate the effects of luteolin-induced apoptosis in non-small lung cancer cell line A549.

METHODS: Cytotoxicity of luteolin (0-80 μ M) was evaluated by 3-(4,5-dimethylthiazol-2-yl)-2,5 diphenyltetrazolium bromide (MTT) assay against A549 human lung cancer cell lines and the morphological changes were observed using a phase-contrast microscope. Cells apoptosis was determined by Hoechst 33342 staining after treatment with various concentrations of luteolin (0-80 μ M) at 24 hours. Thereafter, intracellular reactive oxygen species (ROS) and mitochondrial membrane potential (MMP) changes were also determined.

RESULTS: Luteolin treatment significantly decreased cell viability at the dose of 80 μ M, while treatment of the cells with luteolin at 0-50 μ M caused no significant toxic effect. Hoechst 33342 staining assay confirmed that apoptosis was not detectable in the luteolin-treated cells at 0-20 μ M. The apoptotic cells with fragmented or condensed nuclei were observed in the cells treated with 40, 50 and 80 μ M luteolin. Additionally, ROS production and MMP changes were significantly increased in response to luteolin (40 and 80 μ M) treatment in a concentration-dependent manner.

CONCLUSIONS: These results reveal that luteolin induced lung cancer cells apoptosis through enhancing ROS production and MMP changes which could develop as an anti-cancer therapeutic agent.

Keywords: A549, apoptosis, intracellular reactive oxygen species, mitochondrial membrane potential, lung cancer

INTRODUCTION

Lung cancer is one of the leading causes of death worldwide, and the incidence of non-small cell lung cancer (NSCLC) is approximately 80 % among other subtypes.⁽²⁾ Chemotherapy efficiency is often attended by a number of side effects including nausea and vomiting, neurotoxicity, renal toxicity, and also the recurrence of malignancies.^(12,14) Accordingly, drug developments are needed for higher efficacy with fewer side effects. An abundant number of anti-cancer agents developed from herbal sources have been found to be effective in the treatment and prevention of cancers.^(4,6)

Luteolin, 3',4',5,7-tetrahydroxyflavone, is a natural flavonoid presented in several plants including carrots, broccoli, onion leaves, parsley, celery, sweet bell peppers, and chrysanthemum flowers.⁽¹³⁾ It has been recorded to display various pharmacological effects for example anti-inflammation⁽⁹⁾, anti-oxidant⁽¹⁸⁾, anti-diabetic⁽³⁾ cardioprotection⁽¹⁵⁾ and neuroprotection.⁽¹⁾ Recently, luteolin has been noted as a promising class of anti-cancer agents against many types of malignancies and cancer including melanoma, liver, lung, breast, colon, brain, prostate and epidermal cancer.⁽⁷⁾ However, its effect on lung cancer is not well understood. The present study aimed to investigate the effects of luteolin-induced apoptosis in non-small cell lung cancer cell line A549.

MATERIALS AND METHODS

Chemicals and reagents

Luteolin, dimethylsulfoxide (DMSO), 3-(4,5-Dimethylthiazol-2-yl)-2,5-diphenyltetrazolium bromide (MTT), 2',7'-dichloro-fluorescein diacetate (DCFH-DA), N-acetylcysteine (NAC) and Hoechst 33342 were purchased from Sigma Chemical, Inc. (St. Louis, MO, USA). Tetramethyl rhodamine ethyl ester (TMRE) was purchased from Abcam (MA, USA). Luteolin was dissolved in DMSO and treated to the cells at a final concentration of 5-80 μ M. DMSO concentration in culture medium was always less than 0.1% (v/v) thereby it was not toxic to the cells.

Cell culture

Human non-small cell lung cancer A549 cells were provided from Cell Lines Service (CLS, Eppelheim, Germany) and cultured in DMEM/Ham's F-12 medium containing 2 mM L-glutamine, 10% fetal bovine serum, 100 units/ml penicillin and 100 μ g/ml streptomycin, at 37 °C with a 5 % CO₂ incubator atmosphere.

Cell viability assay

Cell viability was measured using MTT colorimetric assay. A549 cells (10⁴ cells/well) were grown into each well of a 96-well plate and incubated for 24 h. Then, cells were exposed to different concentrations of luteolin (0-80 μ M) for 24 h. After incubation, the medium was discarded and added with MTT solution for 2 h at 37 °C. Formazan product was solubilized with 100 μ L DMSO, and then the intensity was detected at 570 nm using a microplate reader (Biotek, Winooski, VT, USA).

Nuclear staining assay

A549 cells were grown at a density of 5×10^4 cells/well in 24-well plates and treated with luteolin at various concentrations (0-80 μ M) for 24 h at 37 °C. Then, the cells were incubated with 10 μ g/ml Hoechst 33342 for 30 min at 37 °C. The apoptotic cells with condensed chromatin and fragmented nuclei were taken by using a fluorescence microscope (Olympus IX70) supplied with a DP73 digital camera system (Olympus, Tokyo, Japan).

Determination of intracellular ROS production

The intracellular ROS generation was determined using a DCFH-DA method. A549 cells were plated and then treated with luteolin (40 and 80 μ M) for 24 h prior to incubation with 20 μ M DCFH-DA for 1 h in a dark condition. The fluorescent 2', 7'-dichlorofluorescein (DCF), which was converted from DCFH to DCF by the ROS inside the cells, was determined by a fluorescence microplate reader (BioTek, Highland Park, USA) at excitation 485 nm and emission 530 nm.

Measurement of mitochondrial membrane potential (MMP) change

The changes of MMP were evaluated by TMRE mitochondrial membrane potential assay kit. Cells were treated with or without luteolin and then incubated with TMRE for 20 min at 37° C in the dark. MMP was quantified under fluorescence microplate reader using 549/575 nm wavelength (BioTek, Highland Park, USA).

Statistical analysis

All results are presented as mean \pm standard error of the mean (SEM, $n = 4$). The data were analyzed by one-way ANOVA. Statistically significant differences from the control were created when $p < 0.05$.

RESULTS

Effect of luteolin on cell viability and apoptosis in A549 cells

To evaluate the cytotoxicity of luteolin, the cells were seeded and treated with various concentrations (0-80 μM) of luteolin for 24 h, and cell viability was evaluated by MTT assay. Figure 1 shows that 80 μM of luteolin causes significant cytotoxic effects on A549 cells. Morphological observation of cell death after treatment with luteolin was examined in this study by both phase contrast and fluorescence microscopy. Phase contrast microscopy revealed that luteolin induced cell death in A549 cells in comparison to the untreated control (Figure 2A). Distinctive morphological alterations including the loss of cell processes, more rounded morphology, and reduction of viable cells were detected in various concentrations of luteolin (20-80 μM). In addition, fluorescence microscopy was used to examine the nuclear staining and found that the apoptotic cells were not detected in the cells treated with luteolin at 0-20 μM , whereas 40-80 μM luteolin promoted an increase in apoptotic cells, illustrated by condensed and fragmented nuclei (Figure 2B).

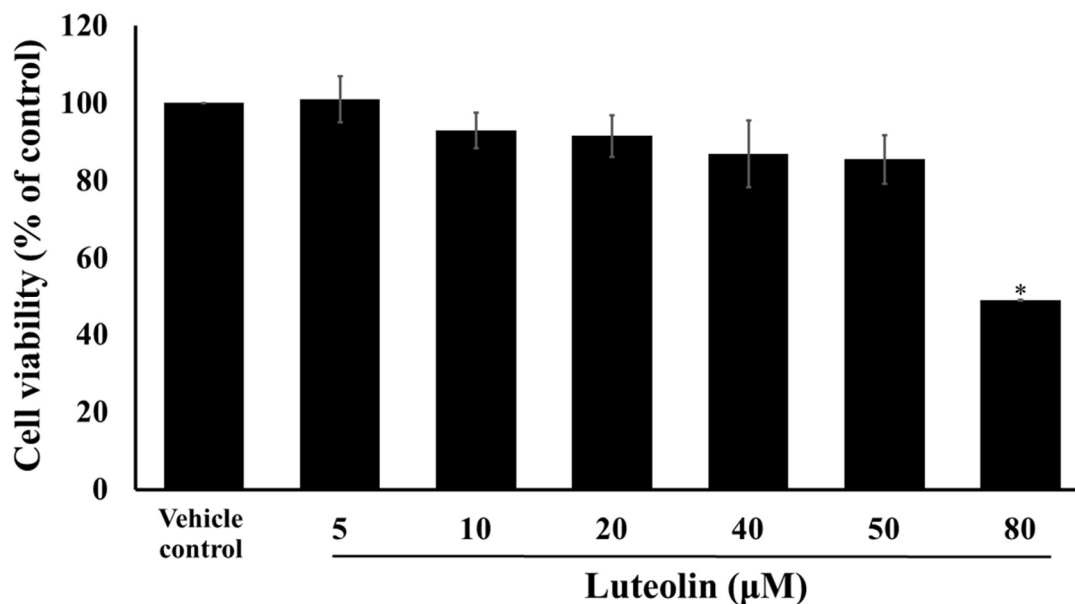


Figure 1. Effect of luteolin on A549 cell viability assessed by MTT assay after 24 h treatment. Percentage of cell viability after treatment with various concentrations are shown as mean \pm SEM of four independent experiments. * $p < 0.05$ versus the control.

Effect of luteolin on intracellular ROS production

We investigated whether luteolin could generate intracellular ROS which is known to activate biochemical changes including apoptosis in the A549 cells. Figure 3 demonstrated that 40 and 80 μM luteolin significantly increased the percentage of ROS generation in A549 cells in a concentration-dependent manner compared to the untreated control group ($p < 0.05$). Furthermore, we found that 5 mM NAC caused a significant reduction of ROS after luteolin treatment as shown in Figure 3 ($p < 0.05$). These results support the evidence that intracellular ROS production play an important role in luteolin-induced apoptosis in A549 cells.

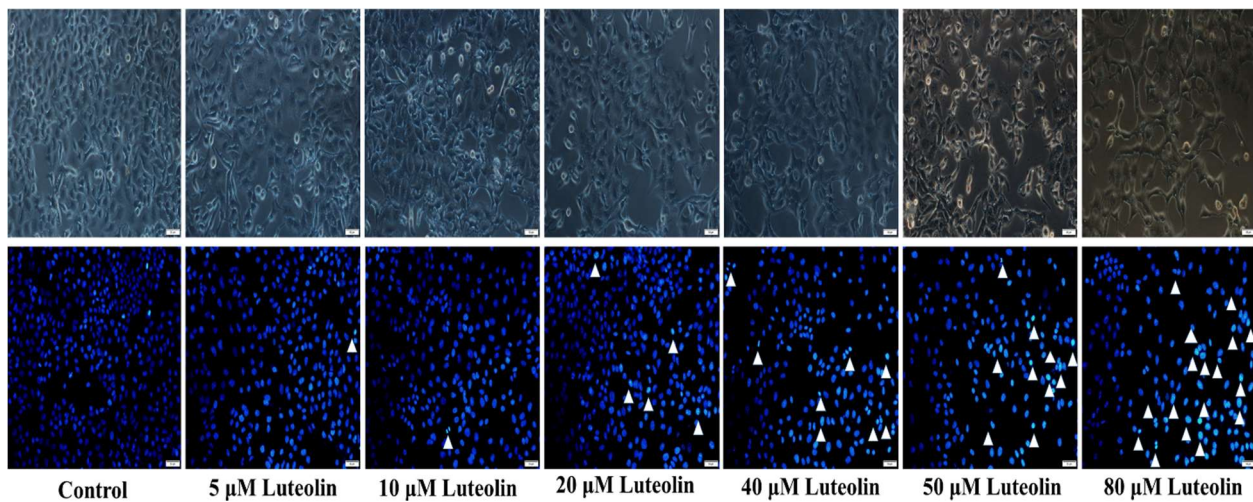


Figure 2. The alterations of cell morphology and apoptosis of A549 cells after treatment with luteolin for 24 h. (a) Inverted microscope evaluated cell morphology on A549 after exposure with 0-80 μM luteolin. (b) Fluorescence staining of Hoechst 33342 examined apoptotic nuclei on A549 after exposure with 0-80 μM luteolin. Scale bar: 50 μm

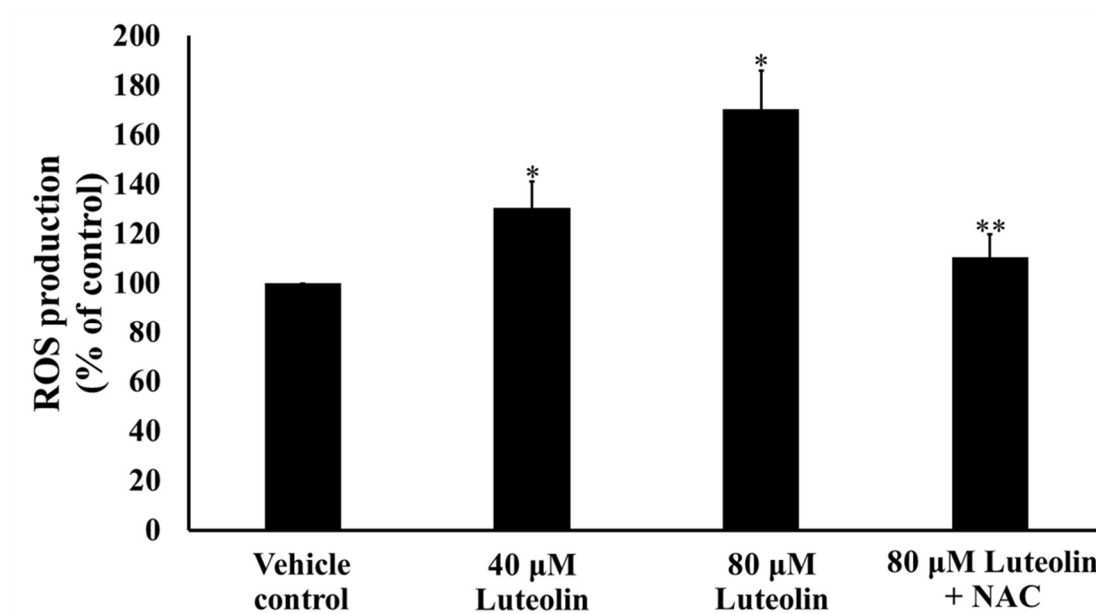


Figure 3 Effect of luteolin on intracellular ROS production in A549 cells by DCFH-DA assay. Data are shown as mean \pm SEM of four independent experiments. * $p < 0.05$ versus the control, ** $p < 0.05$ versus 80 μM luteolin.

Effect of luteolin on MMP changes

The disruption of MMP plays a crucial role in the mechanism of apoptosis thus we evaluated, by TMRE assay, whether luteolin is able to induce A549 cell death via the mitochondrial pathway. As shown in Figure 4, luteolin exposure showed a significant loss of mitochondrial membrane potentials in comparison to the control group ($p < 0.05$), indicating the presence of luteolin mediated the distress of mitochondrial metabolic activity.

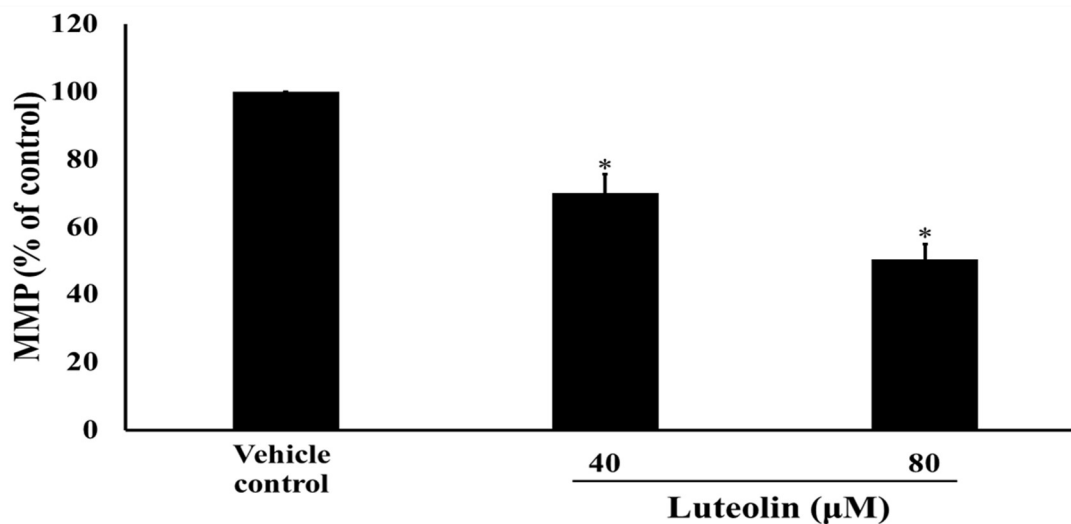


Figure 4 Mitochondrial membrane potential upon treatment with luteolin. A549 cells were exposed to the 0, 40 and 80 μM luteolin. Data are shown as mean ± SEM of four independent experiments. * $p < 0.05$ versus the control.

DISCUSSION

Luteolin is a flavonoid found in fruits, vegetables and medicinal herbs.⁽¹³⁾ Although luteolin is known to induce apoptosis in various types of cancers,^(16,8,10) the precise mechanism of luteolin-induced apoptosis via MMP pathway is not well clarified. This study investigated the effects of luteolin-induced apoptosis in human A549 cells.

We first determined the anti-proliferative effect of luteolin on human lung cancer A549 cell lines and found that luteolin exhibited cytotoxic effect against A549 lung cells. Our experiments were in line with previous reports on gastric cancer, hepatoma, and colon cancer cells proliferation which have been inhibited by luteolin.^(16,8,10)

Further observation elucidated the significance of luteolin on the initiation of apoptosis cell death in A549 cells by both morphological and biochemical assays. Following the apoptosis cell death process, the apparent morphological characteristics of apoptotic cells display nuclear fragmentation and chromatin condensation. Consequently, the apoptotic nucleus further condenses in the late stage and eventually breaks up.⁽¹⁹⁾ The microscopic investigation of the staining assay revealed the alterations in the morphological structures of luteolin exposed cells, when compared to the control.

It is known that various anticancer agents negotiate apoptotic properties by stimulating ROS generation in order to target cancer cells.⁽¹¹⁾ Findings from our study showed that treatment of A549 cells with luteolin augmented the production of intracellular ROS. These results were in good agreement with previous findings which reported an increase of ROS after treatment with luteolin in glioblastoma, non-small cell lung cancer and myeloma.^(5,17,20) Even though these results differ from some published study which were tested on colon cancer cell⁽⁸⁾, this might be associated with the difference type of cell and the concentration of luteolin exposed to the cells.

Mitochondria, the main source of ROS generation, are often recognized as important coordinators of cell death. The changes of MMP lead to an increased of ROS production, and the release of cytochrome C and other apoptogenic proteins. In order to assess the mitochondria function, we used the tetramethylrhodamine ethyl ester (TMRE) fluorescence probe to label the active mitochondria. As shown in Figure 4, the MMP of A549 cells exposed with luteolin was greatly diminished in comparison to the untreated control. This result indicated that MMP changes might be associated with upregulated in ROS production and apoptosis in the cells.

CONCLUSIONS

Our present findings suggest that luteolin suppresses the growth of human A549 cells presumably by ROS-mediated mitochondrial apoptosis pathway. However, further investigations are still needed to explore the specific molecular mechanism as additional information for the anti-cancer activity of luteolin.

ACKNOWLEDGEMENTS

The study was supported by the grant from the General Project and Invention of Prince of Songkla University (no. SCI610456S) and Faculty of Science Research Fund (Contract no. 1-2560-02-004) Prince of Songkla University, Songkhla, Thailand.

REFERENCES

1. Adedara IA, Rosemberg DB, Souza DO, Farombi EO, Aschner M, Rocha JBT. Neuroprotection of luteolin against methylmercury-induced toxicity in lobster cockroach *Nauphoeta cinerea*. *Environ Toxicol Pharmacol* 2016;42:243-251.
2. Al Husaini H, Wheatley-Price P, Clemons M, Shepherd FA. Prevention and management of bone metastases in lung cancer: A review. *J Thorac Oncol* 2009;4(2):251-259.
3. Chen Y, Sun X-B, Lu H, Wang F, Fan X-H. Effect of luteoin in delaying cataract in STZ-induced diabetic rats. *Arch Pharm Res* 2017;40(1):88-95.
4. Cragg GM, Newman DJ. Plants as a source of anti-cancer agents. *J Ethnopharmacol* 2005;100(1-2):72-79.
5. Dong W, Lin Y, Cao Y, Liu Y, Xie X, Gu W. Luteolin induces myelodysplastic syndrome-derived cell apoptosis via the p53-dependent mitochondrial signaling pathway mediated by reactive oxygen species. *Int J Mol Med*. 2018;42(2):1106-1115.
6. Fulda S, Kroemer G. Targeting mitochondrial apoptosis by betulinic acid in human cancers. *Drug Discov Today* 2009;14(17-18):885-890.
7. Jiang K, Wang W, Jin X, Wang Z, Ji Z, Meng G. Silibinin, a natural flavonoid, induces autophagy via ROS-dependent mitochondrial dysfunction and loss of ATP involving BNIP3 in human MCF7 breast cancer cells. *Oncol Rep* 2015;33(6):2711-2718.
8. Kang KA, Piao MJ, Ryu YS, Hyun YJ, Park JE, Shilnikova K. Luteolin induces apoptotic cell death via antioxidant activity in human colon cancer cells. *Int J Oncol* 2017;51(4):1169-1178.
9. Kim HJ, Lee W, Yun J-M. Luteolin inhibits hyperglycemia-induced proinflammatory cytokine production and its epigenetic mechanism in human monocytes: epigenetic changes by luteolin. *Phytother Res* 2014;28(9):1383-1391.
10. Lu X, Li Y, Li X, Aisa HA. Luteolin induces apoptosis in vitro through suppressing the MAPK and PI3K signaling pathways in gastric cancer. *Oncol Lett* 2017;14(2):1993-2000.
11. Marullo R, Werner E, Degtyareva N, Moore B, Altavilla G, Ramalingam SS. Cisplatin induces a mitochondrial-ROS response that contributes to cytotoxicity depending on mitochondrial redox status and bioenergetic functions. *PLoS ONE* 2013;8(11):e81162.
12. McWhinney SR, Goldberg RM, McLeod HL. Platinum neurotoxicity pharmacogenetics. *Mol Cancer Ther* 2009;8(1):10-16.
13. Miean KH, Mohamed S. Flavonoid (myricetin, quercetin, kaempferol, luteolin, and Aapigenin) content of edible tropical plants. *J Agric Food Chem* 2001;49(6):3106–3112.
14. Miller RP, Tadagavadi RK, Ramesh G, Reeves WB. Mechanisms of cisplatin nephrotoxicity. *Toxins* 2010;2(11):2490-2518.
15. Nai C, Xuan H, Zhang Y, Shen M, Xu T, Pan D, Zhang C, Li D. Luteolin exerts cardioprotective effects through improving sarcoplasmic reticulum Ca²⁺-ATPase activity in rats during ischemia/reperfusion in vivo. *Evid Based Complement Alternat Med* 2015;e365854.

16. Selvendiran K, Koga H, Ueno T, Yoshida T, Maeyama M, Torimura T. Luteolin Promotes degradation in signal transducer and activator of transcription 3 in human hepatoma cells: an implication for the antitumor potential of flavonoids. *Cancer Res* 2006;66(9):4826-4834.
17. Wang Q, Wang H, Jia Y, Pan H, Ding H. Luteolin induces apoptosis by ROS/ER stress and mitochondrial dysfunction in gliomablastoma. *Cancer Chemother Pharmacol.* 2017;79(5):1031-1041.
18. Zhang T, Wu W, Li D, Xu T, Zhu H, Pan D, Zhu S, Liu Y. Anti-oxidant and anti-apoptotic effects of luteolin on mice peritoneal macrophages stimulated by angiotensin II. *Int Immunopharmacol* 2014;20(20):346-351.
19. Ziegler U, Groscurth P. Morphological features of cell death. *Cardiovasc Res* 2004;19: 124-128.
20. Zhou M, Shen S, Zhao X, Gong X. Luteoloside induces G0/G1 arrest and pro-death autophagy through the ROS-mediated AKT/mTOR/p70S6K signalling pathway in human non-small cell lung cancer cell lines. *Biochem Biophys Res Commun.* 2017;494(1-2):263-269.

SPONSORS



N.Y.R. Limited Partnership



Smart Heart @Perfect Companion Group Co., Ltd.



Bang Trading 1992 Co., Ltd.



Pornpankorn Scientific Stainless Co., Ltd.



Eppendorf



S.M. CHEMICAL

S.M. Chemical Supplies Co., Ltd.

SPONSORS



ADInstruments



PCL Holding Co., Ltd.



Gibthai Co., Ltd.



Medica Innova Co., Ltd.



Abbott Co., Ltd.



Faculty of Medicine



Chiang Mai University



**The Pharmacological and Therapeutic
Society of Thailand**



Department of Pharmacology, Faculty of Medicine, Chiang Mai University,
110 Intravarorot rd., Sripoom, Mueang Chiang Mai 50220, Thailand

Tel. +66 53 945352

E-mail: pharmacology41@gmail.com

Website: www.pharmacology41.med.cmu.ac.th/web/site/index

Facebook: [@pharmacology41](https://www.facebook.com/pharmacology41)

Line ID: [@pharmacology41](https://www.line.me/tv/pharmacology41)